INFORMATION TO USERS

This manuscript has been reproduced from the microfilm master. UMI films the text directly from the original or copy submitted. Thus, some thesis and dissertation copies are in typewriter face, while others may be from any type of computer printer.

The quality of this reproduction is dependent upon the quality of the copy submitted. Broken or indistinct print, colored or poor quality illustrations and photographs, print bleedthrough, substandard margins, and improper alignment can adversely affect reproduction.

In the unlikely event that the author did not send UMI a complete manuscript and there are missing pages, these will be noted. Also, if unauthorized copyright material had to be removed, a note will indicate the deletion.

Oversize materials (e.g., maps, drawings, charts) are reproduced by sectioning the original, beginning at the upper left-hand corner and continuing from left to right in equal sections with small overlaps.

Photographs included in the original manuscript have been reproduced xerographically in this copy. Higher quality 6" x 9" black and white photographic prints are available for any photographs or illustrations appearing in this copy for an additional charge. Contact UMI directly to order.

ProQuest Information and Learning
300 North Zeeb Road, Ann Arbor, MI 48106-1346 USA
800-521-0600

SEDIMENT-CONTROLLED RADIONUCLIDE TRANSPORT: MATHEMATICAL MODELING AND FIELD APPLICATION

By

SIAMAK ESFANDIARY

A dissertation submitted to Graduate Faculty In Engineering in Partial fulfillment of the requirements for the degree of Doctor of Philosophy, The City University of New York

2001

UMI Number: 3008823

Bell & Howell Information and Learning Company
300 North Zeeb Road
P.O. Box 1346
Ann Arbor, MI 48106-1346

This manuscript has been read and accepted for the Graduate Faculty in Engineering in satisfaction of the dissertation requirement for the degree of Doctor of Philosophy.

4/25/2001
Date

Professor Reza Khanbilvardi
Chair of Examination Committee

4-26-2001
Date

Dean Mumtaz Kassir
Executive Officer

Dr. Lin Ferrand

Dr. Ali M. Sadegh

Dr. Vasil Diyamandoglu

Dr. John Fillos

Supervisory Committee

The City University of New York

ABSTRACT

Sediment-controlled Radionuclide Transport: Mathematical Modeling and Field Application

By

Siamak Esfandiary

Advisor: Professor Reza M. Khanbilvardi, Department of Civil Engineering, CUNY

The contamination of soil is a major concern of environmentalists. The soil contamination can easily be transferred into our body through water and plants. In major accidents, where cleaning up is not an option it is vital to confine the polluted area or to track down the path, through which the contamination is transported and to estimate the rate of transport. The focus of this research is to develop a model to define the transport of radionuclides over the soil surface by erosion and sedimentation induced by rain.

The local equilibrium concept has been used to develop a 2D depth-averaged contaminant transport model to estimate the removal of radionuclides from the soil surface due to erosion and sedimentation process. A 2D depth-averaged surface flow model has been coupled with a 2D depth-averaged sediment transport model. The flow is extremely shallow (about 1-

5 cm) and does not have enough energy to detach and roll the relatively bigger soil grains on the soil surface. Therefore the sediment transport takes place in suspension mode. The results of this coupling have then been used in a 2D depth-averaged contaminant transport model to estimate the rate of radioactive removal by erosion and sedimentation in water.

The model has been applied to a 20 m x 20 m plot in Ukraine, where a one-year experiment was conducted by the Center for Water Resources and Environmental Research in CUNY. The results were compared to the collected field data. It was concluded that the model results were statistically in an acceptable range.

Acknowledgment

This work could not be accomplished without the help and support of a number of people. Among them, my wholehearted gratitude goes to my beloved and beautiful wife Dr. Leyla Rahjou Esfandiary. There is no doubt in my mind that it would have been impossible for me to accomplish this undertaking without her encouragement and unconditional love.

My parents, to whom I owe my life, were the source of inspiration during these years. Although thousands of miles away, I felt and still feel their heart and presence with me all the time.

I also have to thank my father and mother in-law for their trust and unremitting support and encouragement.

My last and foremost gratitude goes to Professor Reza Khanbilvardi, my advisor, who financially and academically supported me for more than four years. He is one of the most gracious men I have ever met in my life and I know for a fact that I am not the only one feeling this way.

Table of Contents

List of Tables

List of Figures

CHAPTER 1

INTRODUCTION AND BACKGROUND

1.1 Introduction

The technological advances in the recent decades have made us and our environment more susceptible to disastrous failures. A good example is the Chernobyl Nuclear Power Plant explosion in Ukraine back in 1986. Not only the whole vicinity of the power plant was contaminated by radionuclides but also some parts of Europe became polluted as the result of that. In an accident with this nature and scale the contaminants are likely to remain in the environment for a long time. The major concern in this situation is to confine the source to prevent the transport of the contaminant or to track down its path to take suitable measures along its course. One of the biggest concerns after the Chernobyl accident was the soil. The soil contamination can easily be transferred into plants, animals, human, rivers and reservoirs through different mechanisms. The goal of this research is to depict a tangible picture of the sediment/erosion-controlled transport of radionuclides over the soil surface by runoff. This chapter discusses the sources, the history and the status of the past and present research in this area.

1.1.1 Environmental radioactivity

There are two sources of radioactivity in the environment:

1- Natural sources

2- Man-made sources

1.1.1.1 Natural Sources

The geological material of earth is naturally radioactive. Radioactive elements in rocks and soils decay, radiation is emitted and new elements form. One of such geological radionuclides is ^{40}K, which finds its way from rocks into soil and eventually into the human foodchain. This means that we have a certain amount of radioactivity in our bodies from natural resources. Our bodies are also exposed to radioactive material through building materials, such as concrete, which are made from geological materials.

The atmosphere contains radioactive gases as well. For instance radon is a radioactive gas, which is the product of decay of some geological radionuclides. Because it originates in earth's surface, it is released under buildings and can accumulate if there is a lack of good ventilation.

We receive certain dosage of radiation from outer space as well. This is called cosmic radiation, and the exposure depends on location. Obviously the radiation exposure increases with altitude, because the atmosphere,

which acts like an invisible shield becomes thinner. It is believed that 85-90% of the annual dosage of radioactive exposure is from natural sources.

1.1.1.2 Man-made Sources

Advances in technology and science have enabled us to develop nuclear weapons and nuclear power plants. We also have incorporated radioactive material in industry and medicine. All these have caused the widespread release of man-made radionuclides into environment. These artificial radionuclides have been generated by nuclear reactions involving fission, activation and decay. Some of the man-made material is radioactive isotopes of naturally occurring elements, such as ^{14}C or ^{90}Sr, and others are entirely artificial, such as plutonium.

1.1.2 A Brief History of Radioactive Contamination of Soil

We can identify the following reasons for the contamination of soils by radioactive material:

1- Nuclear weapons' tests

2- Releases of radionudclides from nuclear power plants

1.1.2.1 Nuclear Weapons Tests

The development of nuclear weapons after the Second World War was accomplished by several tests. Substantial amount of radioactivity entered our atmosphere because of these tests. The released radioactivities were the product of fission. ^{90}Sr and ^{137}Cs were specifically noticeable among the released products. These radionuclides were then transported globally and deposited world wide as radioactive fallout. Obviously the concentration of contaminants (radioactivity) near the test sites was more localized and concentrated.

1.1.2.2 Release of Radionuclides from Nuclear Power Plants

A certain amount of radionuclides are released into environment regularly by nuclear power plants. The intensity and discharge of these releases must be approved by the government. These authorized releases are in the gaseous or particulate form into the atmosphere, suspensions or solutions into the rivers or the sea and solid waste into certain underground repositories. Due to intense research on the mobility of radionuclides, this process is better understood today. Consequently the maximum allowable (authorized) release of radionuclides from power plants has been reduced during the last couple of years. A good example of this is the Sellafield

Nuclear Reprocessing Plant in Cumbria, UK. Scientists believed that the large quantities of plutonium and americium, which were released into the Irish Sea, would be absorbed on to the sediments and thereby immobilized. However, this did not happen. The radioactive materials were strongly absorbed but the sediments were mobile. In particular they were moved into tidal reaches of nearby rivers and were deposited on adjacent fields during flooding. Therefore, the discharged radionuclides into the sea were brought back into the land and contaminated the soil.

Accidental releases of radionuclides from nuclear power plant have been few and far between. The three best documented nuclear catastrophes are:

- Windscale Fire in the UK in 1957
- Three Mile Island in the USA in 1979
- Chernobyl in Ukraine in 1986

One of the most dangerous nuclear accidents in the history of nuclear reactor operations occurred at the Chernobyl Nuclear Power Plant on the 26th of April 1986. This reactor was one of the 16 existing high-power boiling channel-type reactors. This type of reactor features a graphite-moderated light-water coolant system, in which vertical zirconium alloy pressure tubes contain the fuel pins. The accident took place during a test to verify the

ability of the turbine generators to supply energy to coolant pumps in the event of an external power malfunction.

As a result of this accident, consumed fuel and fission products were released into the atmosphere. During the initial explosion and the ten days following the accident, approximately 2.7 X 10^{18} Bq of radioactivity (3-4 % of the core inventory) were released into the environment [Konshin 1992]. The radionuclides, released into the atmosphere, were deposited in the vicinity of the Power Plant (within a radius of 20 miles) or carried by the prevalent weather pattern and deposited by precipitation. As a result, the pattern of the contamination was not, and still is not uniform in the territories of the former Soviet Union and the rest of the Europe.

Because of direct fallout of the radionuclides and the subsequent runoff and sediment transport process, entire basins of several rivers were contaminated. Most of the radionuclides have relatively short half-lives and have since the accident considerably decayed. Only ^{137}Cs and ^{90}Sr are currently present in concentrations, which comprise any real threat to the public health in the impacted regions.

Hydrologic runoff and erosion are the two main processes in which radionuclides deposited in the surface environment migrate widely in both dissolved and particulate forms. Precipitation and flooding erode

radionuclides on the surface soils. They might be deposited again elsewhere or reach rivers or reservoirs. Qualification and quantification of radionuclides transported through runoff systems has been given a considerable attention following radioactive contamination caused by the nuclear accidents.

As a consequence of the extensive environmental contamination after the Chernobyl accident, contaminated runoff has flowed downstream through several different river basins. The main portion of these watersheds lies in the system of Dnieper-Sozh rivers. Extremely high concentrations of different radionuclides were observed in waters of these rivers during the month of May 1986.

Dissolved fractions in runoff components have been estimated to be up to 90% of total radionuclides transported by water flow (Voitsekhovitch et al., 1994). The movement of this fraction is a function of hydrodynamic transport and many interactions between the radionuclides and physical, chemical and biological systems. Soil erosion on the other hand is a complex process itself. The elements involved in this process are not well understood yet. This is especially true when the soil particles are contaminated by radionuclides or other hazardous chemicals.

Almost, all radioactive contamination exists in the very top surface of soil. The vertical migration rate is very much slower than the planar migration. Viewing the vertical migration of radionuclides in soil as a diffusion-convection process considerably simplifies the long-term prediction of the behavior of radionuclides under natural conditions. Vertical migration is a slow process and meticulous inspection of it would be so time consuming as to be impractical [Khanbilvardi et al., 1997; Khanbilvardi et al., 2000; Konsin 1992; Rogowski et al., 1965].

1.2 Past and Present Status of This Research

Mathematical models describing the transport of radionuclides have become more complex during the last two decades. In particular fairly simple 'black box', which was developed for radiological assessment in soil, has advanced to more thorough and realistic models. The main interest of modelers is the potential danger of soil to act as a temporary or permanent source of radionuclides to man. In particular, the following processes are relevant:

1- Suspension of contaminated soil in the atmosphere;

2- Leaching and surface runoff into drinking water;

3- Uptake by plants and crops;

4- Ingestion by grazing animals and humans.

The simplest model was the single 'black box', assuming a given area of soil to a given depth with a stated bulk density. Radionuclide inputs are assumed to be homogenized immediately and to be equally available throughout the box. [Coughtrey 1988].

Rogowski and Tamura (1965) studied the movement of ^{137}Cs by runoff and infiltration on the alluvial Captina silt loam. They applied five millicuries of ^{137}Cs in the form of spray to the 5-m^2 plots of Captina soil in Tennessee under bare, clipped meadow, and tall meadow cover conditions. A linear relationship on a full log scale was found between the soil and ^{137}Cs loss. On the plots with vegetation, it was found that practically all of the ^{137}Cs applied to areas covered with vegetation was initially on the plant and litter material. The leaching of ^{137}Cs from the vegetation began to level off towards the end of the 81-day study period. At the end of the 81-day period, the bare plot had lost 11.9% of the cesium while the clipped meadow and tall meadow plots had lost 5.1% and 2.6% of their cesium, respectively.

Armstrong and Gloyna (1969) presented a general equation to describe radionuclide transport in terms of hydraulic dispersion and convection and detention systems, which sorb and release. They also presented a model to describe sorption by various substrates using

concentration gradient between the equilibrium activity in the substrate and the actual activity. They discussed linear and non-linear equations concerning accuracy of prediction of the transport. They discovered that Freundlich isotherm is adequate in describing sorption by suspended solids, bed sediments and biological systems. However, the use of this equation in the reaction term of the one- dimensional dispersion equation forces it into a non-linear form.

Gloyna, Yousef and Padden (1971) studied the transport of radioactivity in water under continuous release of radionuclides in a small-scale ecosystem. Model rivers were simulated in two channels of a research flume. The control channel of the model river system contained a typical bottom segment and received a potable water supply. The second channel, in addition to bottom sediment, contained a lush community of rooted aquatic plants in one end and received water, which was rich in phytoplankton. Both channels were subjected to a continuous release of ^{134}Cs and ^{85}Sr for periods up to thirty-five days. The distribution of the radionuclides in the bottom sediment, plants, algae and water was determined. Under condition of the release, less than maximum permissible concentration, the radioactivity continued to increase on the surface of the bottom sediments until a quasi-equilibrium level was reached at approximately 30 days after initiation of

release. Once saturation was reached at the sediment surface, radionuclide uptake by the sediment was equal to the radioactivity lost by the surface as a result of migration into the sediment. This migration into the sediment was found to be very slow. It was discovered that the concentration of radionuclides in the sediment was affected by sediment movement. It was recognized that pollution stresses and reduction in pH and toxic material may be responsible for sudden release of radionuclides from both plants and sediments.

Carlsson (1977) presented a model for the movement and loss of ^{137}Cs in a small watershed. He presented a mathematical model, which described the turnover of fallout of ^{137}Cs in a small lake. The model was based on the assumption that the water of the lake receives ^{137}Cs from deposition on the surface of the lake and from removal of the radionuclides from the drainage area. The loss of ^{137}Cs from the water is assumed to occur through outflow and sedimentation. His investigation showed that the activity of ^{137}Cs in the water of the lake depends on both the deposition rate and the cumulative deposition of the radionuclides in the drainage area of the lake. The results also indicated that there is a seasonal variation in the concentration of ^{137}Cs, which depends on the seasonal variations of both the deposition rate and the water turnover in the lake. A large amount of the ^{137}Cs introduced into the

lake was stored in the bottom sediment. The redistribution of ^{137}Cs between the different compartments of the watershed was small and its loss from the watershed was mostly due to physical decay.

Bjurman (1989) observed the urban water transport and wash-off of ^{137}Cs after the Chernobyl accident. He elucidated the transport of ^{137}Cs from a building roof and three storm sewers in Uppsala Sweden during the first rainfall after those, on April 29-30 1986, causing the Chernobyl contamination. Runoff and concentration of ^{137}Cs in storm water were determined. The origin of storm water was determined as well. Surface contamination was measured on July 3, 1986. Total fallout was 25 kBq/m^2. During the rainfall on 11 May, 4 kBq/m^2 were transported from the roof and approximately 1 kBq/m^2 from the sewered areas. From April 30 to July 4 a level of 13-20 kBq/m^2 was present. Measurements from another project showed that the fallout rain events washed off 10 to 16 kBq/m^2 [Amono et al., 1999; Halldin et al., 1990; Korhonen, 1990]. The wash-off by the small rainfall on May 11constituted one third of the remaining decontamination occurring up until July 4. The transport of ^{137}Cs during May 11 event increased when the runoff increased, but was less efficient as the event proceeded. The relations between ^{137}Cs concentrations and runoff implied

that the wash-off of ^{137}Cs in Uppsala was totally dominated by that bound to particles.

Veronov and Aleksakhin (1992) studied the main laws governing the migration of ^{90}Sr and ^{137}Cs in the natural and cultured farming centers of Uzbekistan. The peculiar natural and climatic conditions and also the peculiar features of the agricultural industry create a radiological situation, which is specific for this region. In this region, the distribution of the leading dose-generating radionuclides ^{137}Cs and ^{90}Sr of global origin was studied in 1983-1986 in principal types of natural and cultured farming centers; also the entry of these radionuclides in to the human organism was assessed. They found that radioecological and radiation-related health problems originating from the introduction of radionuclides into the environment must be solved on the basis of radiation-monitoring data, taking into account all the ecological, economic, demographic, social, and other factors determining the influence of radiation upon men and the biota.

Konshin (1992) analyzed the convection-diffusion equation as a basis for modeling the migration of radionuclides. To describe the experimental data adequately within the framework of convection-diffusion equation, it was necessary to introduce migration parameters, which increase as the radionuclides penetrates further down through the soil layer and decrease as

the observation time lengthens. He also studied the applicability of a traditional mathematical model on the basis of 3-year observation of the vertical migration of ^{137}Cs fallout after the Chernobyl accident. The most accurate description of the dependence of the radionuclide concentration on the depth of the soil layer is given by a lognormal distribution. He determined the parameters of this distribution and showed that they are a solution of the Fokker-Planck equation, a special case of which is the convection-diffusion transport equation.

Melkozerova et al. (1995) observed the flow of radioactive sediment in rivers near Chernobyl. They discussed the fate, formation and transport of the radioactive contaminants of Belarussian rivers due to the accident at the Chernobyl Power Plant. They reviewed the data obtained by Belarussian, Ukrainian and Russian Institutes. Of all the extensive sets of data, they presented in particular the results related to the Iput river. On the basis of monitoring data, they analyzed the fate and transportation of ^{137}Cs and ^{90}Sr in the Dnieper-Sozh river system. Their analyses were made using HEC-R-6 model, which was developed by the US Army Corps of Engineers, modified by the Oak Ridge National Laboratory and adapted for the Iput river simulations at Tulane University. They defined a parameter called modulus of runoff to estimate radionuclide runoff from watersheds. They discovered

that over 87% of the ^{137}Cs were transported by fine sediment less than 0.2 mm despite the fact that these particles account for only 53% of the total mass of the transported sediments

Nair et al. (1996) modeled the washout of ^{90}Sr and ^{137}Cs from an experimental plot established in the vicinity of the Chernobyl reactor. A vertical, one dimensional, multiphase, multispecies transport model was developed to simulate the movement of the contaminants in the topsoil during the 160-day period between the Chernobyl event and the experiments as well as the washouts of contaminants by runoff during the experiments and during the 24-hour period thereafter. The model provided very good predictions of the vertical distribution of the total contaminant concentration in the top 10-cm of the soil. However, the concentrations of the individual chemical forms were not predicted as accurately. Their goal was to create a site-specific model rather than a general mathematical model. They defined a number of parameters and coefficients, which are very difficult to estimate. The uncertainty and lack of knowledge about these key parameters makes this model very difficult to apply to different sites.

Khanbilvardi and Sadegh (1997) observed the transport of radionuclides due to erosion and runoff on agricultural watersheds. An experimental plot was selected in the vicinity of Chernobyl Power Plant. It

was devegated and leveled. Redistribution and transport of radionuclides on the plot were analyzed within a one-year period. Artificial rainfall was performed during the dry months of the year. Vertical migration of radionuclides was also studied. The movement of the peak of the vertical distribution in the topsoil was investigated as well. It was elucidated that for the entire one-year cycle, the total amount of ^{137}Cs washed out of the runoff plot by natural processes constituted 0.07% of its initial reserves. The corresponding figure for artificial irrigation came up to less than 1% of its initial reserves. This is lower than the amount of natural radioactive decay, even though the erosion caused by the artificial irrigation led to a considerable loss of soil. An effect of redistribution of ^{137}Cs and ^{90}Sr within the area of the plot was observed, with considerable accumulation in microtopographical depressions, along with soil mass washed out during irrigation. Apart from the planar movement of radionuclides down the slope, the irrigation caused more intense vertical migration.

Amono et al. (1999) studied the transfer capability of long-lived Chernobyl radionuclides from surface soil to river water in dissolved forms. They examined the concentration and speciation of radioactive Cs, Sr and transuranic isotopes, such as Pu and Am, in undisturbed surface soil along the river in the exclusion zone near the Chernobyl Nuclear Power Plant in

order to validate the radioactive contamination characteristics. Almost all radioactivities existed in the very top surface in the undisturbed soil layer. ^{90}Sr in the soil was estimated to be highest in the water soluble and exchangeable fractions, which were easily accessible to river water as dissolved fraction.

1.3 Objectives

The objectives of this research was to investigate the transport of radioactive contaminants on soil surface in dissolved and particulate form due to runoff, erosion and sedimentation. To fulfill the objectives of this study the following tasks will be accomplished:

a) Developing (adapting) a 2D depth-averaged unsteady flow model;

b) Developing a 2D depth-averaged unsteady sediment transport model;

c) Developing a 2D depth-averaged contaminant transport model;

d) Coupling the above mentioned models and finding the appropriate numerical scheme to solve the model;

e) Calibrating the model, based on experimental field values, to find the key parameters;

f) Performing a sensitivity analysis.

1.4 General Model Overview

The erosion process and the movement of the sediments over the soil surface are induced by rainfall [Aziz et al.,1984]. In other words rainfall generates overland flow. If the overland flow is strong enough it can detach soil particles (erosion) and transport them to a new location and deposit them [David et al., 1975]. If the soil particles are contaminated, the contamination is also transported in this process. To include all these major factors into a single model, three separate modules have been considered:

1. **Overland flow module:** The hydrodynamic properties of the overland flow (velocity in the x and y direction and flow depth) are computed in this section. A depth-averaged approach was selected here because the overland flow is extremely shallow (1-5 cm) and one can assume that the flow properties are constant over its depth.
2. **Sediment transport module:** Using the hydrodynamic properties of the flow from the module number one, the net flux of sediment (erosion-deposition) into the water is calculated. At the same time the rate of sediment transport and the sediment redistribution over the soil surface is computed. In the framework of this study only shallow overland flows (1-5 cm) are taken into consideration. It has been established by different field experiments that the bulk

portion of radionuclides is transported mostly by very fine particles [Fennema ,1983; Guo et al., 2000; Lee et al., 1997]. This is the reason, why this research is just focused on the transport of fine particles. Like the first module, working with depth-averaged equations is justifiable here as well.

3. **Contaminant transport module:** The redistribution of the radionuclides is predicted here using the above two modules. The amount of radioactive contamination transported by water in particulate (absorbed) form and dissolved form is computed here. The amount of particulate radionuclides in runoff depends directly on the suspended sediment concentration in water (module 2).

In the following chapters the very details of each module is discussed. Chapter 2 depicts the development of the flow module and the averaging procedure. Chapter 3 and 4 illustrate the sediment transport and the contaminant transport processes and their averaging procedure, respectively. Chapter 5 explains the numerical technique, which is selected to solve the model. The application of the model and the verification results are shown in chapter 6. The conclusions and the suggestions for the future studies are presented in chapter 7.

CHAPTER 2

FLOW MODEL

2.1 Introduction

Horton (1933) described overland flow as follows: "Neglecting interception by vegetation, surface runoff is that part of the rainfall, which is not absorbed by the soil or by infiltration. If the soil has an infiltration capacity i, then when the rain intensity R is less than i the rain is all absorbed and there is no surface runoff. It may be said as the first approximation that if R is greater than i, surface runoff will occur at the rate (R – i)" [Eagleson, 1970]. Horton called (R – i) rainfall excess. He considered the overland flow similar to sheet flow, whose depth might be very small.

Overland flow seldom happens on planar surfaces with homogenous physical and hydraulic properties. Surface roughness, soil hydraulic properties and structure varies over distance. These factors strongly effect the hydrodynamics of the overland flow. These spatial variations significantly influence the soil erosion and contaminant transport as well. Overland flow modeling in the past several decades has been confined to one-dimensional kinematic wave equations. By constraining the overland flow to one dimension and assuming a homogenous plane surface, previous

models ignored the real, measurable spatial variation in the overland flow field. Consequently, significant errors in the distribution of velocity, depth and boundary shear stress may be created.

Dunne and Dietrich (1980) showed that one-dimensional models are unable to simulate the spatial variability of the flow field, however they may successfully predict the average flow depth and the hydrograph on a real hillslope. For their experimental plots, the coefficient of variation of the cross-slope depth ranged from 0.5-0.8.

Kibler and Woolhiser (1970) proposed the kinematic cascade method, in which the real surface was approximated by a series of plane surfaces, each with a different gradient. Borah et al. (1980) used the same idea to develop a more sophisticated kinematic shock fitting technique. Constantinides and Stephenson (1981) extended the kinematic wave model to a two-dimensional overland flow model.

These studies provided a deep insight to the overland flow problem. Yet they were limited by the kinematic wave assumptions. For instance negative or steep slopes were not allowed.

Chow and Ben-Zvi (1973) used a two-dimensional hydrodynamic equation to model the overland flow. They used Lax-Wendorff scheme to solve the model. Yet because of the simplification of the hydrodynamic

equation, all terms related to the convective acceleration were dropped. These terms are significant in flow in terms of spatial variation in hillslope characteristics, which could not therefore be incorporated in the model.

Katapodes and Strelkoff (1979) used a characteristic method to solve the two-dimensional flow model resulting from a dam break. They pointed out all the advantages of this method. However, for the general case of overland flow of spatial variability in slope, roughness and infiltration, characteristic methods are not tractable.

Kawahara and Yokoyama (1980) presented a two-dimensional overland flow model, where they had solved a two-dimensional shallow water equation using finite element method. Spatial variability of roughness and infiltration were not included in their model. Iwasa and Inoue (1982) modeled floods due to dam break using a two-dimensional Saint-Venant equation solved by the Lax-Wendorff scheme. They had not included rainfall and infiltration in their model.

Fennema (1985) compared different numerical solutions of two-dimensional transient water-surface flows, which are used in computational fluid dynamics. He used McCormack, Gabutti, and Beam and Warming methods to analyze the solution of the shallow water equations describing

two-dimensional transient flow. Both negative and positive waves were simulated following a dam break

Zhang and Cundy (1989) developed a two-dimensional hydrodynamic equation. The equation was solved using a numerical scheme based on the explicit, second order accurate, McCormack finite difference scheme. This scheme allows incorporating the real topography of the field and also spatial variation of soil properties.

Zhao et al. (1994) presented a two-dimensional unsteady flow model based on the finite-volume method with a combination of unstructured triangular and quadrilateral grids. The attractive feature of their model was the ability to deal with the wetting and drying processes for floodplain and wetland studies, dam break problems involving discontinuous flows, subcritical and supercritical flows.

In a general case, the flow model should be three-dimensional. However, we may simplify the analysis by considering them two-dimensional flows by using vertically averaged quantities. This method simplifies and abridges the analysis without a significant effect on accuracy.

2.2 Formulation

The Navier-Stokes equations for an incompressible fluid are:

Continuity:

$$\frac{\partial u}{\partial x}+\frac{\partial v}{\partial y}+\frac{\partial w}{\partial z}=0 \qquad (2\text{-}1)$$

Momentum equation:

$$\frac{\partial u}{\partial t}+u\frac{\partial u}{\partial x}+v\frac{\partial u}{\partial y}+w\frac{\partial u}{\partial z}=g_x-\frac{1}{\rho}\frac{\partial}{\partial x}+\frac{\mu}{\rho}\nabla^2 u \qquad (2\text{-}2)$$

$$\frac{\partial v}{\partial t}+u\frac{\partial v}{\partial x}+v\frac{\partial v}{\partial y}+w\frac{\partial v}{\partial z}=g_y-\frac{1}{\rho}\frac{\partial}{\partial y}+\frac{\mu}{\rho}\nabla^2 v \qquad (2\text{-}3)$$

$$\frac{\partial w}{\partial t}+u\frac{\partial w}{\partial x}+v\frac{\partial w}{\partial y}+w\frac{\partial w}{\partial z}=g_z-\frac{1}{\rho}\frac{\partial}{\partial z}+\frac{\mu}{\rho}\nabla^2 w \qquad (2\text{-}4)$$

where:

u, v, w = velocity component in x, y and z direction (LT^{-1}),

$g_{x,y,z}$ = gravitational force per unit mass in x, y and z direction (LT^{-2}),

μ = dynamic viscosity ($ML^{-1}T^{-1}$),

ρ = density (ML^{-3}),

P = pressure($ML^{-1}T^{-2}$), and

∇^2 = Laplace operator = $\frac{\partial^2}{\partial x^2}+\frac{\partial^2}{\partial y^2}+\frac{\partial^2}{\partial z^2}$.

A two-dimensional depth-averaged overland flow can be obtained by integrating equations (2-1)-(2-4) in the z-direction.

Continuity equation

Integrating continuity equation in the z-direction, it yields:

$$\int_{z_b}^{z} \frac{\partial u}{\partial x} dz + \int_{z_b}^{z} \frac{\partial v}{\partial x} dz + w(Z) - w(Z_b) = 0 \qquad (2\text{-}5)$$

Z and Z_b are the z-coordinates of the flow surface and the land, respectively, measured vertically to the plane of the land.

Equation (2-5) can be evaluated using Leibnitz rule:

$$\int_{z_b}^{z} \frac{\partial u}{\partial x} dz = \frac{\partial}{\partial x} \int_{z_b}^{z} u dz - u(Z) \frac{\partial Z}{\partial x} + u(Z_b) \frac{\partial Z_b}{\partial x} \qquad (2\text{-}6)$$

$$\int_{z_b}^{z} \frac{\partial v}{\partial x} dz = \frac{\partial}{\partial x} \int_{z_b}^{z} v dz - v(Z) \frac{\partial Z}{\partial x} + v(Z_b) \frac{\partial Z_b}{\partial x} \qquad (2\text{-}7)$$

The following boundary conditions can be defined for the general overland flow equations:

At the free surface

$$\frac{dZ}{dt} = \frac{\partial Z}{\partial t} + u(Z) \frac{\partial Z}{\partial x} + v(Z) \frac{\partial Z}{\partial y} = w(Z) + R(x, y, t) \qquad (2\text{-}8)$$

or

$$w(Z) = \frac{\partial Z}{\partial t} + u(Z)\ \frac{\partial Z}{\partial x} + v(Z)\ \frac{\partial Z}{\partial y} - R(x,y,t) \qquad (2\text{-}9)$$

where

$R(x,y,t)$ = rainfall rate (LT^{-1}).

At the bed surface :

$$\frac{dZ_b}{dt} = u(Z_b)\ \frac{\partial Z_b}{\partial x} + v(Z_b)\ \frac{\partial Z_b}{\partial y} = w(Z_b) + i(x,y,t) \qquad (2\text{-}10)$$

or

$$w(Z_b) = u(Z_b)\ \frac{\partial Z_b}{\partial x} + v(Z_b)\ \frac{\partial Z_b}{\partial y} - i(x,y,t) \qquad (2\text{-}11)$$

where

$i(x,y,t)$ = infiltration rate (LT^{-1}).

Substituting equation (2-6), (2-7), (2-9) and (2-11) into equation (2-5) yields:

$$\frac{\partial Z}{\partial t} + \frac{\partial(\bar{u}d)}{\partial x} + \frac{\partial(\bar{v}d)}{\partial y} = R(x,y,t) - i(x,y,t) \qquad (2\text{-}12)$$

where

$\bar{u}$ = mean value of u over the depth of the flow (LT^{-1}),

$\bar{v}$ = mean value of v over the depth of the flow (LT^{-1}), and

$d = Z - Z_b$ = depth of the flow measured perpendicular to the plane of the land (L).

Momentum equations:

Assuming negligible vertical acceleration, it follows:

$$\mu \nabla^2 w \approx 0 \tag{2-13}$$

and

$$\frac{Dw}{Dt} \approx 0 \tag{2-14}$$

Equation (2-14) indicates that the left-hand side of equation (2-4) is approximately zero. Therefore equation (2-4) reduces to

$$g_Z - \frac{1}{\rho}\frac{\partial P}{\partial z} = 0 \tag{2-15}$$

Integrating equation (2-15) in the z-direction yields:

$$P = \rho g_Z (z - Z) \tag{2-16}$$

where

P = gage pressure.

It follows from equation (2-16) that:

$$-\frac{1}{\rho}\frac{\partial}{\partial x} = g_z \frac{\partial Z}{\partial x} \tag{2-17}$$

$$-\frac{1}{\rho}\frac{\partial}{\partial y} = g_z \frac{\partial Z}{\partial y} \tag{2-18}$$

Multiplying equation (2-1) once by u and once by v, it follows:

$$u\frac{\partial u}{\partial x}+u\frac{\partial v}{\partial y}+u\frac{\partial w}{\partial z}=0 \tag{2-19}$$

$$v\frac{\partial u}{\partial x}+v\frac{\partial v}{\partial y}+v\frac{\partial w}{\partial z}=0 \tag{2-20}$$

Adding equation (2-19) to (2-2) and (2-20) to (2-3) and using equation (2-17) and (2-18) one acquires [Fennema, 1983; Street, 1996; Tannehill, 1997; Tayfur et al., 1993]:

$$\frac{\partial u}{\partial t}+\frac{\partial u^2}{\partial x}+\frac{\partial (uv)}{\partial y}+\frac{\partial (uw)}{\partial z}=g_x+g_z\frac{\partial Z}{\partial x}+\frac{\mu}{\rho}\nabla^2 u \tag{2-21}$$

$$\frac{\partial v}{\partial t}+\frac{\partial (uv)}{\partial x}+\frac{\partial v^2}{\partial y}+\frac{\partial (vw)}{\partial z}=g_y+g_z\frac{\partial Z}{\partial y}+\frac{\mu}{\rho}\nabla^2 v \tag{2-22}$$

Now let us integrate equations (2-21) and (2-22) in the z-direction. In order to avoid confusion, the integrals have been presented term by term.

$$\int_{Z_b}^{z}\frac{\partial u}{\partial t}dz=\frac{\partial}{\partial t}\int_{Z_b}^{z}udz-u(Z)\frac{\partial Z}{\partial t}+u(Z_b)\frac{\partial Z_b}{\partial t} \tag{2-23}$$

also

$$\int_{Z_b}^{z}udz=\bar{u}d \tag{2-24}$$

so

$$\frac{\partial}{\partial t}\int_{Z_b}^{z}udz=\frac{\partial(\bar{u}d)}{\partial t} \tag{2-25}$$

Assuming that the topography of the field does not change with time, then

$$u(Z_b)\frac{\partial Z_b}{\partial t}=0 \tag{2-26}$$

$$\int_{Z_b}^{Z}\frac{\partial u^2}{\partial x}dz=\frac{\partial}{\partial x}\int_{Z_b}^{Z}u^2dz-u^2(Z)\frac{\partial Z}{\partial x}+u^2(Z_b)\frac{\partial Z_b}{\partial x} \tag{2-27}$$

$$\int_{Z_b}^{Z}\frac{\partial uv}{\partial y}dz=\frac{\partial}{\partial y}\int_{Z_b}^{Z}uvdz-u(Z)v(Z)\frac{\partial Z}{\partial y}+u(Z_b)v(Z_b)\frac{\partial Z_b}{\partial y} \tag{2-28}$$

$$\int_{Z_b}^{Z}\frac{\partial(uw)}{\partial z}dz=u(Z)w(Z)-u(Z_b)w(Z_b) \tag{2-29}$$

Substituting equation (2-9) for w(Z) and (10) for $w(Z_b)$ in (2-29), and adding equations (2-23), (2-27), (2-28) and (2-29), based on the uniform velocity distribution assumption, the left hand side of equation (2-21) yields:

$$LHS(2-21)=\frac{\partial(\bar{u}d)}{\partial t}+\frac{\partial(\bar{u}^2d)}{\partial x}+\frac{\partial(\bar{u}\bar{v}d)}{\partial y}-\bar{u}(R(x,y,t)-i(x,y,t)) \tag{2-30}$$

Similarly the left hand side of equation (22) becomes:

$$LHS(2-22)=\frac{\partial(\bar{v}d)}{\partial t}+\frac{\partial(\bar{u}\bar{v}d)}{\partial x}+\frac{\partial(\bar{v}^2d)}{\partial y}-\bar{v}(R(x,y,t)-i(x,y,t)) \tag{2-31}$$

For the right hand side of equation (2-21) it yields:

$$\int_{Z_b}^{Z}(g_x + g_z\frac{\partial Z}{\partial x})dz = (g_x + g_z\frac{\partial d}{\partial x})d \qquad (2\text{-}32)$$

In turbulent flow, the dynamic viscosity is replaced by an eddy viscosity coefficient. Furthermore, a distinction is made between the stress acting in the x-y plane and stresses acting in the x-z and y-z planes. Considering these facts, for the shear stress term one acquires [Fennema, 1983; Street, 1996]:

$$\varepsilon_{xy}\left(\frac{\partial^2 u}{\partial x^2} + \frac{\partial^2 u}{\partial y^2}\right) + \varepsilon_{zx}\frac{\partial^2 u}{\partial z^2} \qquad (2\text{-}33)$$

where

$\varepsilon_{xy}, \varepsilon_{zx}$ = eddy viscosity ($ML^{-1}T^{-1}$).

Assuming that the bottom shear stress is the effective stress, the first term of equation (2-33) is negligible relative to the second term. So it follows:

$$\int_{Z_b}^{Z}\varepsilon_{zx}\frac{\partial^2 u}{\partial z^2}dz = \varepsilon_{zx}\left(\frac{\partial u}{\partial z}\right)_{z=Z} - \varepsilon_{zx}\left(\frac{\partial u}{\partial z}\right)_{z=Z_b} = \tau_{sx} - \tau_{bx} \qquad (2\text{-}34)$$

where

τ_{sx} = wind shear stress at the surface ($ML^{-1}T^{-1}$), and

τ_{bx} = bottom shear stress ($ML^{-1}T^{-1}$).

The wind shear stress due to wind velocity at the water surface is neglected, and the shear stress at the bottom of the channel can be evaluated using different empirical formulas. For example, the Chezy formula gives

$$\tau_b = \frac{\gamma}{C^2} V^2 \tag{2-35}$$

where

$$V = \sqrt{\bar{u}^2 + \bar{v}^2}\ (LT^{-1}) \tag{2-36}$$

C = Chezy coefficient

Equation (2-35) indicates that [Guo et al., 2000; Julien, 1995; Koboyashi, 1985; US Army Corps of Eng., 1993]

$$\tau_{bx} = \tau_b \cos\theta = \frac{\gamma}{C^2} \bar{u} V \tag{2-37}$$

$$\tau_{by} = \tau_b \sin\theta = \frac{\gamma}{C^2} \bar{v} V \tag{2-38}$$

where

θ = angle between the velocity vector and the x-axis

Assembling all the depth-integrated terms of equation (2-21) yield

$$\frac{\partial(\bar{u}d)}{\partial t} + \frac{\partial(\bar{u}^2 d)}{\partial x} + \frac{\partial(\bar{u}\bar{v}d)}{\partial y} = (g_x + g_z \frac{\partial d}{\partial x})d - \frac{g}{C^2} \bar{u}\sqrt{\bar{u}^2 + \bar{v}^2} \tag{2-39}$$

Applying the same procedure to equation (2-22) gives

$$\frac{\partial(\bar{v}d)}{\partial t} + \frac{\partial(\bar{u}\bar{v}d)}{\partial x} + \frac{\partial(\bar{v}^2 d)}{\partial y} = (g_y + g_z \frac{\partial d}{\partial y})d - \frac{g}{C^2} \bar{v}\sqrt{\bar{u}^2 + \bar{v}^2} \tag{2-40}$$

Equations (2-12), (2-39) and (2-40) can be expressed in a horizontal coordinate system $(\tilde{x},\tilde{y},\tilde{z})$. In this system, a channel may have piecewise constant bottom slope. A rotation of this type is generally accomplished using the following matrices Fennema, 1983 and 1990; Spiegle et al., 1968]:

$$\begin{pmatrix}\tilde{x}\\ \tilde{y}\\ \tilde{z}\end{pmatrix}=\begin{pmatrix}\cos\alpha_x & -\cos\varphi\cos\alpha_x/\sin\varphi & \tan\alpha_x\cos\alpha_z\\ 0 & \cos\alpha_y/\sin\varphi & \tan\alpha_y\cos\alpha_z\\ -\sin\alpha_x & -\sin\alpha_y\cos^2\alpha_x/\sin\varphi & \cos\alpha_z\end{pmatrix}=\begin{pmatrix}x\\ y\\ z\end{pmatrix} \qquad (2\text{-}41)$$

where

$$\cos\alpha_z=\frac{1}{\sqrt{1+\tan^2\alpha_x+\tan^2\alpha_y}} \qquad (2\text{-}42)$$

$$\cos\varphi=\sin\alpha_x\cos\alpha_y \qquad (2\text{-}43)$$

$$\sin\varphi=\sqrt{1-\sin^2\alpha_x\sin^2\alpha_y} \qquad (2\text{-}44)$$

Figure (2-1) shows the definition of α_x, α_y and α_z.

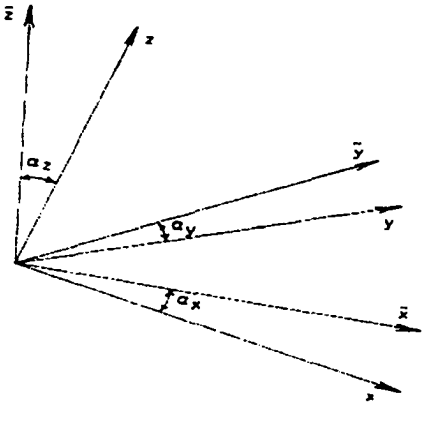

Figure 2-1. Definition of α_x, α_y and α_z [Chaudhry, 1988]

Let us assume that even though $\sin\alpha_x$ and $\sin\alpha_y$ may not be small, but their product is small. That means:

$$\sin\alpha_x \sin\alpha_y \approx \sin^2\alpha_x \approx \sin^2\alpha_y \approx 0 \qquad (2\text{-}45)$$

It follows from equation (2-45) that

$$\sin\varphi = 1 \; ; \; \cos\varphi = 0 \qquad (2\text{-}46)$$

Now it follows [Chaudhry, 1988; Spiegle et al., 1968]

$$\tilde{x} = x\cos\alpha_x + z\tan\alpha_x\cos\alpha_z \qquad (2\text{-}47)$$

$$\tilde{y} = y\cos\alpha_y + z\tan\alpha_y\cos\alpha_z \qquad (2\text{-}48)$$

The dependent variables after transformation become[Chaudhry, 1993; Fennema, 1983]

$$h = \frac{d}{\cos\alpha_z} \qquad (2\text{-}49)$$

$$\tilde{u} = \bar{u}\cos_x \qquad (2\text{-}50)$$

$$\tilde{v} = \bar{v}\cos_y \qquad (2\text{-}51)$$

where

h = flow depth measured vertically (L).

For the partial derivatives it follows [Chaudhry, 1993; Fennema, 1990]:

$$\frac{\partial}{\partial x} = \cos\alpha_x \frac{\partial}{\partial \tilde{x}} + \tan\alpha_x \cos\alpha_z \frac{\partial}{\partial \tilde{z}} \tag{2-52}$$

$$\frac{\partial}{\partial y} = \cos\alpha_y \frac{\partial}{\partial \tilde{y}} + \tan\alpha_y \cos\alpha_z \frac{\partial}{\partial \tilde{z}} \tag{2-53}$$

Since the basic idea of integrating over the depth is to eliminate the derivatives along the z-direction, the presence of $\partial/\partial z$ in equations (2-52) and (2-53) are objectionable. However, because terms like $\tan\alpha_x \cos\alpha_z(\partial/\partial z)$ are of order $\sin^2\alpha_x$, they are negligible.

Introducing the transformation to equations (2-12), (2-39) and (2-40), simplifying and noting that [Chaudhry, 1993]

$$g_x = g\sin\alpha_x \tag{2-54}$$

$$g_y = g\frac{\sin\alpha_y \cos^2\alpha_x}{\sin\varphi} \tag{2-55}$$

$$g_z = -g\cos\alpha_z \tag{2-56}$$

and dropping the ~ symbol, one acquires [Mays, 1996; Sladkevich, 2000; Zhang, 1989]:

$$\frac{\partial h}{\partial t} + \frac{\partial (ud)}{\partial x} + \frac{\partial (vd)}{\partial y} = R(x,y,t) - i(x,y,t) \tag{2-57}$$

$$\frac{\partial (uh)}{\partial t} + \frac{\partial (u^2 h)}{\partial x} + \frac{\partial (uvh)}{\partial y} = gh\left[\cos\alpha_x S_{0x} - (\cos\alpha_x \cos\alpha_z)^2 \frac{\partial h}{\partial x} - S_{fx}\right] \tag{2-58}$$

$$\frac{\partial(vh)}{\partial t}+\frac{\partial(uvh)}{\partial x}+\frac{\partial(v^2h)}{\partial y}=gh\left[\cos\alpha_y S_{0y}-(\cos\alpha_y\cos\alpha_z)^2\frac{\partial h}{\partial y}-S_{fy}\right] \quad (2\text{-}59)$$

where

$$S_{0x}=\sin\alpha_x \quad (2\text{-}60)$$

$$S_{0y}=\sin\alpha_y \quad (2\text{-}61)$$

$$S_{fx}=\frac{u\sqrt{u^2+v^2}}{C^2\cos\alpha_z h} \quad (2\text{-}62)$$

$$S_{fy}=\frac{v\sqrt{u^2+v^2}}{C^2\cos\alpha_z h} \quad (2\text{-}63)$$

If Manning equation is used to compute the friction terms, then

$$S_{fx}=\frac{n^2u\sqrt{u^2+v^2}}{C_0{}^2h^{1.33}} \quad (2\text{-}64)$$

$$S_{fy}=\frac{n^2v\sqrt{u^2+v^2}}{C_0{}^2h^{1.33}} \quad (2\text{-}65)$$

where

n = Manning coefficient, and

C_0 = 1.49 in customary units, 1 in SI units

Equations (2-57), (2-58) and (2-59) can also be written in the following form [Fennema, 1983]

$$U_t + E_x + F_y + S = 0 \quad (2\text{-}66)$$

where

$$U = \begin{pmatrix} h \\ uh \\ vh \end{pmatrix} \tag{2-67}$$

$$E = \begin{pmatrix} uh \\ u^2h + \frac{1}{2}(\cos\alpha_x \cos\alpha_z)^2 gh^2 \\ uvh \end{pmatrix} \tag{2-68}$$

$$F = \begin{pmatrix} vh \\ uvh \\ v^2h + \frac{1}{2}(\cos\alpha_y \cos\alpha_z)^2 gh^2 \end{pmatrix} \tag{2-69}$$

$$S = \begin{pmatrix} -(R(x,y,t) - i(x,y,t)) \\ -gh(\cos\alpha_x S_{0x} - S_{fx}) \\ -gh(\cos\alpha_y S_{0y} - S_{fy}) \end{pmatrix} \tag{2-70}$$

uh = momenta convected in the x-direction

vh = momenta convected in the y-direction.

CHAPTER 3

SEDIMENT TRANSPORT

3.1 Introduction

When the hydrodynamic forces exerted on the sediment particles surpass their threshold for beginning of motion, coarse particles move in contact with the bed surface. Finer particles are brought into suspension when turbulent velocity fluctuations are adequately large to sustain the particles within the mass of fluid without intermittent bed contact [Khanbilvardi et al., 1984; Yang, 1996].

In the framework of the present study, transport of coarse particles is of no importance. Overland flows are mostly known to cause sediment transport in the suspension mode, because the flow is not hydraulically forceful enough to move coarse particles.

Laboratory experiments to predict sediment transport are generally very expensive and time consuming. Hence, there is an imperative need for mathematical models capable of predicting sediment transport. In recent years many numerical models have been developed to estimate the sediment transport rate or sediment redistribution. One-dimensional models include those developed by Witkowska (1974), Thomas and Prasuhn (1977), the

Hydrologic Engineering Center (1977,1993), Han and He (1987), Bhallamudi and Chaudhry (1991). One-dimensional models are not sufficiently mature. Many key aspects of the real phenomena are neglected, which affect the accuracy of the results.

In spit of immaturity of model development, researchers still apply their efforts to extend the existing models to improve the outcomes. They utilized the same concepts and worked on multi-dimensional problems. Two-dimensional models have been developed by Lin and Shen (1984), Rijn (1986), Celik and Rodi (1988), Rijn et al (1990). A quasi-two-dimensional simulation of scour and deposition was developed by Hong-Yuan et al (1997). A two-dimensional, vertically averaged sediment transport model was introduced by Roig,Donnell, Thomas, McAnally and Adamec (1996). Quing-Chao and Jin proposed a sediment transport model using depth-averaged and momentum equations (1999). Weiming, Rodi and Wenka developed a 3-dimensional numerical model for flow and sediment transport in open channels (2000).

3.2 Theoretical Basis and Governing Equations

The equation governing the conservation of mass can be applied to a small cubic control volume to derive the sediment continuity relationship

[Julien, 1995]. The rate of change of mass of sediment per unit volume of water $\partial m/\partial t$, is equal the difference of mass fluxes across the control volume faces. In general we have:

$$\frac{\partial m}{\partial t}+\frac{\partial \hat{q}_x}{\partial x}+\frac{\partial \hat{q}_y}{\partial y}+\frac{\partial \hat{q}_z}{\partial z}=0 \qquad (3\text{-}1)$$

where

m = spatial-averaged sediment concentration inside the control volume (ML^{-3}),

$\hat{q}_x, \hat{q}_y, \hat{q}_z$ = mass fluxes of sediment through the faces of control volume ($ML^{-2}T^{-1}$).

To avoid misinterpretation, the term concentration is replaced by the most common unit for sediment concentration, which is the ratio of the mass of sediment to the volume of water-sediment mixture. Other units include the ratio of the volume of sediment to total volume or the ratio of the sediment weight to total weight. The mathematical relations are as followings [Julien, 1995]:

$$m_v=\frac{\text{sediment volume}}{\text{total volume}}=\frac{\forall_s}{\forall_t}=1-p_0 \qquad (3\text{-}2)$$

$$m_w=\frac{\text{sediment weight}}{\text{total weight}}=\frac{C_v G}{1+(G-1)C_v} \qquad (3\text{-}3)$$

where

P_0 = porosity, and

G = specific gravity $\approx$ 2.65 g/cm^3 in average.

Also

$m_{ppm} = 10^6 m_w$, and

$m_{mg/l} = 10^6 G m_v$

Sediment concentration varies in time and space. Therefore different average values can be considered [Julien, 1995]:

1 - Time - averaged concentration $\overline{m}_{ts} = \frac{1}{t_s}\int_t^{t+t_s} m dt$

2 - Spatial - averaged concentration $\overline{m}_{\forall} = \frac{1}{\forall}\int_{\forall} m d\forall$

3 - flux - averaged concentration (in 1 - D) $\overline{m}_f = \frac{1}{Q}\int_A mud A$

where

Q = flow rate (L^3T^{-1})

u = velocity in the x direction (LT^{-1}).

The resulting sediment concentration m from equation (3-1) is a spatially-averaged concentration inside our control volume. In this present research, the distribution of sediment inside the control volume is assumed to be uniform. Therefore the spatially-averaged sediment concentration suits the assumption. We drop the subscript and superscript from the spatially-averaged concentration and use just the symbol m through out this research.

By expanding equation (3-1), one can realize three different types of mass fluxes across each face:

1- advective fluxes,

2- diffusive fluxes, and

3- mixing fluxes.

Mathematically we can express the above terms as [Yang, 1996]:

$$\hat{q}_x = um - (D_x + \varepsilon_x)\frac{\partial m}{\partial x} \tag{3-4}$$

$$\hat{q}_y = vm - (D_y + \varepsilon_y)\frac{\partial m}{\partial y} \tag{3-5}$$

$$\hat{q}_z = \underbrace{wm}_{\text{advective fluxes}} - \underbrace{(D_z + \varepsilon_z)\frac{\partial m}{\partial z}}_{\text{diffusive and mixing fluxes}} - \underbrace{\omega m}_{\text{settling flux}} \tag{3-6}$$

where

u, v, w = flow velocity in x, y and z direction respectively (LT^{-1}),

ω = particle fall velocity (LT^{-1}),

$D_{x,y,z}$ = molecular diffusion coefficient in x, y and z direction respectively (L^2T^{-1}),

$\varepsilon_{x,y,z}$ = turbulent mixing coefficient in x, y and z direction (L^2T^{-1}).

The transport of sediments imparted by velocity currents is described by advective fluxes. The rate of mass transport per unit area conveyed by advection is acquired from the product of sediment concentration and velocity components. Molecular diffusion refers to the scattering of sediment particles by random molecular motion, as described by Fick's law. Turbulent mixing or turbulent diffusion induces the scattering of sediment particles due to turbulent fluid motion [Van rijn, 1994; Wu et al., 2000; Zhang et al., 1987]. In turbulent flow ε the turbulent mixing coefficient is several orders of magnitude greater than D molecular diffusion coefficient.

The general mathematical form describing the conservation of mass for dilute incompressible sediment suspension subject to mixing, diffusion and advection (constant D, ε_x, ε_y, ε_z) is obtained after substituting equations (3-4), (3-5) and (3-6) into (3-1) [Guo et al., 2000; Roig et al., 1996; Rose, 1985]

$$\frac{\partial m}{\partial t}+\frac{\partial um}{\partial x}+\frac{\partial vm}{\partial y}+\frac{\partial wm}{\partial z}=\frac{\partial \omega m}{\partial z}+(D+\varepsilon_x)\frac{\partial^2 m}{\partial x^2}+(D+\varepsilon_y)\frac{\partial^2 m}{\partial y^2}(D+\varepsilon_z)\frac{\partial^2 m}{\partial z^2} \tag{3-7}$$

As mentioned before, in turbulent flows, molecular diffusion coefficient D, is negligible compared to ε and it vanishes. In this research, the deriving force behind the sediment transport is the overland flow, which

is a turbulent sheet flow over the soil surface. This fact indicates that the only mechanism inducing diffusion is turbulent mixing mechanism. Equation (3-7) reduces to [Alanson, 1981; Ariaturai et al., 1976]:

$$\frac{\partial m}{\partial t}+\underbrace{\frac{\partial um}{\partial x}+\frac{\partial vm}{\partial y}+\frac{\partial wm}{\partial z}}_{\text{advective terms}}=\underbrace{\frac{\partial \omega m}{\partial z}}_{\text{settlingterm}}+\underbrace{\varepsilon_x\frac{\partial^2 m}{\partial x^2}+\varepsilon_y\frac{\partial^2 m}{\partial y^2}+\varepsilon_z\frac{\partial^2 m}{\partial z^2}}_{\text{turbulent mixing terms}} \quad (3\text{-}8)$$

A two-dimensional depth-averaged sediment transport equation can be obtained by integrating equation (3-8) in the z-direction. To avoid confusion the integration has been performed term by term. Using the Leibnitz rule it follows:

$$\int_{Z_b}^{z}\frac{\partial m}{\partial t}dz=\frac{\partial}{\partial t}\int_{Z_b}^{z}mdz+m(Z_b)\frac{\partial Z_b}{\partial t}+m(Z)\frac{\partial Z}{\partial t}=\frac{\partial(\overline{mh})}{\partial t}+m(Z)\frac{\partial(Z)}{\partial t} \quad (3\text{-}9)$$

$$\int_{Z_b}^{z}\frac{\partial(um)}{\partial x}dz=\frac{\partial}{\partial x}\int_{Z_b}^{z}(um)dz+u(Z_b)m(Z_b)\frac{\partial Z_b}{\partial x}-u(z)m(z)\frac{\partial Z}{\partial x}$$

$$=\frac{\partial(\overline{umh})}{\partial x}+u(Z_b)m(Z_b)\frac{\partial Z_b}{\partial x}-u(z)m(z)\frac{\partial Z}{\partial x} \quad (3\text{-}10)$$

similarly

$$\int_{Z_b}^{z}\frac{\partial(vm)}{\partial y}dz=\frac{\partial(\overline{vmh})}{\partial y}+v(Z_b)m(Z_b)\frac{\partial Z_b}{\partial y}-v(z)m(z)\frac{\partial Z}{\partial y} \quad (3\text{-}11)$$

$$\int_{Z_b}^{z}\frac{\partial(wm)}{\partial z}dz=w(Z)m(Z)-w(Z_b)m(Z_b) \quad (3\text{-}12)$$

$$\int_{Z_b}^{z} \frac{\partial(\omega m)}{\partial z} dz = \omega(Z)m(Z) - \omega(Z_b)m(Z_b) \qquad (3\text{-}13)$$

$$\int_{Z_b}^{z} \varepsilon_x \frac{\partial^2 m}{\partial x^2} dz = \varepsilon_x \frac{\partial}{\partial x}\int_{Z_b}^{z} \frac{\partial m}{\partial x} dz + (\varepsilon_x \frac{\partial m}{\partial x}\Big|_{Z_b}) \frac{\partial Z_b}{\partial x} - (\varepsilon_x \frac{\partial m}{\partial x}\Big|_{Z}) \frac{\partial Z}{\partial x}$$

$$= \varepsilon_x \frac{\partial^2 (h\bar{m})}{\partial x^2} + \varepsilon_x m(Z_b) \frac{\partial Z_b}{\partial x} - \varepsilon_x m(Z) \frac{\partial Z}{\partial x} + (\varepsilon_x \frac{\partial m}{\partial x}\Big|_{Z_b}) \frac{\partial Z_b}{\partial x}$$

$$- (\varepsilon_x \frac{\partial m}{\partial x}\Big|_{Z}) \frac{\partial Z}{\partial x}$$

(3-14)

$$\int_{Z_b}^{z} \varepsilon_y \frac{\partial^2 m}{\partial y^2} dz = \varepsilon_y \frac{\partial}{\partial y}\int_{Z_b}^{z} \frac{\partial m}{\partial y} dz + (\varepsilon_y \frac{\partial m}{\partial y}\Big|_{Z_b}) \frac{\partial Z_b}{\partial y} - (\varepsilon_y \frac{\partial m}{\partial y}\Big|_{Z}) \frac{\partial Z}{\partial y}$$

$$= \varepsilon_y \frac{\partial^2 (h\bar{m})}{\partial y^2} + \varepsilon_y m(Z_b) \frac{\partial Z_b}{\partial y} - \varepsilon_y m(Z) \frac{\partial Z}{\partial y} + (\varepsilon_y \frac{\partial m}{\partial y}\Big|_{Z_b}) \frac{\partial Z_b}{\partial y}$$

$$- (\varepsilon_y \frac{\partial m}{\partial y}\Big|_{Z}) \frac{\partial Z}{\partial y}$$

(3-15)

$$\int_{Z_b}^{z} \varepsilon_z \frac{\partial^2 m}{\partial z^2} dz = (\varepsilon_z \frac{\partial m}{\partial z}\Big|_{Z}) - (\varepsilon_z \frac{\partial m}{\partial z}\Big|_{Z_b}) \qquad (3\text{-}16)$$

On the other hand [Fetter, 1993]

$$\overline{um} \approx \bar{u}\,\bar{m} \tag{3-17}$$

$$\overline{vm} \approx \bar{v}\,\bar{m} \tag{3-18}$$

Equation (3-8) takes the form of

$$\frac{\partial(h\bar{m})}{\partial t} + \frac{\partial(h\bar{u}\,\bar{m})}{\partial x} + \frac{\partial(h\bar{v}\,\bar{m})}{\partial y} = \varepsilon_x^* \frac{\partial^2(h\bar{m})}{\partial x^2} + \varepsilon_y^* \frac{\partial^2(h\bar{m})}{\partial y^2} + q(x,y,t) \tag{3-19}$$

where

$q(x,y,t)$ = source and sink term ($ML^{-2}T^{-1}$), and

$\varepsilon^*_{x,y}$ = effective turbulent mixing coefficient in x and y direction

respectively (L^2T^{-1}).

All the additional terms in equations (3-9) through (3-18) contribute to the diffusion process. Therefore a new effective turbulent mixing coefficient has been introduced. The source and sink term quantifies the net erosion and deposition. Mathematically q(x,y,t) can be expressed as follows [Nicholson, 1984]:

$$q(x,y,t) = \begin{cases} -r\omega m & : \quad \tau \prec \tau_D \\ -\omega m & : \quad \tau_D \le \tau \prec \tau_E \\ \dfrac{\partial M}{\partial t} - \omega m & : \quad \tau \ge \tau_E \end{cases} \tag{3-20}$$

where

$$r = \begin{cases} \frac{\tau}{\tau_D} & : \tau \prec \tau_D \\ 1 & : \tau \geq \tau_D \end{cases} \tag{3-21}$$

$$\frac{\partial M}{\partial t} = \begin{cases} E(\frac{\tau}{\tau_E} - 1.0) & : \tau \geq \tau_E \\ 0 & : \tau \prec \tau_E \end{cases} \tag{3-22}$$

τ = bed shear stress = $\rho_w(u^*)^2$ ($ML^{-1}T^{-2}$) [Roig et al., 1996],

ρ_w = water density (ML^{-3}),

u^* = bed shear velocity = $\frac{\sqrt{g}\left[\sqrt{(u^2+v^2)}\right]n}{\sqrt{C_0}h^{(1/6)}}$ (LT^{-1}) [US Army Corps of Eng., 1993], (3-23)

C_0=1.49 in BI units, 1.0 in SI units,

n = manning coefficient,

τ_E = limiting shear stress for erosion ($ML^{-1}T^{-2}$),

τ_D = limiting shear stress for deposition ($ML^{-1}T^{-2}$),

E = erosion constant ($ML^{-2}T^{-1}$).

CHAPTER 4

CONTAMINANT TRANSPORT MODEL

4.1 Introduction

Radionuclides (or radioactive substances) are the result of nuclear weapon development and test, energy generation and some industrial application. Some radionuclides occur naturally and have useful applications in science, medicine and technology. Radionuclides are similar to organic pollutants in that they sorb to particulate matter. However, they are different in two rudimentary ways:

1- The radionuclides listed in Table 4-1 do not volatilize [Chapra, 1997].

2- They decompose by a simple first-order decay function. They are not subject to the variety of decomposition mechanism, such as photolysis, biodegradation, etc. that act to break down organic compounds [Chapra, 1997].

Radioactive concentration units are measured in radioactivity units (Ci curi or Bq becquerel) rather than in mass units. One curi corresponds to the disintegration of 3.7e+10 atoms per second. It is approximately equal to the decay rate of 1 g of radium. 3.7e10 becquerel are equivalent to a Ci.

Table 4-1. Listing of some radionuclides of interest in water-quality modeling [Chapra, 1997]

Radionuclides	
Name	**Symbol**
Cesium-137	^{137}Cs
Strantium-90	^{90}Sr
Plutonium-239,240	$^{239,240}Pu$
Lead-210	^{210}Pb

4.2 Overview

The local and instantaneous equilibrium assumptions were used to develop a mechanistic framework to describe the transfer of radionuclides on soil surface. The local equilibrium assumption leads to solid-liquid partitioning concept. The main reason for solid-liquid partitioning is to depict a more mechanistically tangible characterization of the radionuclides mass balance. Especially it is known that several important mechanisms act selectively on one or the other of two forms. For example erosion acts solely on the particulate form of contaminant on the soil surface or diffusion acts only on the dissolved form of the contaminant

Using the above-mentioned assumptions, the total radioactive contaminant is separated into two separate components; dissolved component and particulate or absorbed component. These components are assumed to represent fixed fractions of the total concentration.

The following framework, Figure 4-1, is suggested for the transport of radionuclide by overland flow [Khanbilvardi et al., 2000; Nair et al., 1996]:

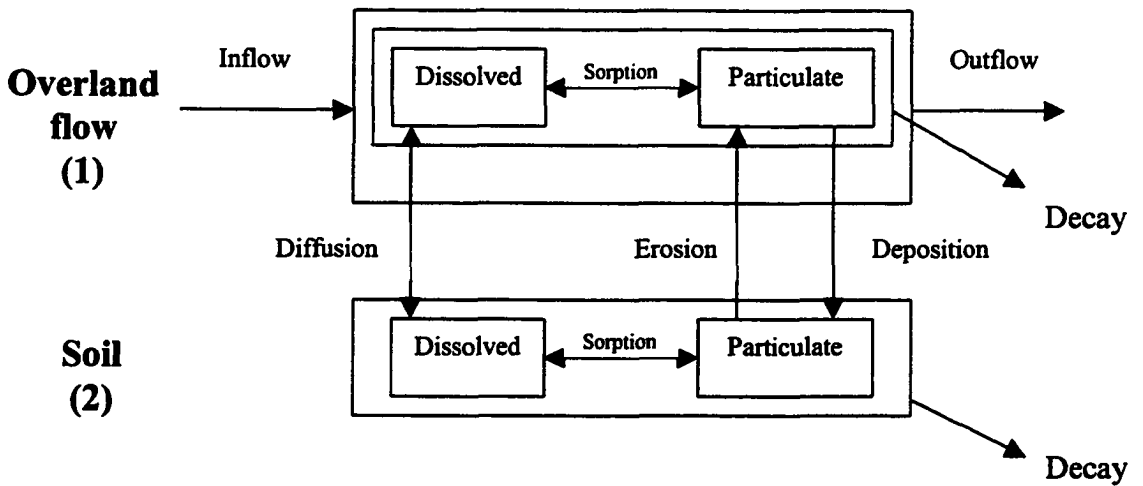

Figure 4-1. Schematic for the suggested framework

4.3 Theory and Formulation

4.3.1 Sorption

Sorption is a process, whereby a dissolved substance is transferred to and becomes associated with solid material [Wallach et al., 1992]. The sorbed substance is called sorbate and the solid is called sorbent. Sorption includes absorption, adsorption, chemisorption and ion exchange. Absorption occurs, when the sorbent (in this case soil grain) is porous so that the solute can diffuse into the particle and be sorbed onto interior surfaces.

Adsorption includes the processes by which the solute clings to sorbent. Chemisorption occurs, when the solute is incorporated on sorbent by a chemical reaction. Ion exchange is caused by positively and negatively charged sites on the sorbent and the sorbate [Fetter, 1997]. In this research there will be no attempt to separate these phenomena. Here the term sorption will simply indicate the overall result of the various processes.

The ability of a soil to adsorb a solute from a certain solution can be determined by batch test. A known mass of the soil is mixed and allowed to equilibrate with a solution containing a known concentration of the sorbate of interest. The soil is then separated from the solution. The concentration of the sorbate is then measured. The difference between the initial concentration and the concentration after the test is the amount of that was adsorbed by the soil. During the test soil samples can be taken from the mixture. The samples can be separated by centrifuge. The concentration of sorbate as well as concentration of solution can be measured. The sampling is repeated for different concentrations and the results plotted. Figure 4.2 shows a graph of this type, which are called isotherms.

Numerous different models have been proposed to mathematically represent the isotherms. The two most common are:

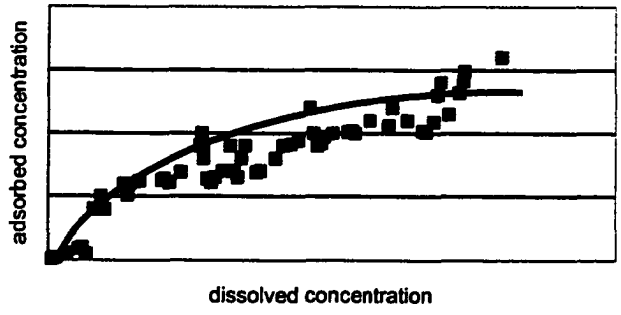

Figure 4.2 Sorption data (isotherm)

1-*Freundlich sorption isotherm:*

This isotherm is defined by a nonlinear relationship

$$C_{sorbed} = KC_d^N \qquad (4\text{-}1)$$

where

C_{sorbed} = mass of solute sorbed per dry unit weight of solid

K and N = constants

C_d = concentration of solute in solution (dissolved concentration)

The most important shortcoming of this isotherm model is the fact that theoretically there is no upper limit for the sorption.

2-*Longmuir sorption isotherm:*

This isotherm model was developed with the concept that a sorbent possesses a limited number of sorption sites. When all the sites are occupied the sorbent will no longer sorb solute from the solution.

$$C_{sorbed} = \frac{(C_{sorbed})_{max} \beta C_d}{1 + \beta C_d} \qquad (4\text{-}2)$$

where

β = a coefficient used to fit the data

When $C_{sorbed} << (C_{sorbed})_{max}$ plenty of sites are available on the sorbent and equation (4-2) becomes a linear relation (Figure 4.3)

$$C_{sorbed} = K_d C_d \qquad (4\text{-}3)$$

where

K_d = a partition coeffiecient

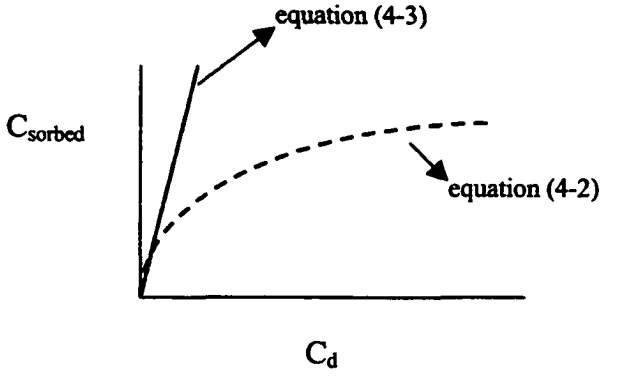

Figure 4.3 Langmuir isotherm

The latter case implies that if the dissolved concentration is decreased or increased a certain proportion, the solid concentration will display the same proportional decrease or increase.

4.3.2 Dissolved Fraction and Particulate Fraction

Fast sorption kinetics assumption leads us to the local equilibrium concept. Using the local equilibrium concept we can basically separate the total contamination into the dissolved form and particulate form. For example, when soil is contaminated by a certain organic chemical the contaminant is sorbed onto the soil grains. When the soil becomes saturated and all the pore spaces are occupied with water then only a fraction of the contaminant will remain on the soil particles. The rest will be held by water. The fraction on the soil particles is the particulate or sorbed fraction and the fraction in water is the dissolved fraction. The sum of these two is the total soil contamination. The same concept can be used to define the same fractions for surface water, which is containing and transporting contaminated suspended sediment and fine soil particles. After the contaminated soil particles enter the water a portion of the contamination will be held only in water in dissolved form. The rest will remain on the soil

particle, which is the particulate fraction. The sum of these two is the total contamination in water.

Using the above framework for the surface water transporting suspended solids, it follows [Chapra, 1997]:

$$C_w = C_{pw} + C_{dw} \tag{4-4}$$

$$C_{pw} = m\, C_{sorbed} \tag{4-5}$$

where

C_w = total contaminant concentration in water

C_{pw} = particulate concentration in water

m = suspended solid concentration in water

Using equation (4-3) in (4-5) and substituting the result in equation (4-4) one obtains:

$$C_w = C_{dw} + m\, K_{dw}\, C_{dw} \tag{4-6}$$

where

K_{dw} = partition coefficient in water.

The dissolved fraction in water is defined as

By combining (4-6) and (4-7) it yields:

$$F_{dw} = \frac{C_{dw}}{C_w} \tag{4-7}$$

$$F_{dw} = \frac{1}{1 + K_{dw} m} \tag{4-8}$$

Equation (4-4) indicates that the sum of these two fractions is one. So it follows:

$$F_{pw} = 1 - F_{dw} \tag{4-9}$$

or

$$F_{pw} = \frac{K_{dw} m}{1 + K_{dw} m} \tag{4-10}$$

The same technique can be implemented to derive these fractions for soil or any porous media. The dissolved concentration in soil can be defined as:

$$C_{ds} = \phi C_{dp} \tag{4-11}$$

where

C_{ds} = dissolved concentration in soil

ϕ = porosity

C_{dp} = dissolved concentration in pore water.

The particulate concentration is defined as:

$$C_{ps} = (1 - \phi)\rho C_{sorbed} \tag{4-12}$$

and

$$C_{sorbed} = K_{ds} C_{dp} \tag{4-13}$$

where

K_{ds} = partition coefficient in soil.

Equation (4-4) can also be written for soil. It yields:

$$C_s = C_{ps} + C_{ds} \tag{4-14}$$

where

C_s = total concentration in soil.

Substituting equation (4-13) into (4-12) and then (4-12) and (4-11) into (4-14) it follows:

$$C_s = (1- \phi)\rho\, C_{sorbed} + \phi\, C_{dp} \tag{4-15}$$

where

ρ = soil density.

The dissolved fraction in soil is defined as:

$$F_{ds} = \frac{C_{ds}}{C_s} \tag{4-16}$$

$$F_{ds} = \frac{1}{\varphi + \varrho K_{ds}(1-\varphi)} \tag{4-17}$$

Substituting (4-15) into (4-16) one obtains:

Similarly

$$F_{ps} = 1- F_{ds} \tag{4-18}$$

where

F_{ps} = the particulate fraction in soil.

4.3.3 Diffusion

A solute in water will move from an area of greater concentration to an area of lower concentration. This process is called molecular diffusion or just diffusion. Diffusion occurs as long as a concentration gradient exists, even if there is no flow [Fetter, 1993]. Molecular diffusion results from the random Brownian motion of water molecules. A similar kind of random motion occurs on a large scale due to eddies and is called turbulent diffusion. Both turbulent and molecular diffusion have a tendency to minimize the concentration gradient [Armstrong et al., 1967].

In 1855 the physiologist Adolf Fick proposed the following model of diffusion [Chapra, 1997]:

$$J_s = -D\frac{\partial c}{\partial s} \qquad (4\text{-}19)$$

where

J_s = mass flux of solute per unit area per unit time in s direction (s is an arbitrary axis)

D = a diffusion coefficient

c = solute concentration

The minus sign indicates that the concentration moves from the higher concentration to the lower concentration. This model is known as Fick's first law. The diffusion coefficient D is a parameter, which quantifies the rate of diffusion.

As it can be seen in figure (4-1) the diffusive mass transfer takes place only between the dissolved fraction of the total contamination in water and the dissolved fraction of total contamination in soil. A mass balance for water in figure (4-1) can be written as:

$$\left(\frac{\partial(AhC_w)}{\partial t}\right)_{diffusion} = AJ \qquad (4\text{-}20)$$

where

A = cross-sectional area of the interface between soil and water

h = water depth (flow depth).

A finite difference approximation can be used to estimate the derivative at the interface between the soil and water. Initially it is assumed that the water is clear (rain water) and the dissolved concentration in water is less than the dissolved concentration in soil. It follows:

$$J = -D\frac{\partial C}{\partial s} \approx D\frac{C_{ds} - C_{dw}}{l} = \frac{D}{l}(C_{ds} - C_{dw}) = v_d(C_{ds} - C_{dw}) \qquad (4\text{-}21)$$

where

l = mixing length, which is the length over which the diffusive mixing takes place

v_d = diffusive mixing velocity

Substituting equation (4-21) in (4-20) and canceling out the cross-sectional area we get:

$$\left(\frac{\partial(hC_w)}{\partial t}\right)_{diffusion} = v_d(C_{ds} - C_{dw}) = v_d(F_{ds}C_s - F_{dw}C_w) \qquad (4\text{-}22)$$

4.3.4 Transport Equation

Using a simple mass balance and integrating the resulting equation over the flow depth the same equation as equation (3-19) can be obtained for the contaminant transport in water:

$$\frac{\partial(C_w h)}{\partial t} + \frac{\partial(vhC_w)}{\partial x} + \frac{\partial(uhC_w)}{\partial y} = \frac{\partial}{\partial x}\left(\varepsilon_x h \frac{\partial C_w}{\partial x}\right) + \frac{\partial}{\partial y}\left(\varepsilon_y h \frac{\partial C_w}{\partial y}\right) + qc(x,y,t) + \varphi(x,y,t) \qquad (4\text{-}23)$$

$$qc(x,y,t) = (q(x,y,t)/\rho s) * Fps * Cs \qquad (4\text{-}24)$$

$$\varphi(x,y,t) = -\lambda h C_w + V_d(F_{ds}C_s - F_{dw}C_w) \qquad (4\text{-}25)$$

where

C_w = total contaminant concentration in water (BqL^{-3})

C_s = total contaminant concentration in soil surface (BqL^{-3})

C_{abs} = concentration of contaminant on soil grains (BqL^{-3})

λ = first order decay rate (T^{-1})

V_d = diffusive mixing velocity (LT^{-1})

The change of the soil-water interface contaminant concentration can be written as:

$$\frac{\partial(C_s)}{\partial t} = \frac{-(qc(x,y,t)+\varphi(x,y,t))}{h(x,y,t)} \qquad (4\text{-}26)$$

CHAPTER 5

AN ANALYTICAL SOLUTION FOR THE FLOW MODEL AND THE FLOW MODEL'S ACCURACY

5.1 Introduction

There is no analytical solution available for the 2D-depth averaged overland flow equations. In order to obtain an analytical solution first the problem must be reduced to a one-dimensional one. By doing so one of the velocity components (velocity in the x-direction or velocity in the y-direction) is eliminated. Once the model is one-dimensional some assumptions are made to simplify the problem. After these two steps, an analytical solution is obtainable by imposing a sin transformation on the spatial derivative of the equations.

5.2 Solution Procedure

The one-dimensional shallow water equations (or the Saint Venant equations) are frequently used as the mathematical representation of flows on planar land segments. They are comprised of the continuity and momentum equations as:

$$\frac{\partial y}{\partial t}+\frac{\partial (Vy)}{\partial x}=R(x,t)-i(x,t)=N(x,t) \qquad 0<x<L\ ,t>0 \qquad (5\text{-}1)$$

$$S_f=S_0-\frac{\partial y}{\partial x}-\frac{V}{g}\frac{\partial V}{\partial x}-\frac{1}{g}\frac{\partial V}{\partial t}-\frac{NV}{gy} \qquad (5\text{-}2)$$

where

$y(x,t)$ = overland flow depth

$V(x,t)$ = depth-averaged flow velocity

L = length of the hillslope

S_0 = slope of the land

$N(x,t)$ = net lateral inflow into the overland flow section (rainfall – infiltration)

S_f = slope of the total energy line

g = gravitational acceleration

S_f is related to the flow depth and velocity through a friction relationship like Chezy equation. According to Chezy law:

$$V(x,t)=C\sqrt{y(x,t)S_f(x,t)} \qquad (5\text{-}3)$$

where

C = Chezy coefficient

The problem has been reduced to a one-dimensional problem but still there is no known analytical solution to solve the full 1D Saint Venant

equations. Thus, certain simplifications must be applied. One such simplification is obtained by neglecting all but first two terms on the right – hand side of equation (5-2) leading to

$$S_f = S_0 - \frac{\partial y}{\partial x} \qquad (5\text{-}4)$$

Combining equations (5-1), (5-3) and (5-4) leads to the diffusion wave approximation

$$\frac{\partial y}{\partial t} = \frac{\partial}{\partial x}(Cy^{3/2}(S_0 - \frac{\partial y}{\partial x})^{1/2}) = N(x,t) \qquad (5\text{-}5)$$

Govindaraju et al (1990) used a sine transformation for the spatial part of the solution to obtain analytical expressions for the overland flow and discharges. The choice of this spatial representation of the flow was not arbitrary. It was observed by Govindaraju et al. that the sine functions are the eigenfunctions of the corresponding homogenous problem while utilizing the diffusion wave approximation for overland flows. We shall use their analysis in this study. The depth of the overland flow profile may be approximately expressed as:

$$y(x,t) = h(t)\sin(\frac{\pi x}{2L}) \qquad (5\text{-}6)$$

where

h(t) = flow depth at the downstream end

The flow discharge at any space and time point is the product of the flow depth and depth averaged velocity, and is given as

$$q(x,t) = Ch^{2/3}\sin^{3/2}(\frac{\pi x}{2L})\,(S_0 - h\frac{\pi}{2L}\cos(\frac{\pi x}{2L}))^{1/2} \qquad (5\text{-}7)$$

The initial and boundary conditions, which are applicable here, are:

$$y(x,0) = 0 \qquad 0 \le x \le L \qquad (5\text{-}8)$$

$$y(0,t) = 0 \qquad (5\text{-}9)$$

$$\frac{\partial y(L,t)}{\partial x} = 0 \qquad (5\text{-}10)$$

Equation (5-6) constitutes an approximation to the true solution and in general, is different from it. Substituting equation (5-6) in to (5-5) and integrating over the spatial domain, results in the following ordinary differential equation for the flow depth at the downstream end:

$$\frac{dh}{dt} + \frac{\pi}{2L}CS_0^{1/2}h^{3/2} - g(t) = 0 \qquad (5\text{-}11)$$

where

$$g(t) = \frac{\pi}{2L}\int_0^L N(x,t)dx \qquad (5\text{-}12)$$

= spatially averaged net lateral inflow

It is reasonable to assume that there is no spatial variation of rainfall over the scale of a single hillslope. Equation (5-11) thus uses an average spatial infiltration. If the soil surface is fairly impervious, then there is no

approximation in using the representation in equation (5-10). If the soil is pervious, one first needs to calculate the infiltration to estimate N(x,t) as a function of rainfall and infiltration; g(t) is then estimated by equation (5-12). However, g(t) is a time-dependent function. This function may be approximated to any degree of accuracy by discretizing it into a series of piecewise constants. Let us say that this value is g_r over the time interval $(\tau,\tau+\Delta\tau)$. The solution to equation (5-11) is then obtained as [Govindaraju et al (1990)]:

$$\frac{1}{6a}\log\left[\frac{u^2-au+a^2}{(u+a)^2}\right]+\frac{1}{a\sqrt{3}}\tan^{-1}\left(\frac{2u-a}{a\sqrt{3}}\right)-k=\frac{}{4L}C\sqrt{S_0(\tau\ -t)} \tag{5-13}$$

where

$$k=\frac{1}{6a}\log\left[\frac{u_\tau^{\,2}-au_\tau+a^2}{(u_\tau+a)^2}\right]+\frac{1}{a\sqrt{3}}\tan^{-1}\left(\frac{2u_\tau-a}{a\sqrt{3}}\right) \tag{5-14}$$

$$a=-\left[\frac{2g_\tau\ L}{\pi C\sqrt{S_0}}\right]^{1/3} \tag{5-15}$$

$$u=u(t)=\sqrt{h(t)} \tag{5-16}$$

The solution in equations (5-13) and (5-14) are applicable over the time interval $(\tau,\tau+\Delta\tau)$. After the rain stops (and assuming that there is no infiltration), there is no net lateral inflow contribution to overland flow. The

solution to equation (5-11) for the receding part of the hydrograph is then given as [Govindaraju et al (1990)]

$$h(t) = \left(\frac{4Lu_r}{4L - u_r C\sqrt{S_0}(t_r - t)} \right)^2 \qquad (5\text{-}17)$$

where

t_r = duration of rainfall

$u_r = \sqrt{h(t_r)}$

It is important to realize that although this is an analytical solution but it is based on a "sin" transformation, which is an approximation of the true solution.

The performance of the analytical solution was compared to the data obtained from an experiment conducted by Singer and Walker (1983). The experimental set-up consisted of a laboratory flume 0.55 m by 3.0 m. Water was supplied through a rain simulator, overland flow or a combination of both. During each experiment the slope was set at 9% and the duration of each run was 30 minutes. In these experiments, approximately 20% of the simulated rainwater seemed to have infiltrated. The agreement between the experimental results and the analytical solution is presented in Figure 5-1 is reasonably good.

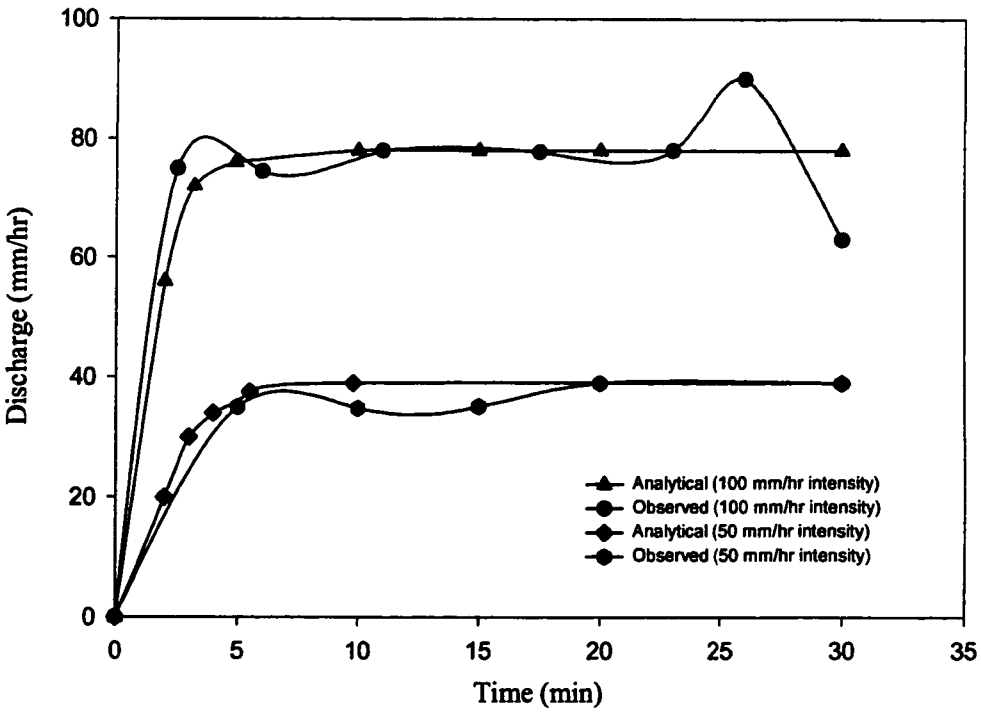

Figure 5-1. Comparison of analytical solution vs. observed data

5.3 Flow Model Accuracy

A simple one-dimensional problem is solved in order to evaluate the accuracy of the flow model. It is the case of the overland flow on a one-dimensional plane surface, for which the hydrodynamic equations have been

solved numerically using the characteristic formulation and is shown to be very accurate [Zhang et al. 1989]. This example is necessarily simple, chosen to test the accuracy of the hydrodynamic model.

To test the model accuracy, rainfall from a smooth impermeable plane surface was simulated. The results of the simulation were compared with those obtained using the characteristic method by Woolhiser and Ligget (1967). The simulated rising hydrographs from the two models and Kinematic wave model are shown in Figure 2. These results were computed for the case defined by the following conditions:

Length = 12 m

Manning coefficient =0.01

Rain intensity = 10 cm/hr

Froude number = F = 2

Kinematic wave number = $\frac{S_0 L}{F^2 h_0} = 1$

where

h_0 = normal depth

The computation grid was taken as Δx = 1.0 m, the time increment was Δt=0.12 s. The results show that the agreement between the hydrodynamic model and the characteristic solution is very good. Since the

kinematic wave number is much less than 10 for this case, the solution by the kinematic wave equation is not satisfactory.

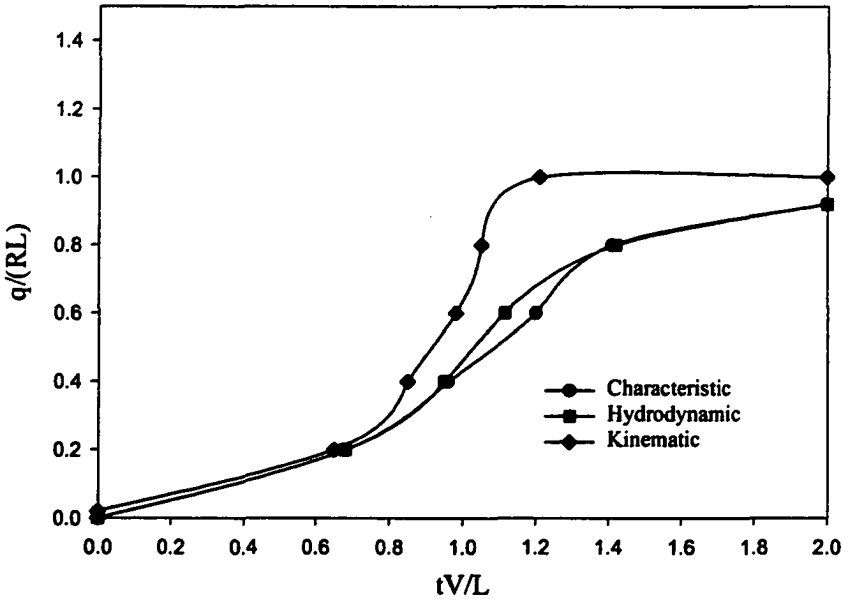

Figure 5-2 Comparison of the hydrodynamic model with the characteristic and kinematic solution (R = rain intensity, q = unit discharge, V = normal flow velocity)

CHAPTER 6

NUMERICAL SOLUTION

6.1 Introduction

In the previous chapters the conceptual parts of this model were discussed and the governing equations were formulated. The objective of this chapter is to review the numerical technique, which was chosen to solve the partial differential equations of the flow model, the sediment transport model and the contaminant transport model.

Reviewing the equations one can realize that the governing equations of the flow model are a set of hyperbolic non-linear partial differential equations, whereas the governing equations of the sediment and contaminant transport models are parabolic equations. The fact that the equations describing the flow are non-linear makes them much more difficult to handle. Specially, in this research, where the model is a 2D depth-averaged model there are no analytical solutions available.

Numerical solutions of the equations may be obtained by finite difference methods in which the continuous domain is replaced by discrete intervals. The derivatives of the sets of partial differential equations are replaced by algebraic equations in terms of the dependent variables (e.g., h,

u, v, m) at the discrete points of independent variables (x, y, t) [Fennema, 1983].

6.2 Numerical Solution Technique

Lax and Wendorff (1960) investigated a number of difference methods, which became popular for solving hyperbolic systems. These methods, known as two-step schemes, are based on second order Taylor series expansion in time [Abbott, 1979; Fennema, 1990]. MacCormack (1969) introduced a simpler variation of Lax-Wendorff scheme. His scheme gained a wide acceptance in computational fluid mechanics.

MacCormack scheme consists of a two-step predictor-corrector sequence. For equation (2-63) the method takes the form [Chaudry, 1993; Tannehill, 1997; Zhang, 1989]:

Predictor Step:

$$U(i,j,\xi) = U(i,j,n) - \frac{\Delta t}{\Delta x}\nabla_x E(i,j,n) - \frac{\Delta t}{\Delta y}\nabla_y F(i,j,n) - \Delta t S(i,j,n) \tag{6-1}$$

Corrector step:

$$U(i,j,\zeta) = U(i,j,\xi) - \frac{\Delta t}{\Delta x}\Delta_x E(i,j,\xi) - \frac{\Delta t}{\Delta y}\Delta_y F(i,j,\xi) - \Delta t S(i,j,\xi) \tag{6-2}$$

in which U(i,j,ξ) and U(i,j,ζ) are intermediate values for U. The new vector U at time n+1 is acquired from :

$$U(i,j,n+1) = (U(i,j,\xi) + U(i,j,\zeta)) / 2 \qquad (6\text{-}3)$$

where

ξ and ζ = dummy variables

Δ = forward differencing

∇ = backward differencing

In the presented form backward differences are used in the predictor step and forward differences are used in the corrector step. The forward and backward differencing can be alternated between the predictor and corrector steps as well as between the two spatial derivatives in a sequential fashion. This eliminates any bios due to one-sided differencing. The sequences shown in table 6-1 are used in this study.

Table 6-1. Sequence table for the flow model

	Step 1	Step 2	Step 3	Step 4
Predictor	$\nabla_x\nabla_y$	$\Delta_x\Delta_y$	$\nabla_x\Delta_y$	$\Delta_x\nabla_y$
Corrector	$\Delta_x\Delta_y$	$\nabla_x\nabla_y$	$\Delta_x\nabla_y$	$\nabla_x\Delta_y$

The MacCormack scheme is also suitable for the sediment transport and contaminant transport equations (parabolic). This scheme is known to yield a good prediction at a reasonable computation price [Chapra, 1997].

6.2.1 Boundary Conditions

Two different types of boundary conditions have been considered in this study, open and close boundaries. The only open boundary is the outlet, where the flow has been considered to be uniform. All the other three boundaries have been considered to be close boundaries. Reflection boundaries can be easily incorporated in the MacCormack scheme for close boundaries. Fictitious points outside the computational domain are replaced by immediate interior points. Antisymmetric reflection is incorporated by changing the sign of the normal component of velocity (Figure 6-1).[Constantindis, 1981; Morris, 1978]

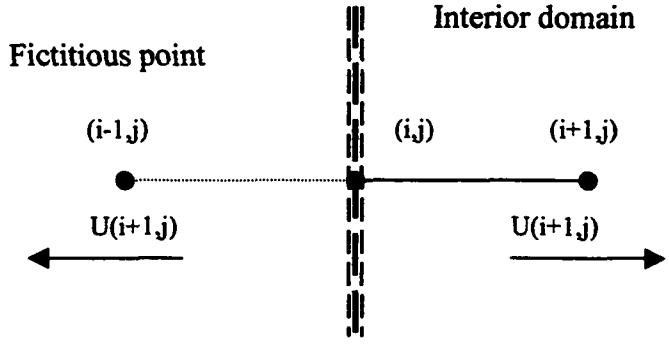

Figure 6-1. Reflection boundary

6.2.2 Stability

The MacCormack scheme is stable if the Courant-Friedrichs-Lewy (CFL) condition is satisfied [Fennema, 1983]. This condition for two-dimensional flow may be written as [Zhang et al., 1989] :

$$C_n = \frac{(V+\sqrt{gh})\Delta t}{\Delta y \Delta x}\sqrt{\Delta y^2 + \Delta x^2} \leq 1 \qquad (6\text{-}4)$$

where

V = resultant velocity at the grid point.

The numerical scheme is stable only if this condition is satisfied in every grid point. This condition is heuristic and is derived from the linearized form of the governing equations for one-dimensional flows, some numerical experimentation should be done before selecting an actual upper limit of the value of C_n.

6.2.3 Artificial Viscosity

High-frequency Oscillations could be produced by the dispersive errors in the MacCormack scheme near the steep gradients. Artificial viscosity might be added to the scheme to dampen these oscillations. In this procedure we first compute the following parameters using the computed values of h, v and u at n+1 time level [Chaudhry, 1993]. For example for h:

$$\upsilon_{\xi}(i,j)\frac{|h(i+1,j)-2h(i,j)+h(i,j)|}{|h(i+1,j)|+|2h(i,j)|+|h(i-1,j)|} \tag{6-5}$$

$$\upsilon_{\eta}(i,j)=\frac{|h(i,j+1)-2h(i,j)+h(i,j-1)|}{|h(i,j+1)|+|2h(i,j)|+|h(i,j-1)|} \tag{6-6}$$

At points, where h(i,j-1) or h(i,j+1) do not exist:

$$\upsilon_{\eta}(i,j)=\frac{|h(i,j+1)-h(i,j)|}{|h(i,j+1)|+|h(i,j)|} \tag{6-7}$$

or

$$\upsilon_{\eta}(i,j)=\frac{|h(i,j)-h(i,j-1)|}{|2(i,j)|+|h(i,j-1)|} \tag{6-8}$$

Then the following equations are determined

$$\varepsilon_{\xi}(i\text{-}1/2,j) = \kappa \max\,(\nu_{\xi}(i\text{-}1,j),\ \nu_{\xi}(i,j)) \tag{6-9}$$

$$\varepsilon_{\xi}(i,j\text{-}1/2) = \kappa \max\,(\nu_{\eta}(i,j\text{-}1),\ \nu_{\eta}(i,j)) \tag{6-10}$$

where

κ = dissipation constant. (a value of 0.3 is recommended for the first trial)

The final value of the variable f at the new time step is computed as:

$$f(i,j,n+1) = f(i,j,n+1) + [\varepsilon_{\xi}(i+1/2,j) * (f(i+1,j,n+1) - f(I,j,n+1)) - \varepsilon_{\xi}(i-1/2,j) * (f(i,j,n+1) - f(i-1,j,n+1))] + [\varepsilon_{\eta}(i,j+1/2) * (f(i,j+1,n+1) - f(i,j,n+1)) - \varepsilon_{\eta}(i-1/2,j) * (f(i,j,n+1) - f(i,j-1,n+1))] \quad (6\text{-}11)$$

in which f refers to u, v and h. Equation (6-11) can be considered as a FORTRAN replacement statement.

6.2.4 Computational Procedure

The computational process is described here, to cover three distinct parts of the simulation processes. They are:

1- ***Hydrodynamic Computations***: Flow velocity in x and y directions as well as flow depth is calculated in this part.

2- ***Sediment Transport Computations***: Suspended solid concentration is calculated based on the above hydrodynamic results.

3- ***Contaminant Transport Computations***: The change of the soil surface contamination as well as sediment-controlled contaminant transport in water is computed in this part.

These steps are intentionally separated to save computation time. The hydrodynamic part needs a longer computation time. Due to the nature of the equations in this part smaller time increments are needed for the difference equations than the other two parts. This way with one hydrodynamic run several different sediment transport and contaminant transport scenarios can be executed. The complete procedure is described sequentially in the following flowchart (Figure 6-2).

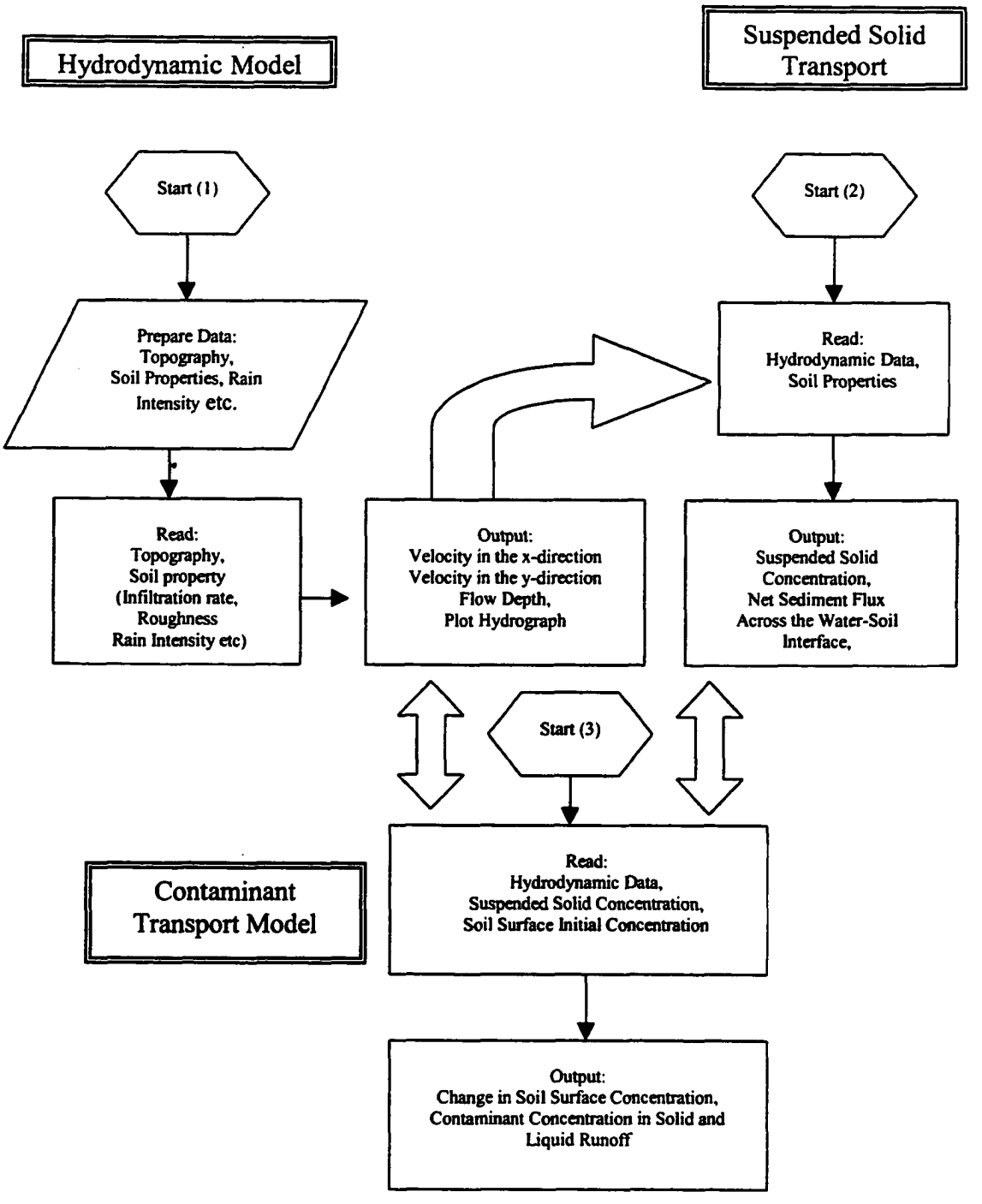

Figure 6-2. Model general flowchart

CHAPTER 7

MODEL APPLICATION

7.1 Introduction

The contaminant transport model developed in this research was applied to an experimental runoff plot near the Chernobyl Nuclear Power Plant (NPP). This plot was designed and constructed by the Center for Water Resources and Environmental Research (CUNY) in Ukraine to conduct a one-year long experiment on the erosion-controlled transfer of radionuclides. The plot was located 12 km to the south-southeast from the Chernobyl NPP. Artificial rainfall was performed to induce erosion in a controlled environment. Liquid and solid runoff were collected and studied. In the following sections the details of the research area, experimental procedure and the data collection process is discussed. At the end of this chapter the results of the model simulation and the collected data are compared.

7.2 Physiographical Characteristics of the Research Area

The Chernobyl NPP is located in Northern Ukraine (Figure 7-1) within the geographical zone of Kiev Polesye. This zone is characterized by moderate/continental climate with positive balance of humidity at relatively

high temperatures and low humidity in the summer, and low temperatures and high humidity and snow cover in winter. The main temperature characteristic of the area are presented in Table 7-1.

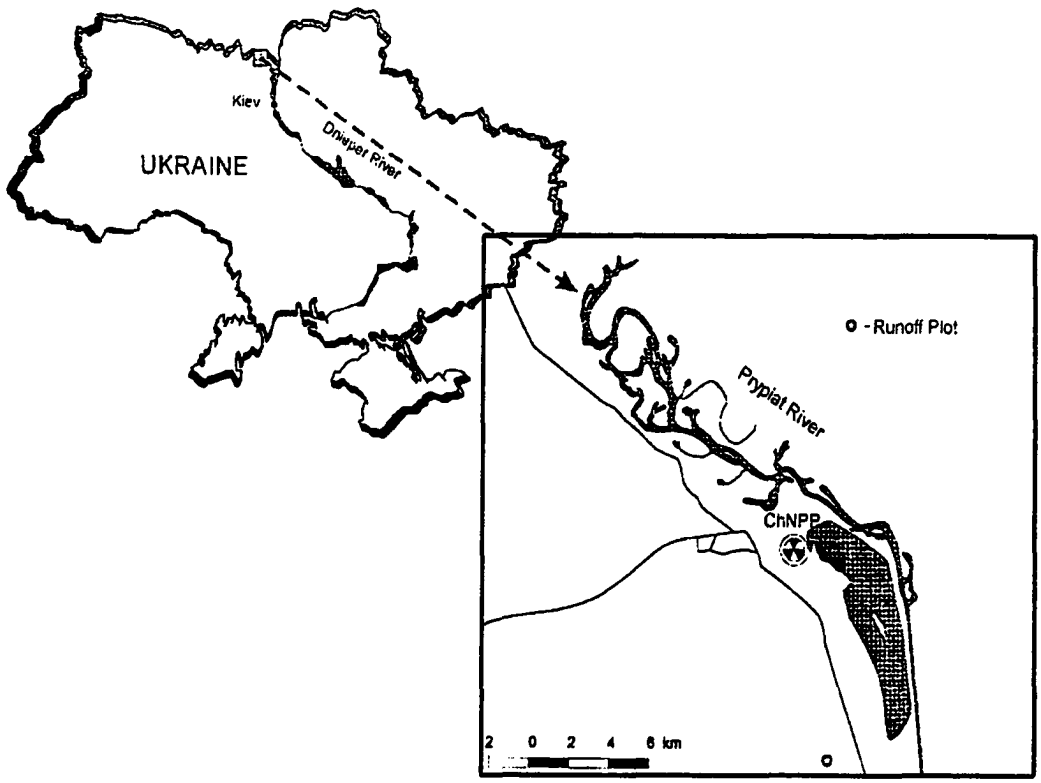

Figure 7-1. Location map for the runoff plot near the Chernobyl NPP

Table 7-1. Characteristic temperature in the area of the Chernobyl NPP

Parameter	January	July
Monthly Average Temperature	- 5.6° C	19.1° C
Absolute Extremum	- 44.9° C	45.2° C
Daily Average Temperature	5.7° C	11.1° C
Daily Maximum Temperature	28.1° C	18.2° C

The annual average relative humidity is 77 percent. The maximum daily precipitation (with 0.01 percent probability) is 190 mm. The maximum 20 minute precipitation (with 0.01 percent probability) is 72 mm. The earliest date for snow cover to appear is October 6, the latest date is December 15. The earliest date for snow cover to thaw is February 21, the latest date is April 22. The number of days with snow cover is 90-102. The average depth of snow cover in open space is 8 cm, the maximum is 41 cm.

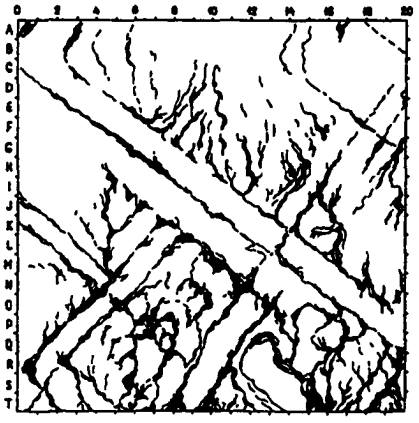

Figure 7-2. The top view of the runoff plot

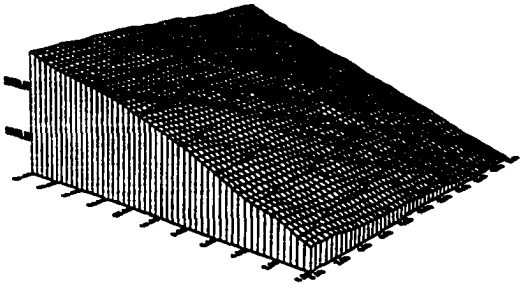

Figure 7-3. The perspective view of the runoff plot

The dominant wind direction is northwesterly. The average annual wind velocity is 4.2 m/s. the maximum wind velocity (with 0.01 percent probability) is 47.3 m/s

The experimental runoff plot, Figure 7-2 and 7-3, is located on a gentle (6° mean) southern slope of a hill with absolute elevation of 140 m. this hill dominates the landscape. The topsoil here is typically soddy-podzolic, sandy-loam, low-thickness (14-18 cm) one, with leached and poorly structured soil-forming rock. The predominant grain-size fraction is coarse silt.

7.3 Instrumentation of the Runoff Plot

To study the erosion/sedimentation-controlled radionuclide transfer, a 20 m x 20 m runoff plot was designed and constructed. It was surrounded by wooden curbs from its three lateral sides and by a runoff chute from the lower side. Figure 7-4 shows the instrumentation and experimental setup in detail.

The frame of the chute was made of wood, while the runoff bed was made of sheet metal with corrosion-resistant coating. The chute was placed into a prepared trench so that its upper edge was 3-6 cm lower than the soil surface. A screen was buried in the soil beyond this edge to prevent both

liquid and solid runoff from leaking to outside the chute. In one of the lower corners of the chute, a discharge window was made under which a discharge

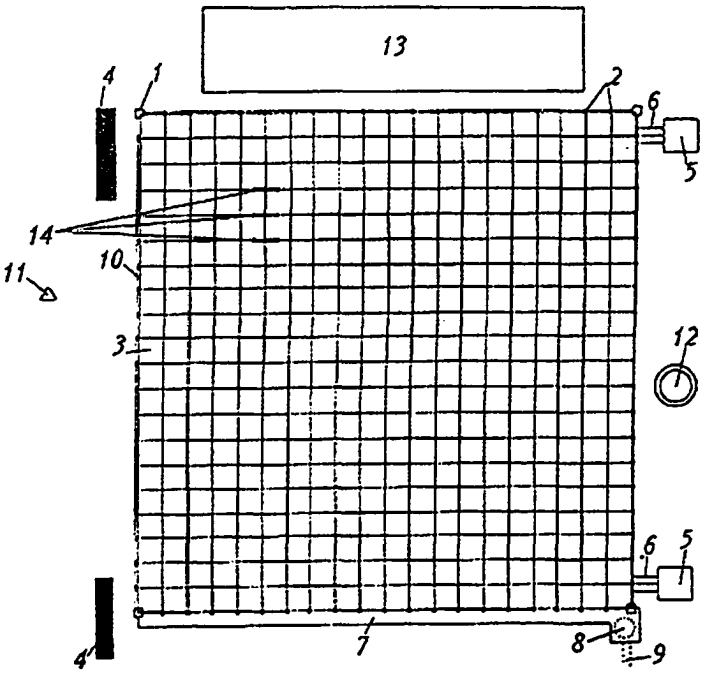

1- *Corner pillars;*
2- *Fixing pegs;*
3- *Elementary (meter) squares;*
4- *Soil trail pits;*
5- *Hydrophysical spots;*
6- *Pipelines to the tensiometers*
7- *Runoff chute;*
8- *Receiving tank for liquid and solid runoff;*
9- *Water discharge channel;*
10- *Wooden boundary curb;*
11- *Benchmark for leveling;*
12- *Rain gauge;*
13- *Area for irrigation equipment*
14- *Profiles 1,2 and 3 to study microtopographical changes of the plot.*

Figure 7-4. Scheme of the runoff plot

tank with a capacity of 50 liters was placed. The entire length of the chute was covered on top to protect it against direct entering of rainwater, while the liquid and solid runoff could easily pass into it. The design of the chute allows for its periodic inspection and collection of the solid runoff.

7.4 Preparation of the Plot and Initial Samplings

First, the runoff plot was devegated. Then it was broken down into 40 subareas of 1 m X 1 m elementary squares, with downslope lines lettered from A to T, and lines along the slope numbered from 1 to 20. The exposed dose intensity (EDI) was then measured for gamma radiation in order to assess the amount and the uniformity of the radioactive contamination. These measurements were made at the center of each elementary square by a scintillation radiometer SRP-88N. The probe was located at about 60 cm above the ground to ensure obtaining an integrated flux of gamma quants from the area of 1 sq. m and a certain smoothening of the picture. The error of a single measurement did not exceed 1 μr/h. the observed variation of the EDI measurements was 200-232 μr/h with the arithmetical mean value of 217 μr/h.

The leveling survey was conducted to determine the elevation and slopes on the plot. Altogether, 441 measurements were performed with the accuracy of 1 mm.

Soil samples were taken to obtain a number of soil properties such as grain-size distribution, content of radio cesium and other gamma emitting radionuclides, humus, exchangeable cations and agrochomicals pollutants in natural conditions, prior to experiments. The samples were taken at the center of each square element by pressing metal rings to a depth of 5 cm. The total number of samples taken was 400. Only 25 of these samples were studied as the representative of the plot.

To determine the soil water/physical properties, such as coefficient of permeability, changes in suction pressure when wetted and dried, six monoliths- undisturbed samples, 6000 cm^3 in volume, of the upper one-meter layer of the soil- were taken from two soil sections. The coefficients of permeability measured in the lab fluctuated between 3.1 and 4.8 m/day.

7.5 Artificial Rainfall

The intensity and the amount of the artificial rainfall were calculated based on the precipitation pattern in the area and taking into account mainly heavy showers able to induce erosion. According to the long-term

observations for the northern part of the Kiev region, the bulk of precipitation falls in the months June through August, and over 60% of precipitation in these months is of the heavy shower type. The maximum daily amount of precipitation observed has reached 120 mm, but this occurs no more than once in ten years. The duration of abundant precipitation does not exceed 12 hours, its intensity varying within 0.02-1.85 mm/min. The duration of such maximum intensity precipitation is no longer than 8 to 12 minutes.

To obtain a clear picture of erosion process, the intensity of the artificial rainfall has to be 3-4 times that of the natural rainfall, i.e. 7-8 mm/min, with duration of 6 to 8 minutes. More prolonged precipitation exceeding 10 minutes would cause additional factors not to be accounted for with due accuracy.

To perform the artificial rainfall, water was supplied by three irrigation machines, KO-002 with 6.5 m^3 capacity. Taking into consideration the wind drift of the rainfall cloud, the two machines were placed on the upper northern side of the plot, while the third one was placed on the upper western part. This was aimed at making the most use of wind to cover the entire area with artificial rainwater. All the machines started ejecting water jets under a pressure of 8 atmosphere up and forward simultaneously. The

rainfall lasted six minutes. It appeared that some 90% of the water fell on the plot; the rest was either ejected or wind-drifted beyond it.

7.6 Study of Grain-size Distribution

The study was carried out using the areometric method, by the device PZPS # 18, 88, and TU-25-75, 1122-75. The method is based on measuring the density of the slurry prepared from the soil in question.

A specimen is taken from the soil sample with natural moisture content, its dry weight being 10-15 grams, and placed inside a porcelain cup; then after adding 20 ml of the 5% solution of $Na_2P_2O_7$, it is left for 6-8 hours. In addition another specimen is taken from the soil to determine the soil skeleton density and moisture content, which are used to calculate the dry weight of the specimen.

Upon dispersing, some distilled water is added to specimen and it is ground by means of a rubber pestle. Then the slurry is poured into a glass vessel, distilled water is added again until the volume of the slurry reaches 0.4-0.6 liters, and it is being shaken for half an hour. After shaking, the slurry is strained through a 0.1-mm sieve, and distilled water is added again until the volume of the slurry reaches 1 liter. The coarser particles remaining on the sieve are dried, and the weight of particles larger than 0.1 mm

calculated. The finer fractions, which went through the sieve, after stirring, measuring its temperature and allowing for sedimentation, are placed into a device, where the density of the slurry is determined at various depths and at certain time intervals. Then the percentages of all fractions are calculated.

Since the PZPS device can be used only to determine the content of soil fractions in the range of 0.001 mm to 0.01 mm, the content of coarser fractions, 0.02 to 0.05 mm, was determined by means of the floating areometer TU-25-11, 1122-75. The results of grain-size analyses of soils from the runoff plot are given in Figure 6-5.

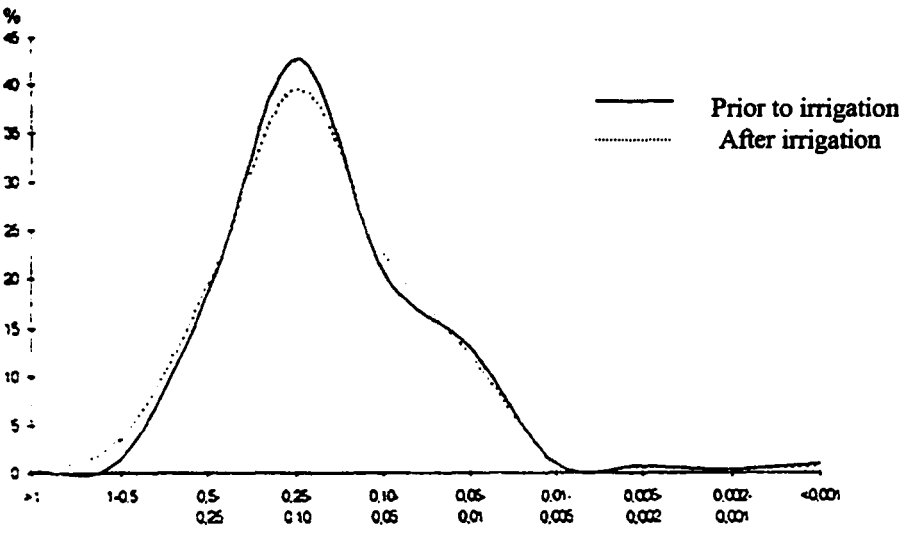

Figure 7-5. Grain-size distribution on the runoff plot prior and after irrigation

7.7 Changes in Topography of The Runoff Plot During One Year

To study the changes of the topography and microtopography (changes in elevation of 1-2 mm over a distance of 10-20 cm) after the rainfall simulations, a method of "needle profiles" has been developed and emplyed in practice. The following actions were undertaken:

1. Three profiles were set up along the slope to characterize the sections most prone to erosion and to cross the main furrows.
2. At the distance of 5 cm from the western end of each profile, a wooden benchmark was hammered into the ground, to serve for leveling and finding the profile.
3. Each of these profiles were intersected by short (1 m long) transversal profiles perpendicular to the main ones.
4. At every 10 cm along the short profiles, metal needles 15 cm long were punched into the soil, so that their upper ends were flush with the surface.
5. Using a surveyor's level and a wooden ruler, elevations of each needle top were obtained.
6. After the rainfall simulation, the new positions of the needle tops were measured with the accuracy of 1 mm; their positions either

remained the same – even with the ground – or changed (came up at places of erosion and disappeared under the soil at places of deposition).

As a result, for the 330 points located at places most vulnerable to erosion, data were obtained regarding their coordination before and after rainfall events, as well as data regarding changes in their final elevation caused by erosion and accumulation.

The data indicated that the annual soil losses amounted to 2.1 mm for the western and central profiles, and 1.2 mm for the eastern profiles. Taking into consideration that the needled profiles were installed on the most erosion-prone areas of the runoff plot, the real washout of the soil is close to that for the eastern profiles, that is 1.2 mm, which corresponds to the Type IV of the erosion intensity – "strong erosion".

7.8 Annual Balance of The Soil Mass

To determine the mass of the soil taken out of the plot (either by washout due to natural and man-made runoff, or removed on the roots of vegetation), the volume of the soil taken out is multiplied by its average density:

20 m X 20 m X 0.012 m X 1610 kg/m^3 = 773 kg

This value is of the same magnitude as the total amount of measured annual natural and man-made solid runoff, which was 380 kg; the difference is probably related to the fact that the previous value (773 kg) included the soil taken out by vegetation. Indeed, when the soil mass removed with the roots during the two cycles of weeding, was calculated it appeared to be quit close to this difference (773 – 380 =393 kg)

The distribution of the soil washout (in kilograms) by season during the one-year cycle is given in Table 7-2.

Table 7-2. Soil Washout in kg from the Runoff Plot During One-Year Experiment

	Fall 1995	Winter 1995-96	Spring 1996	Summer 1996	Fall 1996	**Total**
Natural Solid Runoff	6	0	6	4	5	**21**
Man-made Solid Runoff	98	0	56	22	183	**359**
Devegatation and Weeding	111	0	0	0	282	**393**
TOTAL	**215**	**0**	**62**	**26**	**470**	**773**

7.9 Characteristics of The Radioactive Contamination

The distribution of the ^{137}Cs in the upper 5-cm layer of topsoil on the runoff plot has been studied by analyzing results of gamma-spectrometric measurements for 25 samples taken from the nodes of 4 m X 4 m net before and after each rainfall simulation and during the entire annual cycle. The

^{137}Cs concentration in the soil fluctuated between 1.9 and 11.3 kBq/kg. Its arithmetic mean value was 5.51 kBq/kg with standard deviation of 2.85. As we see the ^{137}Cs concentration is highly variable, which may be explained by both spotty character of fallout and nonhomogeneity of depths reached by the radionuclides within the plot.

Artificial rainfall caused a significant redistribution of radionuclides in the upppermost soil layer. In some places their concentration became lower, while in others it became higher. At first glance it seems that both decrease and increase in the ^{137}Cs concentration can be explained by washout of the uppermost layer of the topsoil and accordingly by deeper portions of the soil profile getting into the sampler. Depending on the nature of the vertical distribution of the nuclide (separation of the maximum from the surface or simple exponential distribution) the resulting outcome may be different. The Influence of the thickness variations of the sampled soil on the arithmetical mean value of mass concentration of ^{137}Cs, as evaluated by detailed study of vertical distribution of this nuclide in two trial pits (Figure 6-4) is rather distinct. So increase in the thickness of the sampled layer from 5 cm to 7 cm leads to the decrease in weighted average values of this concentration by26-27 percent.

7.10 Annual Balance of ^{137}Cs on The Runoff Plot

As per measurements made in the beginning of the one-year cycle of research for 25 samples taken from the uppermost 5-cm layer of topsoil on the runoff plot, the amount of ^{137}Cs was as follows:

20m X 20m X 0.5m X 1610 kg/m^3 X 5.51 kBq/kg =177,422 kBq.

Knowing the masses of the natural solid runoff, man-made solid runoff, soil removal on the roots of vegetation, and seasonal alterations of ^{137}Cs concentrations in these masses, it is possible to calculate both the total amount of radiocesium removal from the runoff plot and its distribution by constituent elements and season (Table 7-3).

7.11 Model Runs and Simulations

The model was calibrated with the available data, which were collected during the one-year cycle of the experiment. Those data, which

Table 7-3. Removal of ^{137}Cs in kBq from the runoff plot during the one-year experiment

	Fall 1995	Winter 1995-96	Spring 1996	Summer 1996	Fall 1996	**Total**
Natural Solid Runoff	49	0	33	22	25	**129**
Man-made Solid Runoff	630	0	174	122	897	**1832**
Devegatation and Weeding	637	0	0	0	1210	**1847**
TOTAL	**1316**	**0**	**207**	**144**	**2132**	**3799**

were not available, were taken from literature and previous research material.

Three artificial rain operations were simulated with the first module. In all three simulations (runs) the rain intensity and the infiltration rate were equal and constant. A time-dependent infiltration rate did not show a significant change in the results of the model. It was also assumed that the change of the topography of the plot is negligible. So the initial grid elevations were kept for all three runs. This assumption is justified due to the fact that the average change in elevation across the plot was about 1.2 mm, which does not have any significant effect on the model results. In extreme cases, where the topography change is significant, it can be easily incorporated into the module 1 as a subroutine, where the hydrodynamics (velocity in the x and y directions and the flow depth) are computed.

Using the results of the module 1, the second module was run to compute the sediment transport, soil detachment and deposition and the sediment discharge from the plot after each rain simulation. Like module one, module two also had to be calibrated first. Certain key coefficients and inputs, useful for the model, were not measured during the one-year experiment. Their initial values were obtained from the literature. Among them the critical shear stress for detachment and erosion constant were

extremely important. These two inputs depend highly on the grain-size distribution. Therefore some adjustments had to be made after each simulation to reflect the changes of the grain-size on the sediment discharge. Figure 7-5 shows clearly a change in the grain-size of plot after the rainfalls were performed. Table 7-2 also shows a decreasing pattern in the sediment discharge from the runoff plot between the first and the third artificial rainfall. There was a jump in the sediment yield in the fourth rainfall simulation. This jump can easily be explained by the fact that there was a weeding and devegatation operation performed before the artificial rainfall. These operations extricate the soil structure so the surface runoff can detach the soil particles much easier.

Most of the coefficients and constants in the third module were obtained from the literature and previous experiments conducted by other scientists and research groups [Brunjes et al., 1999; Carlsson, 1978; Hillel, 1980; Rogowski, 1965]. The ^{137}Cs concentration on the soil surface before each artificial rainfall was available, which was used for each individual run.

Followings are the model inputs for the three runs, which were performed to simulate three artificial rainfall operations.

Module 1:

- Infiltaration rate = 0.003 cm/s

- Rain intensity = 0.0135 cm/s
- Rain duration = 420 seconds

Module 2:

- Erosion Constant = 0.0003 $g/cm^2.t$
- Limiting shear stress for erosion = 0.04 Pa
- Limiting shear stress for deposition = 0.02 Pa
- Soil average density = 1.61 g/cm^3

Module 3:

- Soil porosity = 0.5
- ^{137}Cs diffusion coefficient = 1.21e-6 cm^2/s
- ^{137}Cs partition coefficient = 5e+5 cm^3/g
- Diffusive mixing velocity = 4.137e-6 cm/s

The erosion constant was decreased about 10% for the second and third run and the limiting shear stress for erosion was increased about 10% for the second and the third run. The arguments for these adjustments have already been explained above.

Figure 7-6 illustrates the plot's hydrograph, which is produced by the model.

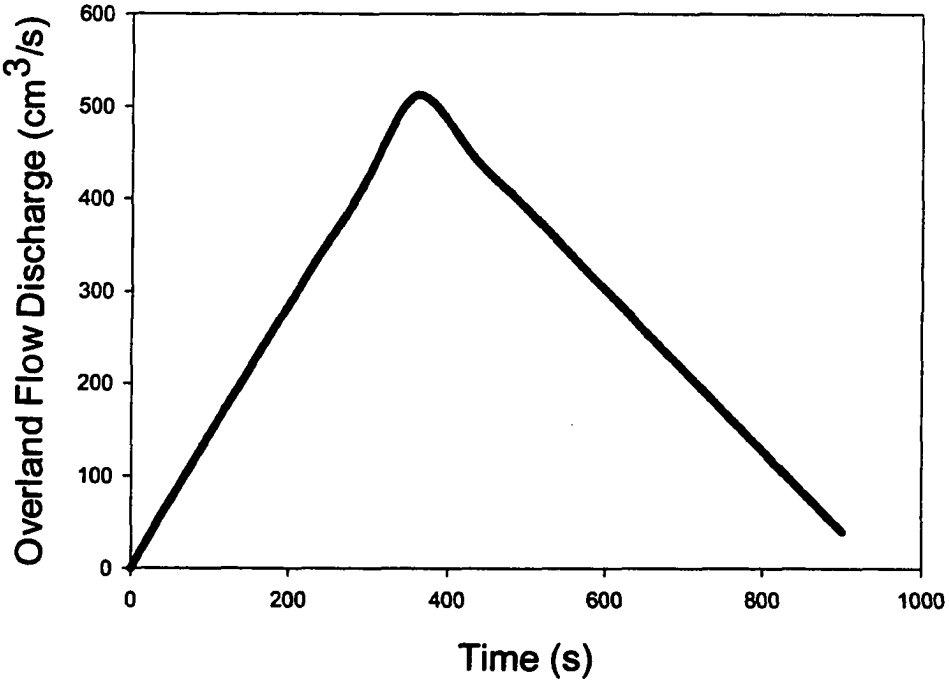

Figure 7-6. The Hydrograph of the Runoff Plot

Figure 7-7 pictures the changes of the sediment discharge versus time. It clearly shows a reduction in the total sediment yield from the plot, when the artificial rain simulation is repeated. By comparing Figure 7-7 to Figure 7-6 one can realize that the peak of the overland flow and the peak of the sediment discharge occur almost at the same time. This can change if the size of the plot becomes larger considerably or the topsoil structure over the

plot is not homogeneous such that at some regions the erosion process may start faster.

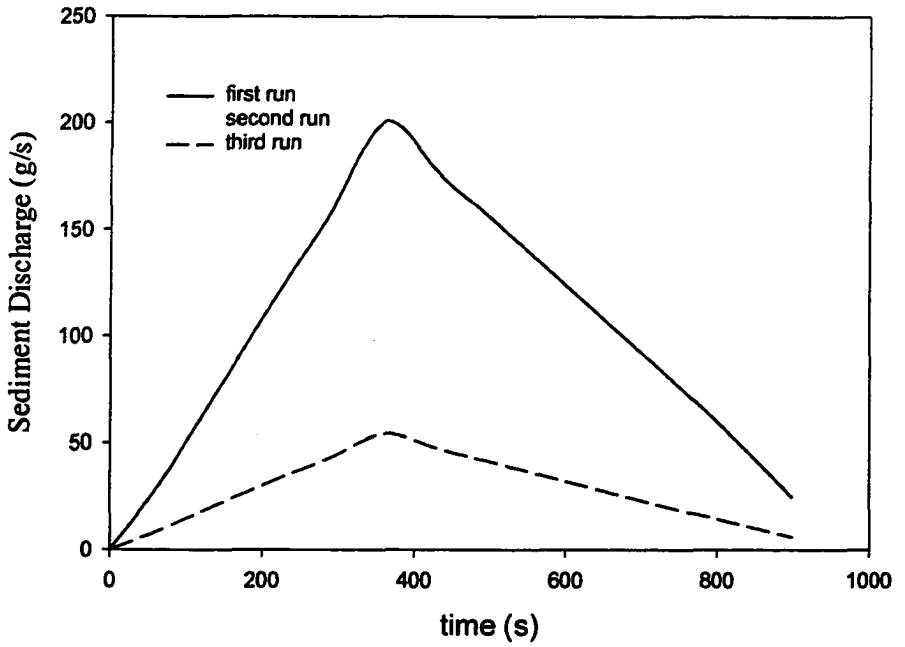

Figure 7-7. Sediment discharge vs. time

The simulation results have been presented in Table 7-3. A comparison between the collected data and simulated data are shown in Table 7-4. The minus sign indicates an underestimation of the model relative to the collected data from the runoff plot.

Table 7-4. The results of the model runs

	RUN #1	RUN #2	RUN #3
Sediment yield (kg)	96	47	26
Radioactive yield (kBq)	630	117	98

Table 7-5. Relative computational error of the model

	RUN #1	RUN #2	RUN #3
Sediment yield (kg)	-2%	-16%	-15%
Radioactive yield (kBq)	0%	-32%	-%19

It can be concluded from the results that in general the model has underestimated the sediment and radioactive discharges. The results can be drastically improved by fine-tuning the key inputs such as limiting shear stress for erosion and erosion constant. For this purpose a thorough and comprehensive test ust be conducted on the soil structure and its mechanical properties to evaluate the key parameters. In the following section the sensitivity of the model toward certain parameters is discussed.

7.12 Sensitivity Analysis

Sensitivity analysis is performed to show how the model reacts toward the changes of the key parameters. Variations in the value of different parameters have unequal effects on the final result. This model proved to be very sensitive in terms of mechanical properties of the soil such as erosion constant, limiting shear stress for erosion and soil roughness coefficient (Manning's coefficient). Other soil parameters such as soil density were also among the very important inputs, which can effect the radioactive discharge drastically (Figures 7-8 through 7-11). The first module, where the

hydrodynamic properties of the system are computed, has the infiltration rate, rain duration and intensity as its inputs. The effect of these parameters on the plot's overland flow peak discharge is illustrated in Figure 7-12 through 7-14. The peak discharge is selected as a representative of the hydrodynamic properties of the plot. An increase in the peak discharge implies a growth in the radioactive and sediment yield of the plot.

The graphs indicate that the model is very sensitive toward the changes of the soil roughness (Manning's coefficient). Figure 7-10 shows that a 14% increase in this parameter causes a 100% growth in the sediment yield. The effect of this parameter on the hydrodynamic results (module 1) is not as severe. The second most important input is the limiting shear stress for erosion. Figure 7-9 suggests that a 10% error in estimating this parameter can cause the model to show a 50% reduction in the sediment yield. The other sediment-related parameter, which is of great importance is the erosion constant. Figure 7-8 shows that a 10% overestimation of this parameter will cause a 10% increase in the calculation of the sediment yield. The soil density has almost the same but reverse effect on the total radioactive (contamination) loss from the plot (Figure 7-11). That means a 10% increase in the density of the topsoil causes a 10% reduction in the total loss, which

indicates that the heavier soil types (or compact soils) are less likely to be affected by erosion-controlled transfer of radionuclides.

Figure 7-12 through 7-14 illustrate the sensitivity of the first module toward rain intensity, rain duration and infiltration rate. A close comparison of the figures suggests that the rain duration is the most important parameter in this module. A one-minute increase in the rain duration causes a 14% growth in the peak discharge (cm^3/s) (Figure 7-13). The rain intensity is the second significant input of this module. The analyses indicated that the peak discharge shows a 10% increase, when the rain intensity changes only 4% (Figure 7-12). And at last the peak discharge shows a 6% increase, when the infiltration rate reduces 10%.

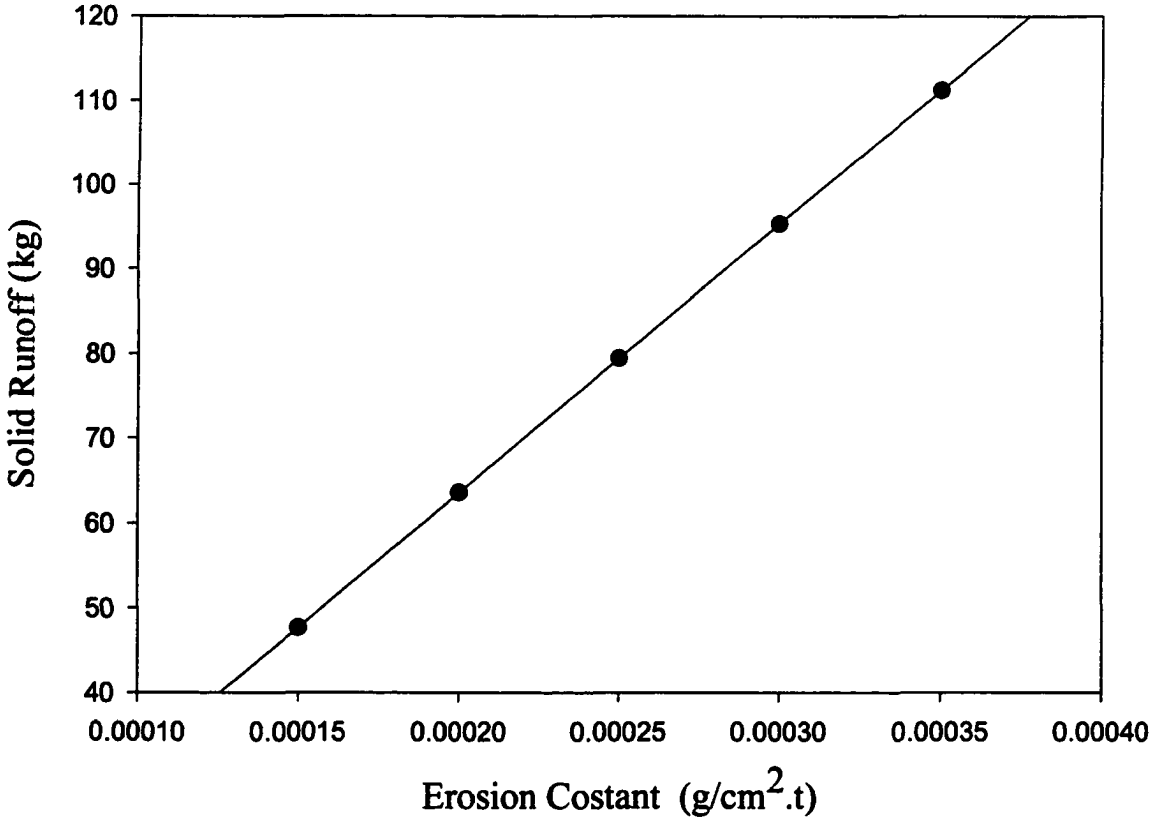

Figure 7-8. Erosion constant vs. solid runoff
(limiting shear stress for erosion = 0.04 Pa)

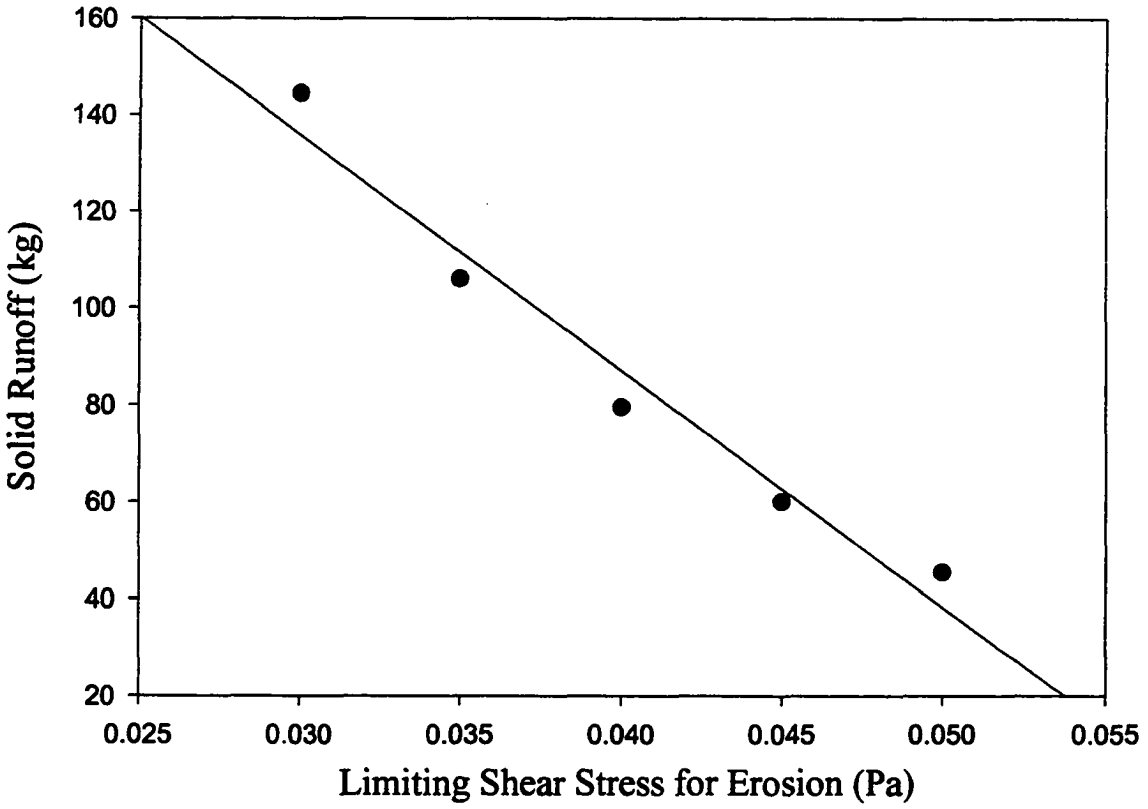

Figure 7-9. Limiting shear stress vs. solid runoff

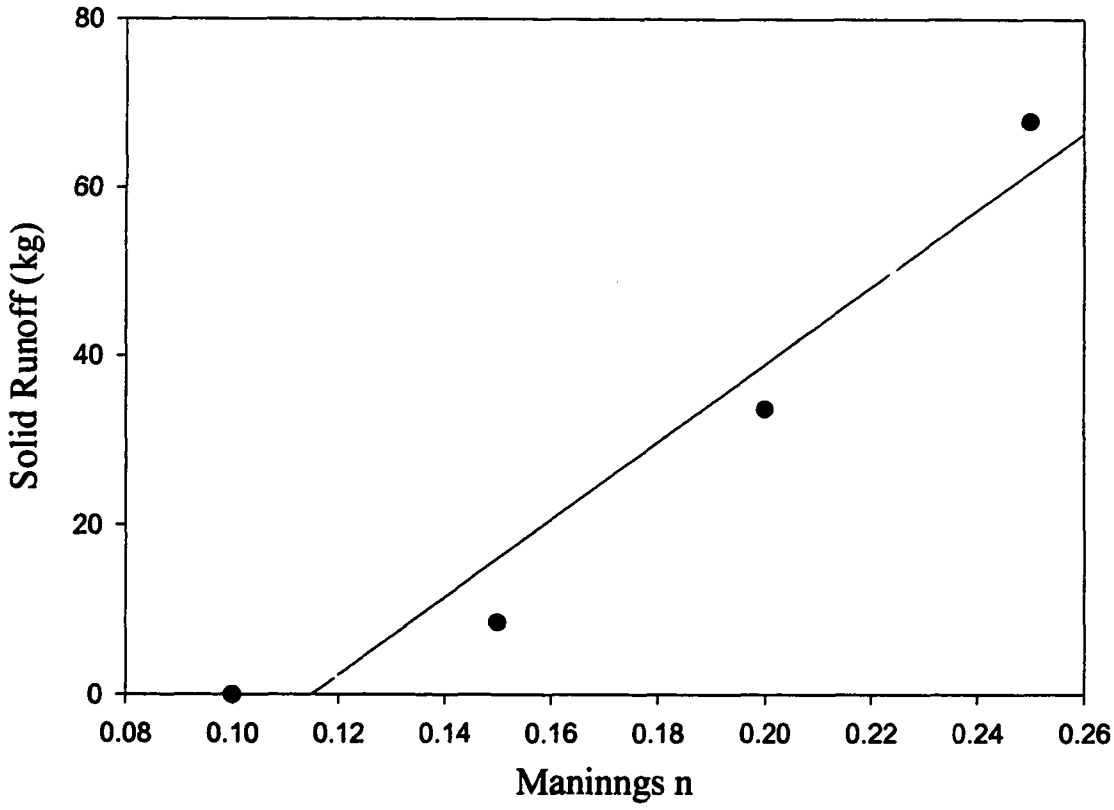

Figure 7-10. Mannings coefficient vs. solid runoff

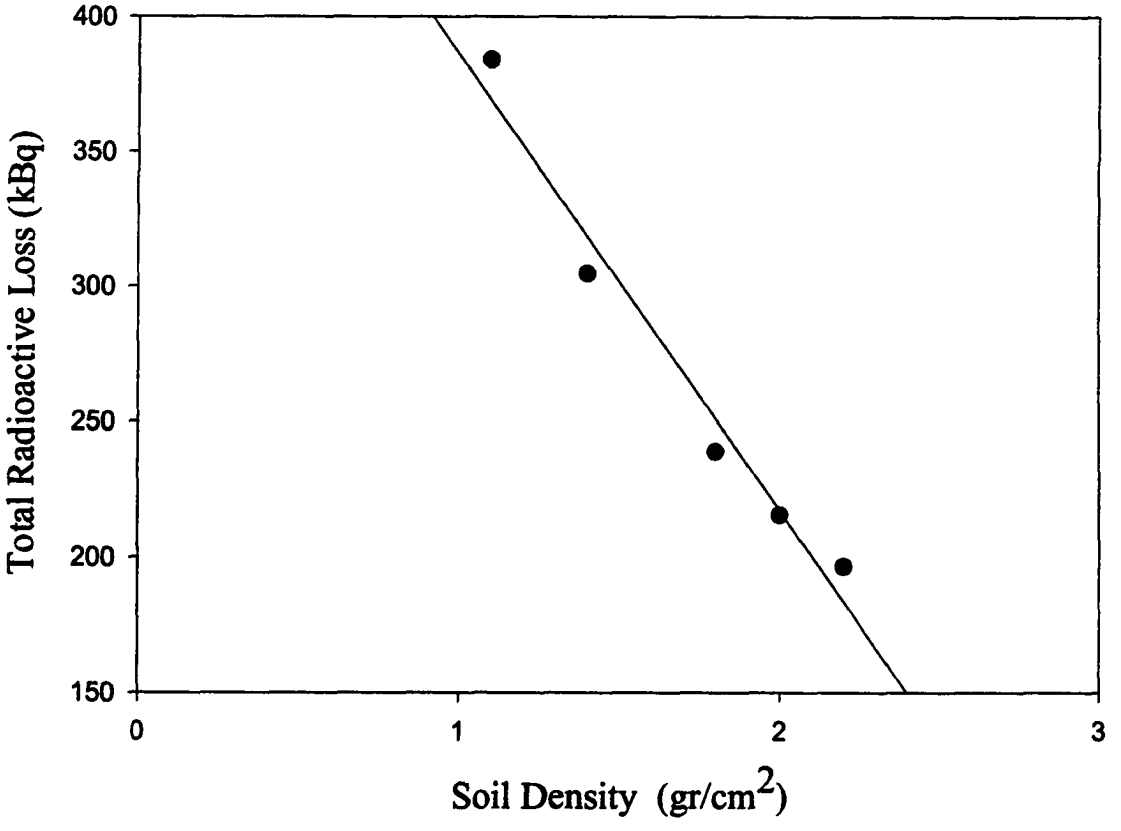

Figure 7-11. Soil density vs. total radioactive loss

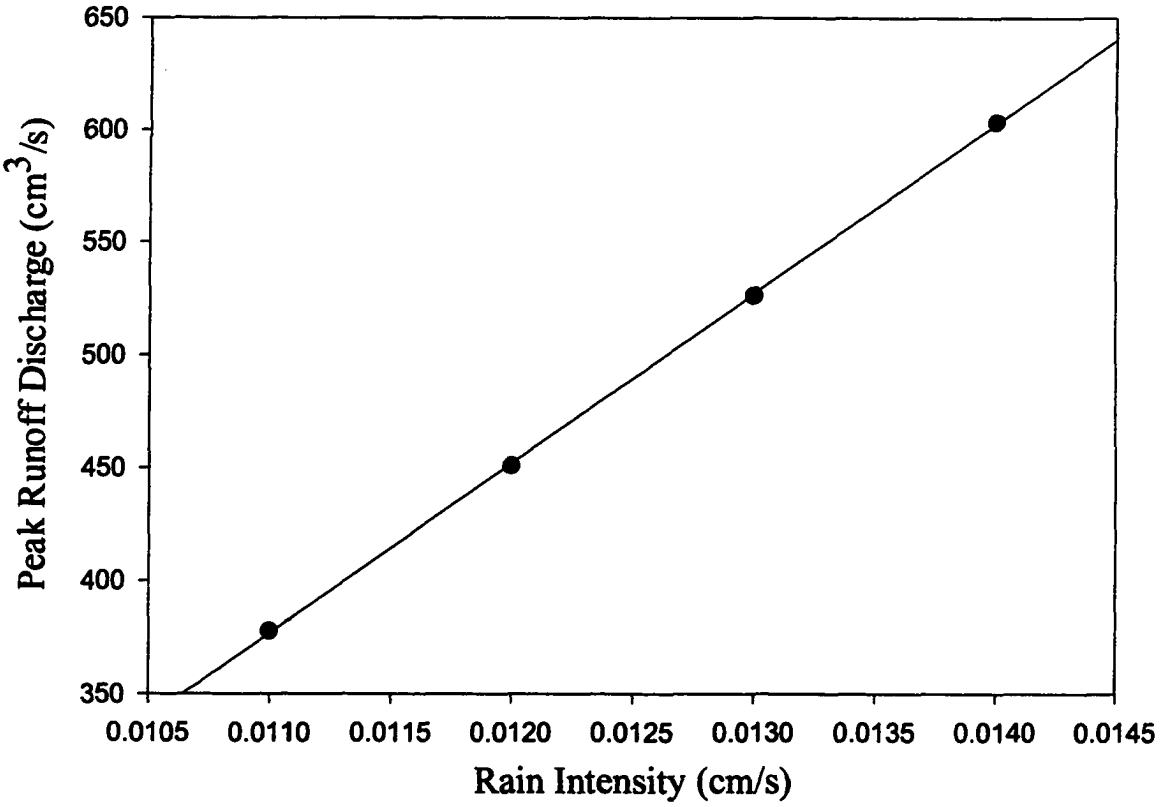

Figure 7-12. Rain intensity vs. peak runoff discharge

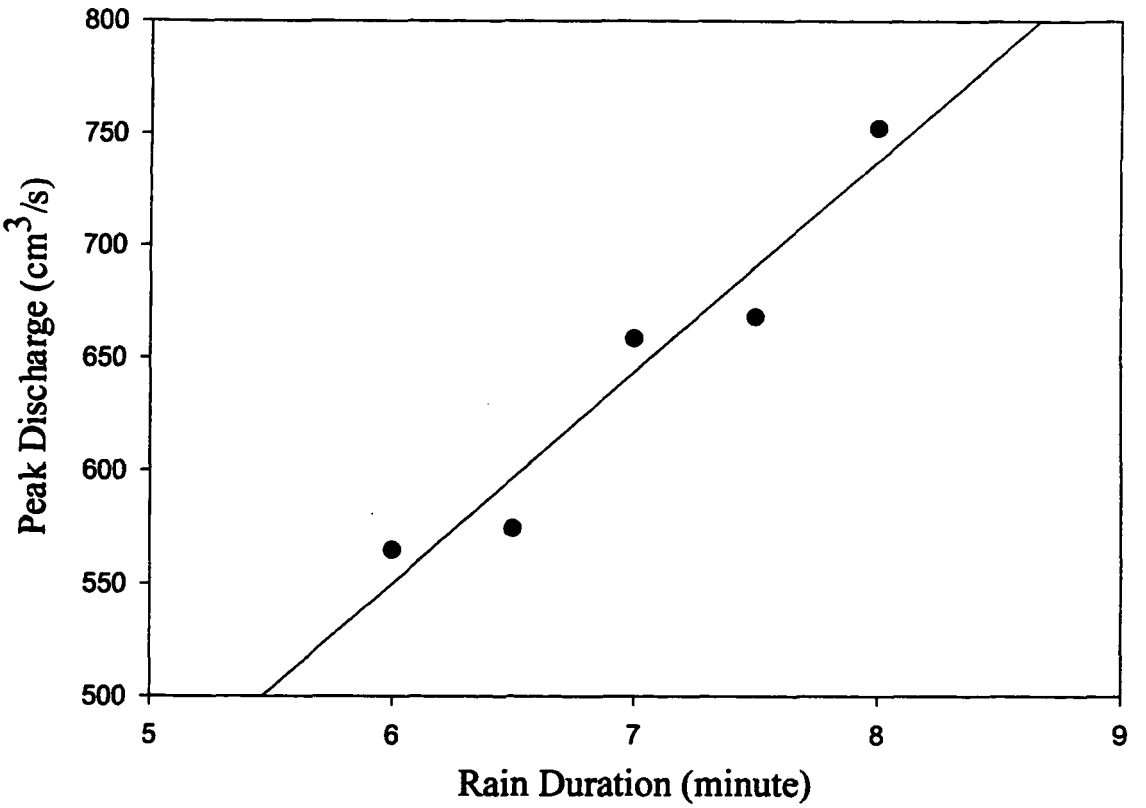

Figure 6-13. Rain duration vs. peak runoff discharge

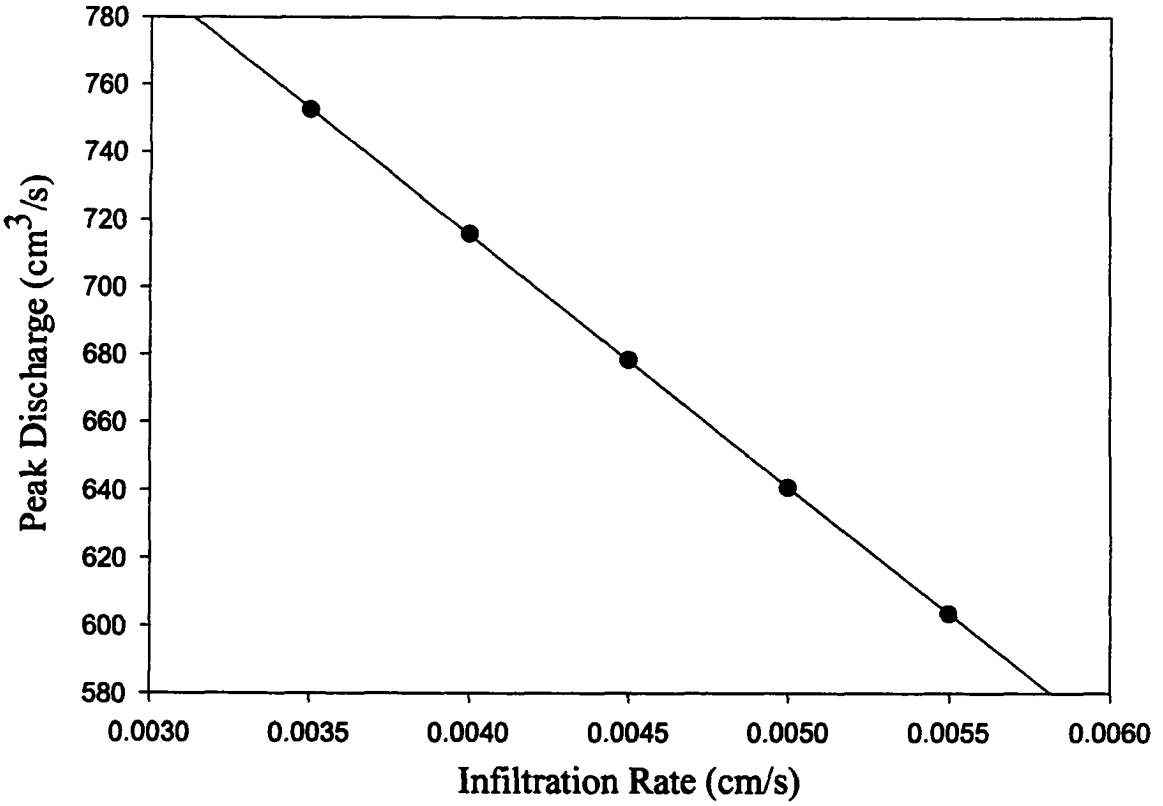

Figure 7-14. Infiltration rate vs. peak runoff discharge

CHAPTER 8

CONCLUSIONS AND SUGGESTIONS

8.1 Summery

A mathematical model is developed to predict the sediment/erosion-controlled radioactive transport on soil surface. The objective of this research was to depict a more realistic picture of the radioactive transport process on soil surface. To accomplish this goal three modules were coupled together:

1- Hydrodynamic module (module 1);

2- Sediment transport module (module 2);

3- Contaminant transport module (module 3).

In the first module the hydrodynamic properties of the system (velocity in the x-direction and y-direction and the depth of flow) are computed. By averaging the governing equations in the z-direction, the 3D equations were transformed to 2D depth-averaged equations. Because the overland flow is extremely shallow (1-5 cm), the averaging process does not have a considerable effect on the accuracy of the model. The equations were solved using the MacCormack scheme. This scheme is a two-step second order (in time and space) explicit finite difference scheme. It is known to

yield a good prediction at a reasonable computation price [Chapra, 1997; Tannehill, 1997].

The second module uses the hydrodynamic properties of the system, which are computed in the first module, to calculate the amount of suspended sediment transported by the overland flow. The governing equations in this part have also been averaged over the depth. The same numerical technique is implemented in this module as well.

The third module computes the amount of radioactive loss due to erosion and sedimentation by using the results of the first and the second module. This module is capable of computing the dissolved and the particulate radioactive transport separately or together.

The model was applied to an experimental runoff plot, which was designed and constructed by the Center for Water Resources and Environmental Research at the CUNY in Ukraine near the Chernobyl NPP. During the one-year cycle of research at the runoff plot the erosion-controlled transfer of the radionuclides was studied. Four artificial rainfall simulations were performed. The amount of solid and liquid runoff was measured after each rainfall. The annual balance of the soil loss and the corresponding amount of radioactive transfer were calculated. The results of

the model runs were compared to the actual data and the relative computational error was calculated.

Comparison of the model with the available data indicated that the model is able to predict the total radioactive loss from the soil surface with satisfactory accuracy. The overall accuracy of the model can be improved by measuring the key parameters in the laboratory or on site precisely.

The focus in this study was more on the erosion process. The simplifications and assumptions, which were made here, might not be justifiable if the focus was on other aspects of this process. This model has the capability and the flexibility to be expanded and coupled with a subsurface contaminant transport model. This coupling will generate a link between the groundwater quality, surface water quality and soil contamination.

8.2 Future Prospects

The possibility of linking this model to GIS should be studied in the future. This option will optimize the use of the first module and simplifies the application of the model to real watersheds and eliminates the surveying and mapping processes. The GIS is also useful for the second module, where the spatial distribution of the soil properties becomes very important.

Rainfalls with duration more than 10 minutes affect the soil structure and the transport mechanisms. The assumptions of this model may not be applicable for such cases. More research and experiments are required to make the necessary adjustments in the model for such cases in future.

More complicated sorption processes can be incorporated into this model for more accurate results and for contaminants, whose sorption process can best be described by non-linear sorption models.

Additional study is needed to develop extra features for the model to analyze multi-component systems. In this case only module 3 needs to be modified. Because the structure of the module changes, more efficient numerical techniques and algorithm must be applied for more accurate and faster computing.

The interaction between the contaminants and soil particles and their effect on the sediment-related key parameters like the erosion constant and the limiting shear stress for erosion should also be studied.

Developing and adopting a visual interface for the FORTRAN codes can improve the data presentation and analysis for more complex systems.

APPENDIX

FORTRAN 90 CODES

```
!!!!!!!!!!!!!!!!!!!!!!!!!!!!!!!!!!!!!!!!!!!!
!!!!!!!!!!!!!!!!!!!!!!!!!!!!!!!!!!!!!!!!!!!!
!!                                          !!
!! A FOUR-TIME-STEP NUMERICAL SOLUTION      !!
!!         FOR A DEPTH-AVERAGED             !!
!!          2-D  OVERLAND FLOW              !!
!!                   BY                     !!
!!          SIAMAK ESFANDIARY               !!
!!                                          !!
!!!!!!!!!!!!!!!!!!!!!!!!!!!!!!!!!!!!!!!!!!!!
!!!!!!!!!!!!!!!!!!!!!!!!!!!!!!!!!!!!!!!!!!!!


implicit none
integer  count, m, n, raindur,kk, maxnod !, zz
parameter(maxnod=10)
!real alphay(maxnod,maxnod), alphax(maxnod,maxnod)
real  elev(maxnod,maxnod), s0x(maxnod,maxnod s0y(maxnod,maxnod))
real  h(maxnod,maxnod), v(maxnod,maxnod), u(maxnod,maxnod)
real  hp(maxnod,maxnod), vp(maxnod,maxnod), up(maxnod,maxnod)
real  hc(maxnod,maxnod), vc(maxnod,maxnod), uc(maxnod,maxnod)
real  hbar(maxnod,maxnod), vbar(maxnod,maxnod), ubar(maxnod,maxnod)
real  momx(maxnod,maxnod), momy(maxnod,maxnod), momxp(maxnod,maxnod)
real  momyp(maxnod,maxnod), momxc(maxnod,maxnod),momyc(maxnod,maxnod)
real  sfx(maxnod,maxnod), sfy(maxnod,maxnod),sfyp(maxnod,maxnod)
real  sfxp(maxnod,maxnod), epsylx(maxnod,maxnod), parax(maxnod,maxnod)
real  paray(maxnod,maxnod), epsyly(maxnod,maxnod), var(maxnod,maxnod)
!real qx(maxnod,maxnod), qy(maxnod,maxnod), qt2(maxnod,maxnod)
real  rain, infilt, mann, dur, kmax
real g, net, havg, time ,tr

parameter (mann=0.2,  g=981.0,  delt=0.001, discof=0.6)
parameter (delx=400.0, dely=400.0, m=6, n=6)
character*1 key




!!!!!!!!!!!!!!!!!!!!!!!!!!!!
!!!!!!!!!!!!!!!!!!!!!!!!!!!!
!!                        !!
!!     OPENING FILES      !!
!!                        !!
!!!!!!!!!!!!!!!!!!!!!!!!!!!!
!!!!!!!!!!!!!!!!!!!!!!!!!!!!


 !print*,'enter the number of rows and coloumns:'
```

```
 !read*,m, n

open (unit=1,file='ukraine-cm-6.txt' ,status='old')
!open (unit=2,file='outS0x.txt' ,status='unknown')
!open (unit=3,file='outS0y.txt' ,status='unknown')
open (unit=4,file='outpth.txt' ,status='unknown')
open (unit=41,file='outhbar.txt' ,status='unknown')
open (unit=42,file='outhbar-2.txt' ,status='unknown')
!open (unit=5,file='outptv.txt' ,status='unknown')
open (unit=51,file='outvbar.txt' ,status='unknown')
open (unit=52,file='outvbar-2.txt' ,status='unknown')
!open (unit=6,file='outptu.txt' ,status='unknown')
open (unit=61,file='outubar.txt' ,status='unknown')
open (unit=62,file='outubar-2.txt' ,status='unknown')
open (unit=71,file='hydrogrph.txt' ,status='unknown')
open(unit=100,file='art-test.txt',status='unknown')

read (1,*) ((elev(i,j),j=1,n),i=1,m)
print*,'rain intensity :'
read*, rain

         dur=4000000.0
         infilt=0.006
         raindur=360000
         tr=int(raindur/60000.0)

write(4,10300)rain,infilt,tr

       dtdx=delt/delx
       dtdy=delt/dely

print*,'Do you want the artificial viscosity to be performed?(y/n)'
read*,KEY
print*,'Please wait'
print 10500
print 10600
write(71,10500)


!!!!!!!!!!!!!!!!!!!!!!!!!!!!!
!!!!!!!!!!!!!!!!!!!!!!!!!!!!!
!!                          !!
!!  COMPUTING SLOPES (S0)   !!
!!                          !!
!!!!!!!!!!!!!!!!!!!!!!!!!!!!!
!!!!!!!!!!!!!!!!!!!!!!!!!!!!!

do 80 i=1,m-1
   do 70 j=1,n

       s0x(i,j)=-(elev(i+1,j)-elev(i,j))/delx
       s0x(m,j)=s0x(m-1,j)
       !alphax(i,j)=dasind(S0x(i,j))

   70 continue
80 continue
```

```
do 100 i=1,m
   do 90 j=1,n-1

       s0y(i,j)=-(elev(i,j+1)-elev(i,j))/dely
       s0y(i,n)=s0y(i,n-1)
       !alphay(i,j)=dasind(S0y(i,j))

   90 continue
100 continue

!write(2,10000)((S0x(i,j),j=1,n-1),i=1,m)
!write(2,10000)((alphax(i,j),j=1,n-1),i=1,m)
!write(3,10100)((S0y(i,j),j=1,n),i=1,m-1)
!write(3,10100)((alphay(i,j),j=1,n),i=1,m-1)

!!!!!!!!!!!!!!!!!!!!!!!!
!!!!!!!!!!!!!!!!!!!!!!!!
!!                      !!
!! INITIAL CONDITIONS !!
!!                      !!
!!!!!!!!!!!!!!!!!!!!!!!!
!!!!!!!!!!!!!!!!!!!!!!!!

do 290 i=1,m
   do 280 j=1,n

       h(i,j)=0.02
       v(i,j)=0.0
       u(i,j)=0.0
       momx(i,j)=0.0
       momy(i,j)=0.0
       sfx(i,j)=0.0
       sfy(i,j)=0.0

   280 continue
290 continue

       count=0

!!!!!!!!!!!!!!!!!!!!!!!!!!!!
!!!!!!!!!!!!!!!!!!!!!!!!!!!!
!!                        !!
!!   FINITE DIFFERENCE    !!
!!     COMPUTATIONS       !!
!!                        !!
!!!!!!!!!!!!!!!!!!!!!!!!!!!!
!!!!!!!!!!!!!!!!!!!!!!!!!!!!


       kmax=dur/delt

do 5000 k=1,kmax

   if (k.eq.raindur) rain=0

       net=(rain-infilt)
```

```
!!!!!!!!!!!!!!!!
!!!!!!!!!!!!!!!!
!!              !!
!!   COUNT=0    !!
!!              !!
!!!!!!!!!!!!!!!!
!!!!!!!!!!!!!!!!

! count=0
! time step=k
! prediction step
! boundary on i=1
! do j=2,n

   if (count.eq.0) then

do 300 j=2,n

    hp(1,j)=h(1,j)-(dtdx)*(momx(1,j)+momx(2,j))&
    -(dtdy)*(momy(1,j)-momy(1,j-1))+delt*net

    momyp(1,j)=momy(1,j)-(dtdx)*(u(1,j)*v(1,j)*h(1,j)+u(2,j)*v(2,j)&
    *h(2,j))-(dtdy)*((v(1,j)**2)*h(1,j)+0.5*g*(h(1,j)**2)-(v(1,j-1)&
    **2)*h(1,j-1)-0.5*g*(h(1,j-1)**2))+g*h(1,j)*delt*(s0y(1,j)-
sfy(1,j))

    up(1,j)= 0.0
    vp(1,j)=momyp(1,j)/hp(1,j)
      !vp(1,j)=0.0

300 continue

! count=0
! prediction step
! boundary on j=1
! do i=2,m

do 310 i=2,m

   hp(i,1)=h(i,1)-(dtdx)*(momx(i,1)-momx(i-1,1))&
   -(dtdy)*(momy(i,1)+momy(i,2))+delt*net

  momxp(i,1)=momx(i,1)-(dtdx)*((u(i,1)**2)*h(i,1)+0.5*g*(h(i,1)**2)-&
  (u(i-1,1)**2)*h(i-1,1)-0.5*g*(h(i-1,1)**2))-(dtdy)*(u(i,1)*v(i,1)&
  *h(i,1)+u(i,2)*v(i,2)*h(i,2))+g*h(i,1)*delt*(s0x(i,1)-sfx(i,1))

   up(i,1)=momxp(i,1)/hp(i,1)
   !up(i,1)=0.0
   vp(i,1)=0.0

310 continue

!!!!!!!!!!!!!!!!!!!!!!!!!!!!
!point(1,1)

   hp(1,1)=(hp(1,2) + hp(2,1))/2.0
```

```
   vp(1,1)=(vp(1,2) + vp(2,1))/2.0
up(1,1)=(up(1,2) + up(2,1))/2.0

! count=0
! time step k
! prediction step
! do i=2,m
! do j=2,n

do 330  i=2,m
   do 320   j=2,n

       hp(i,j)=h(i,j)-(dtdx)*(momx(i,j)-momx(i-1,j))&
       -(dtdy)*(momy(i,j)-momy(i,j-1))+delt*net

   momxp(i,j)=momx(i,j)-(dtdx)*((u(i,j)**2)*h(i,j)+0.5*g*(h(i,j)**2)-&
   u(i-1,j)**2)*h(i-1,j)-0.5*g*(h(i-1,j)**2))-(dtdy)*(u(i,j)*v(i,j)&
   *h(i,j)-u(i,j-1)*v(i,j-1)*h(i,j-1))+g*h(i,j)*delt*(s0x(i,j)-&
   sfx(i,j))

   momyp(i,j)=momy(i,j)-(dtdx)*(u(i,j)*v(i,j)*h(i,j)-u(i-1,j)*v(i-1,j)&
   *h(i-1,j))-(dtdy)*((v(i,j)**2)*h(i,j)+0.5*g*(h(i,j)**2)-(v(i,j-1)&
   **2)*h(i,j-1)-0.5*g*(h(i,j-1)**2))+g*h(i,j)*delt*(s0y(i,j)-sfy(i,j))

   up(i,j)=momxp(i,j)/hp(i,j)
   vp(i,j)=momyp(i,j)/hp(i,j)


   320 continue
330 continue


do 336 i=1,m
   do 335 j=1,n

       sfxp(i,j)=(mann**2)*up(i,j)*sqrt(up(i,j)**2+vp(i,j)**2)&
         /(hp(i,j)**(1.33))
       sfyp(i,j)=(mann**2)*vp(i,j)*sqrt(up(i,j)**2+vp(i,j)**2)&
         /(hp(i,j)**(1.33))


   335 continue
336 continue


! count=0
! time step=k
! correction step
! do i=1,m-1
! do j=1,n-1

do 350 i=1,m-1
    do 340 j=1,n-1

       hc(i,j)=h(i,j)-(dtdx)*(momxp(i+1,j)-momxp(i,j))&
       -(dtdy)*(momyp(i,j+1)-momyp(i,j))+delt*net
```

```
      momxc(i,j)=momx(i,j)-(dtdx)*((up(i+1,j)**2)*hp(i+1,j)+0.5*g*&
      (hp(i+1,j)**2)-(up(i,j)**2)*hp(i,j)-0.5*g*(hp(i,j)**2))-(dtdy)&
      *(up(i,j+1)*vp(i,j+1)*hp(i,j+1)-up(i,j)*vp(i,j)*hp(i,j))+&
      g*hp(i,j)*delt*(s0x(i,j)-sfxp(i,j))

      momyc(i,j)=momy(i,j)-(dtdx)*(up(i+1,j)*vp(i+1,j)*hp(i+1,j)&
      -up(i,j)*vp(i,j)*hp(i,j))-(dtdy)*((vp(i,j+1)**2)*hp(i,j+1)+0.5&
      *g*(hp(i,j+1)**2)-(vp(i,j)**2)*hp(i,j)-0.5*g*(hp(i,j)**2))+g*&
      hp(i,j)*delt*(s0y(i,j)-sfyp(i,j))


      uc(i,j)=momxc(i,j)/hc(i,j)
      vc(i,j)=momyc(i,j)/hc(i,j)


   340 continue
350 continue

! count=0
! time step=k
! correction step
! boundary on i=m
! do j=1,n-1

do 360 j=1,n-1


   !qx(m,j)=up(m-1,j)*hp(m-1,j)
   !qy(m,j)=vp(m-1,j)*hp(m-1,j)
   !qt2(m,j)=((qx(m,j)**2)+(qy(m,j)**2))
   !hc(m,j)=(qt2(m,j)/g)**(1.0/3.0)
   hc(m,j)=hc(m-1,j)
   vc(m,j)=vc(m-1,j)
   uc(m,j)=uc(m-1,j)

360 continue


! count=0
! time step=k
! correction step
! boundary on j=n
! do i=1,m-1

do 370 i=1,m-1

   hc(i,n)=h(i,n)-(dtdx)*(momxp(i+1,n)-momxp(i,n))&
   -(dtdy)*(momyp(i,n-1)+momyp(i,n))+delt*net

   momxc(i,n)=momx(i,n)-(dtdx)*((up(i+1,n)**2)*hp(i+1,n)+&
   0.5*g*(hp(i+1,n)**2)-(up(i,n)**2)*hp(i,n)-0.5*g*(hp(i,n)**2)&
   )-(dtdy)*(up(i,n-1)*vp(i,n-1)*hp(i,n-1)+up(i,n)*vp(i,n)*&
   +hp(i,n))g*hp(i,n)*delt*(s0x(i,n)-sfxp(i,n))

   uc(i,n)=momxc(i,n)/hc(i,n)
```

```
   !uc(i,n)=0.0
   vc(i,n)=0.0

370 continue

!!!!!!!!!!!!!!!!!!!!!!!!!!!!!!!!!!!!
!point(m,n)

   hc(m,n)=(hc(m,n-1)+hc(m-1,n))/2.0
   vc(m,n)=(vc(m,n-1)+vc(m-1,n))/2.0
   uc(m,n)=(uc(m,n-1)+uc(m-1,n))/2.0


! END OF COUNT=0
!!!!!!!!!!!!!!!!!!!!!!!!!!!!!!!!!!!!!!!!!!!!!!!!!!!!!!!!!!!!!!!!!!!!!!!!!!!!!!
!!!!!!!!!!!!!!!!!!!!!!!!!!!!!!!!!!!!!!!!!!!!!!!!!!!!!!!!!!!!!!!!!!!!!!!!!!!!!!

!!!!!!!!!!!!!!!!!
!!!!!!!!!!!!!!!!!
!!             !!
!!   COUNT=1   !!
!!             !!
!!!!!!!!!!!!!!!!!
!!!!!!!!!!!!!!!!!

! count=1
! time step k+1
! prediction step

    elseif(count.eq.1) then

do 410 i=1,m-1
   do 400 j=1,n-1


      hp(i,j)=h(i,j)-(dtdx)*(momx(i+1,j)-momx(i,j))&
      -(dtdy)*(momy(i,j+1)-momy(i,j))+delt*net

      momxp(i,j)=momx(i,j)-(dtdx)*((u(i+1,j)**2)*h(i+1,j)&
      +0.5*g*(h(i+1,j)**2)-(u(i,j)**2)*h(i,j)-0.5*g*(h(i,j)**2))&
      -(dtdy)*(u(i,j+1)*v(i,j+1)*h(i,j+1)-u(i,j)*v(i,j)*h(i,j))&
      +g*h(i,j)*delt*(s0x(i,j)-sfx(i,j))

      momyp(i,j)=momy(i,j)-(dtdx)*(u(i+1,j)*v(i+1,j)*h(i+1,j)-u(i,j)&
      *v(i,j)*h(i,j))(dtdy)*((v(i,j+1)**2)*h(i,j+1)+0.5*g*(h(i,j+1)**&
      2)-(v(i,j)**2)*h(i,j)-0.5*g*(h(i,j)**2))+g*h(i,j)&
      *delt*(s0y(i,j)-sfy(i,j))

      up(i,j)=momxp(i,j)/hp(i,j)
      vp(i,j)=momyp(i,j)/hp(i,j)


   400 continue
410 continue

! count=1
! time step=k+1
```

```
! prediction step
! boundary on j=n
! do i=1,m-1

do 420 i=1,m-1

   hp(i,n)=h(i,n)-(dtdx)*(momx(i+1,n)-momx(i,n))&
   -(dtdy)*(momy(i,n-1)+momy(i,n))+delt*net

   momxp(i,n)=momx(i,n)-(dtdx)*((u(i+1,n)**2)*h(i+1,n)+0.5*g&
   *(h(i+1,n)**2)-(u(i,n)**2)*h(i,n)-0.5*g*(h(i,n)**2))-(dtdy)&
   *(u(i,n-1)*v(i,n-1)*h(i,n-1)+u(i,n)*v(i,n)*h(i,n))&
   +g*h(i,n)*delt*(s0x(i,n)-sfx(i,n))

   up(i,n)=momxp(i,n)/hp(i,n)
   !up(i,n)=0.0
   vp(i,n)=0.0

420 continue

! count=1
! time step=k+1
! prediction step
! boundary on i=m
! do j=1,n-1

do 430 j=1,n-1

   !qx(m,j)=up(m-1,j)*hp(m-1,j)
   !qy(m,j)=vp(m-1,j)*hp(m-1,j)
   !qt2(m,j)=((qx(m,j)**2)+(qy(m,j)**2))
   !hp(m,j)=(qt2(m,j)/g)**(1.0/3.0)
   hp(m,j)=hp(m-1,j)
   vp(m,j)=vp(m-1,j)
   up(m,j)=up(m-1,j)

430 continue

!!!!!!!!!!!!!!!!!!!!!!!!!!!!!!!!
!!!!!point(m,n)

   hp(m,n)=(hp(m-1,n)+hp(m,n-1))/2.0
   vp(m,n)=(vp(m-1,n)+vp(m,n-1))/2.0
   up(m,n)=(up(m-1,n)+up(m,n-1))/2.0


do 436 i=1,m
   do 435 j=1,n

      sfxp(i,j)=(mann**2)*up(i,j)*sqrt(up(i,j)**2+vp(i,j)**2)&
        /(hp(i,j)**(1.33))
      sfyp(i,j)=(mann**2)*vp(i,j)*sqrt(up(i,j)**2+vp(i,j)**2)&
        /(hp(i,j)**(1.33))

   435 continue
436 continue
```

```
! count=1
! time step=k+1
! correction step
! boundary on i=1
! do j=2,n

do  440 j=2,n

   hc(1,j)=h(1,j)-(dtdx)*(momxp(1,j)+momxp(2,j))&
   -(dtdy)*(momyp(1,j)-momyp(1,j-1))+delt*net

   momyc(1,j)=momy(1,j)-
(dtdx)*(up(1,j)*vp(1,j)*hp(1,j)+up(2,j)*vp(2,j)&
   *hp(2,j))-(dtdy)*((vp(1,j)**2)*hp(1,j)+0.5*g*(hp(1,j)**2)-(vp(1,j-
1)&
   **2)*hp(1,j-1)-0.5*g*(hp(1,j-1)**2))+g*hp(1,j)*delt*(s0y(1,j)-
sfyp(1,j))

   uc(1,j)=0.0
   vc(1,j)=momyc(1,j)/hc(1,j)
   !vc(1,j)=0.0

440 continue

! count=1
! time step=k+1
! correction step
! boundary on j=1
! do i=2,m

do 450 i=2,m

   hc(i,1)=h(i,1)-(dtdx)*(momxp(i,1)-momxp(i-1,1))&
   -(dtdy)*(momyp(i,1)+momyp(i,2))+delt*net

   momxc(i,1)=momx(i,1)-
(dtdx)*((up(i,1)**2)*hp(i,1)+0.5*g*(hp(i,1)**2)-&
   (up(i-1,1)**2)*hp(i-1,1)-0.5*g*(hp(i-1,1)**2))-
(dtdy)*(up(i,1)*vp(i,1)&
   *hp(i,1)+up(i,2)*vp(i,2)*hp(i,2))+g*hp(i,1)*delt*(s0x(i,1)-
sfxp(i,1))

   uc(i,1)=momxc(i,1)/hc(i,1)
   !uc(i,1)=0.0
   vc(i,1)=0.0

!endif

450 continue

!!!!!!!!!!!!!!!!!!!!!!!!!!!!
!point(1,1)

   hc(1,1)=(hc(1,2) + hc(2,1))/2.0
   vc(1,1)=(vc(1,2) + vc(2,1))/2.0
   uc(1,1)=(uc(1,2) + uc(2,1))/2.0
```

```
! count=1
! time step=k+1
! correction step

do 470 i=2,m
   do 460 j=2,n

        hc(i,j)=h(i,j)-(dtdx)*(momxp(i,j)-momxp(i-1,j))&
        -(dtdy)*(momyp(i,j)-momyp(i,j-1))+delt*net

        momxc(i,j)=momx(i,j)-(dtdx)*((up(i,j)**2)*hp(i,j)+0.5*g*&
          (hp(i,j)**2)-(up(i-1,j)**2)*hp(i-1,j)-0.5*g*(hp(i-1,j)**2))&
        -(dtdy)*(up(i,j)*vp(i,j)*hp(i,j)-up(i,j-1)*vp(i,j-1)*hp(i,j-1))&
        +g*hp(i,j)*delt*(s0x(i,j)-sfxp(i,j))

        momyc(i,j)=momy(i,j)-(dtdx)*(up(i,j)*vp(i,j)*hp(i,j)-up&
          (i-1,j)*vp(i-1,j)*hp(i-1,j))-(dtdy)*((vp(i,j)**2)*hp(i,j)&
        +0.5*g*(hp(i,j)**2)-(vp(i,j-1)**2)*hp(i,j-1)-0.5*g*(hp(i,j-
1)**2))&
        +g*hp(i,j)*delt*(s0y(i,j)-sfyp(i,j))

        uc(i,j)=momxc(i,j)/hc(i,j)
        vc(i,j)=momyc(i,j)/hc(i,j)

   460 continue
470 continue

! END OF COUNT=1
!!!!!!!!!!!!!!!!!!!!!!!!!!!!!!!!!!!!!!!!!!!!!!!!!!!!!!!!!!!!!!!!!!!!!!!!!!!
!!!!!!!!!!!!!!!!!!!!!!!!!!!!!!!!!!!!!!!!!!!!!!!!!!!!!!!!!!!!!!!!!!!!!!!!!!!

!!!!!!!!!!!!!!!!!
!!!!!!!!!!!!!!!!!
!!               !!
!!   COUNT=2     !!
!!               !!
!!!!!!!!!!!!!!!!!
!!!!!!!!!!!!!!!!!

! count=2
! time step=k+2
! prediction step
! boundary on i=1
! do j=1,n-1

elseif (count.eq.2) then

do 500 j=1,n-1

   hp(1,j)=h(1,j)-(dtdx)*(momx(1,j)+momx(2,j))&
   -(dtdy)*(momy(1,j+1)-momy(1,j))+delt*net

   momyp(1,j)=momy(1,j)-(dtdx)*(u(1,j)*v(1,j)*h(1,j)+u(2,j)*v(2,j)&
   *h(2,j))-(dtdy)*((v(1,j+1)**2)*h(1,j+1)+0.5*g*(h(1,j+1)**2)-(v(1,j)&
   **2)*h(1,j)-0.5*g*(h(1,j)**2))+g*h(1,j)*delt*(s0y(1,j)-sfy(1,j))
```

```
      up(1,j)=0.0
      vp(1,j)=momyp(1,j)/hp(1,j)
      !vp(1,j)=0.0

  500 continue

  ! count=2
  ! time step k+2
  ! prediction step
  do 520 i=2,m
     do 510 j=1,n-1

         hp(i,j)=h(i,j)-(dtdx)*(momx(i,j)-momx(i-1,j))&
         -(dtdy)*(momy(i,j+1)-momy(i,j))+delt*net

         momxp(i,j)=momx(i,j)-(dtdx)*((u(i,j)**2)*h(i,j)+0.5*g*&
          (h(i,j)**2)-(u(i-1,j)**2)*h(i-1,j)-0.5*g*(h(i-1,j)**2))&
         -(dtdy)*(u(i,j+1)*v(i,j+1)*h(i,j+1)-u(i,j)*v(i,j)*h(i,j))&
          +g*h(i,j)*delt*(s0x(i,j)-sfx(i,j))


         momyp(i,j)=momy(i,j)-(dtdx)*(u(i,j)*v(i,j)*h(i,j)-u(i-1,j)&
         *v(i-1,j)*h(i-1,j))-(dtdy)*((v(i,j+1)**2)*h(i,j+1)+&
         0.5*g*(h(i,j+1)**2)-(v(i,j)**2)*h(i,j)-0.5*g*(h(i,j)**2))&
         +g*h(i,j)*delt*(s0y(i,j)-sfy(i,j))

         up(i,j)=momxp(i,j)/hp(i,j)
         vp(i,j)=momyp(i,j)/hp(i,j)

      510 continue
  520 continue

  ! count=2
  ! time step= k+1
  ! prediction step
  ! boundary on j=n
  ! do i=2,m

  do 530 i=2,m

     hp(i,n)=h(i,n)-(dtdx)*(momx(i,n)-momx(i-1,n))&
     -(dtdy)*(momy(i,n-1)+momy(i,n))+delt*net

     momxp(i,n)=momx(i,n)-(dtdx)*((u(i,n)**2)*h(i,n)+0.5*g&
     *(h(i,n)**2)-(u(i-1,n)**2)*h(i-1,n)-0.5*g*(h(i-1,n)**2))&
     -(dtdy)*(u(i,n-1)*v(i,n-1)*h(i,n-1)+u(i,n)*v(i,n)*h(i,n))&
     +g*h(i,n)*delt*(s0x(i,n)-sfx(i,n))

     up(i,n)=momxp(i,n)/hp(i,n)
     !up(i,n)=0.0
     vp(i,n)=0.0

  530 continue

  !!!!!!!!!!!!!!!!!!!!!!!!!!!!!!!!
  !point(1,n)
```

```
      hp(1,n)=(hp(1,n-1)+hp(2,n))/2.0
      vp(1,n)=(vp(1,n-1)+vp(2,n))/2.0
      up(1,n)=(up(1,n-1)+up(2,n))/2.0


do 536 i=1,m
   do 535 j=1,n

        sfxp(i,j)=(mann**2)*up(i,j)*sqrt(up(i,j)**2+vp(i,j)**2)&
          /(hp(i,j)**(1.33))
        sfyp(i,j)=(mann**2)*vp(i,j)*sqrt(up(i,j)**2+vp(i,j)**2)&
          /(hp(i,j)**(1.33))

   535 continue
536 continue

! count=2
! time step=k+2
! boundary on j=1
! correction step
! do i=1,m-1

do 540 i=1,m-1

   hc(i,1)=h(i,1)-(dtdx)*(momxp(i+1,1)-momxp(i,1))&
   -(dtdy)*(momyp(i,1)+momyp(i,2))+delt*net

   momxc(i,1)=momx(i,1)-(dtdx)*((up(i+1,1)**2)*hp(i+1,1)&
   +0.5*g*(hp(i+1,1)**2)-(up(i,1)**2)*hp(i,1)-0.5*g*(hp(i,1)**2))&
   -(dtdy)*(up(i,1)*vp(i,1)*hp(i,1)+up(i,2)*vp(i,2)*hp(i,2))&
   +g*hp(i,1)*delt*(s0x(i,1)-sfxp(i,1))


   uc(i,1)=momxc(i,1)/hc(i,1)
   !uc(i,1)=0.0
   vc(i,1)=0.0

540 continue

! count=2
! time step=k+2
! correction step

do 560 i=1,m-1
   do 550 j=2,n

        hc(i,j)=h(i,j)-(dtdx)*(momxp(i+1,j)-momxp(i,j))&
        -(dtdy)*(momyp(i,j)-momyp(i,j-1))+delt*net

        momxc(i,j)=momx(i,j)-(dtdx)*((up(i+1,j)**2)*hp(i+1,j)+&
          0.5*g*(hp(i+1,j)**2)-(up(i,j)**2)*hp(i,j)-0.5*g*(hp(i,j)**2))&
        -(dtdy)*(up(i,j)*vp(i,j)*hp(i,j)-up(i,j-1)*vp(i,j-1)*hp(i,j-
1))+&
        g*hp(i,j)*delt*(s0x(i,j)-sfxp(i,j))

        momyc(i,j)=momy(i,j)-(dtdx)*(up(i+1,j)*vp(i+1,j)*hp(i+1,j)&
          -up(i,j)*vp(i,j)*hp(i,j))-(dtdy)*((vp(i,j)**2)*hp(i,j)+&
```

```
          0.5*g*(hp(i,j)**2)-(vp(i,j-1)**2)*hp(i,j-1)-0.5&
        *g*(hp(i,j-1)**2))+g*hp(i,j)*delt*(s0y(i,j)-sfyp(i,j))

        uc(i,j)=momxc(i,j)/hc(i,j)
        vc(i,j)=momyc(i,j)/hc(i,j)

   550 continue
560 continue

! count=2
! time step=k+2
! correction step
! boundary on i=m
! do j=1,n

do 570 j=1,n

   !qx(m,j)=uc(m-1,j)*hc(m-1,j)
   !qy(m,j)=vc(m-1,j)*hc(m-1,j)
   !qt2(m,j)=((qx(m,j)**2)+(qy(m,j)**2))
   !hc(m,j)=(qt2(m,j)/g)**(1.0/3.0)
   hc(m,j)=hc(m-1,j)
   vc(m,j)=vc(m-1,j)
   uc(m,j)=uc(m-1,j)

570 continue

! END OF COUNT=2
!!!!!!!!!!!!!!!!!!!!!!!!!!!!!!!!!!!!!!!!!!!!!!!!!!!!!!!!!!!!!!!!!!!!!!!!!!!
!!!!!!!!!!!!!!!!!!!!!!!!!!!!!!!!!!!!!!!!!!!!!!!!!!!!!!!!!!!!!!!!!!!!!!!!!!!

!!!!!!!!!!!!!!!!!
!!!!!!!!!!!!!!!!!
!!               !!
!!   COUNT=3     !!
!!               !!
!!!!!!!!!!!!!!!!!
!!!!!!!!!!!!!!!!!

! count=3
! time step=k+3
! prediction step
! boundary on j=1
! i=1,m-1

elseif (count.eq.3) then

do 600 i=1,m-1

    hp(i,1)=h(i,1)-(dtdx)*(momx(i+1,1)-momx(i,1))&
    -(dtdy)*(momy(i,1)+momy(i,2))+delt*net

    momxp(i,1)=momx(i,1)-(dtdx)*((u(i+1,1)**2)*h(i+1,1)+&
      0.5*g*(h(i+1,1)**2)-(u(i,1)**2)*h(i,1)-0.5*g*(h(i,1)**2))&
    -(dtdy)*(u(i,1)*v(i,1)*h(i,1)+u(i,2)*v(i,2)*h(i,2))&
    +g*h(i,1)*delt*(s0x(i,1)-sfx(i,1))
```

```
      up(i,1)=momxp(i,1)/hp(i,1)
        !up(i,1)=0.0
      vp(i,1)=0.0

600 continue

! count=3
! time step k+3
! prediction

do 620 i=1,m-1
    do 610 j=2,n

       hp(i,j)=h(i,j)-(dtdx)*(momx(i+1,j)-momx(i,j))&
       -(dtdy)*(momy(i,j)-momy(i,j-1))+delt*net

       momxp(i,j)=momx(i,j)-(dtdx)*((u(i+1,j)**2)*h(i+1,j)&
         +0.5*g*(h(i+1,j)**2)-(u(i,j)**2)*h(i,j)-0.5*g*(h(i,j)**2))&
       -(dtdy)*(u(i,j)*v(i,j)*h(i,j)-u(i,j-1)*v(i,j-1)*h(i,j-1))&
       +g*h(i,j)*delt*(s0x(i,j)-sfx(i,j))

       momyp(i,j)=momy(i,j)-(dtdx)*(u(i+1,j)*v(i+1,j)*h(i+1,j)&
         -u(i,j)*v(i,j)*h(i,j))-(dtdy)*((v(i,j)**2)*h(i,j)+0.5*g&
       *(h(i,j)**2)-(v(i,j-1)**2)*h(i,j-1)-0.5*g*(h(i,j-1)**2))&
       +g*h(i,j)*delt*(s0y(i,j)-sfy(i,j))

       up(i,j)=momxp(i,j)/hp(i,j)
       vp(i,j)=momyp(i,j)/hp(i,j)

   610 continue
620 continue

! count=3
! time step=k+3
! prediction step
! boundary on i=m
! do j=1,n

do 630 j=1,n

    !qx(m,j)=up(m-1,j)*hp(m-1,j)
    !qy(m,j)=vp(m-1,j)*hp(m-1,j)
    !qt2(m,j)=((qx(m,j)**2)+(qy(m,j)**2))
    !hp(m,j)=(qt2(m,j)/g)**(1.0/3.0)
    hp(m,j)=hp(m-1,j)
    vp(m,j)=vp(m-1,j)
    up(m,j)=up(m-1,j)

630 continue

do 636 i=1,m
   do 635 j=1,n

       sfxp(i,j)=(mann**2)*up(i,j)*sqrt(up(i,j)**2+vp(i,j)**2)&
         /(hp(i,j)**(1.33))
       sfyp(i,j)=(mann**2)*vp(i,j)*sqrt(up(i,j)**2+vp(i,j)**2)&
         /(hp(i,j)**(1.33))
```

```
   635 continue
636 continue


! count=3
! time step=k+3
! correction step
! boundary on i=1
! do j=1,n-1

do 640 j=1,n-1

   hc(1,j)=h(1,j)-(dtdx)*(momxp(1,j)+momxp(2,j))&
   -(dtdy)*(momyp(1,j)-momyp(1,j-1))+delt*net

   momyc(1,j)=momy(1,j)-(dtdx)*(up(1,j)*vp(1,j)*hp(1,j)&
   +up(2,j)*vp(2,j)*hp(2,j))-(dtdy)*((vp(1,j)**2)*hp(1,j)&
   +0.5*g*(hp(1,j)**2)-(vp(1,j1)**2)*hp(1,j-1)-0.5*g*(hp(1,j-1)**2))+&
   g*hp(1,j)*delt*(s0y(1,j)-sfyp(1,j))

   uc(1,j)=0.0
   vc(1,j)=momyc(1,j)/hc(1,j)
   !vc(1,j)=0.0

640 continue

! count=3
! time step=k+3
! correction step

do 660 i=2,m
   do 650 j=1,n-1

      hc(i,j)=h(i,j)-(dtdx)*(momxp(i,j)-momxp(i-1,j))&
      -(dtdy)*(momyp(i,j+1)-momyp(i,j))+delt*net

      momxc(i,j)=momx(i,j)-(dtdx)*((up(i,j)**2)*hp(i,j)+0.5*&
        g*(hp(i,j)**2)-(up(i-1,j)**2)*hp(i-1,j)-0.5*g*(hp(i-1,j)**2))&
      -(dtdy)*(up(i,j+1)*vp(i,j+1)*hp(i,j+1)-up(i,j)*vp(i,j)*hp(i,j))&
      +g*hp(i,j)*delt*(s0x(i,j)-sfxp(i,j))

      momyc(i,j)=momy(i,j)-(dtdx)*(up(i,j)*vp(i,j)*hp(i,j)&
        -up(i-1,j)*vp(i-1,j)*hp(i-1,j))-(dtdy)*((vp(i,j+1)**2)&
        *hp(i,j+1)+0.5*g*(hp(i,j+1)**2)-(vp(i,j)**2)*hp(i,j)&
      -0.5*g*(hp(i,j)**2))+g*hp(i,j)*delt*(s0y(i,j)-sfyp(i,j))

      uc(i,j)=momxc(i,j)/hc(i,j)
      vc(i,j)=momyc(i,j)/hc(i,j)

   650 continue
660 continue

! count=3
! time step=k+3
! correction step
! boundary on j=n
```

```
! do i=2,m
do 670 i=2,m

   hc(i,n)=h(i,n)-(dtdx)*(momxp(i,n)-momxp(i-1,n))&
   -(dtdy)*(momyp(i,n-1)+momyp(i,n))+delt*net

   momxc(i,n)=momx(i,n)-
(dtdx)*((up(i,n)**2)*hp(i,n)+0.5*g*(hp(i,n)**2)-&
   (up(i-1,n)**2)*hp(i-1,n)-0.5*g*(hp(i-1,n)**2))-(dtdy)*(up(i,n-
1)*vp(i,n-1)&
   *hp(i,n-1)+up(i,n)*vp(i,n)*hp(i,n))+g*hp(i,n)*delt*(s0x(i,n)-
sfxp(i,n))

   uc(i,n)=momxc(i,n)/hc(i,n)
   !uc(i,n)=0.0
   vc(i,n)=0.0

670 continue

!!!!!!!!!!!!!!!!!!!!!!!!!!
!point(1,1)

   hc(1,n)=(hc(1,n-1)+hc(2,n))/2.0
   vc(1,n)=(vc(1,n-1)+vc(2,n))/2.0
   uc(1,n)=(uc(1,n-1)+uc(2,n))/2.0

! END OF COUNT=3
!!!!!!!!!!!!!!!!!!!!!!!!!!!!!!!!!!!!!!!!!!!!!!!!!!!!!!!!!!!!!!!!!!!!!!!!!!!
!!!!!!!!!!!!!!!!!!!!!!!!!!!!!!!!!!!!!!!!!!!!!!!!!!!!!!!!!!!!!!!!!!!!!!!!!!!

   endif
!!!!!!!!!!!!!!!!!!!!!!!!!!!!!!!!!!!!!!!!!!!!!!!!!!!!!!!!!!!!!!!!!!!!!!!!!!!
!!!!!!!!!!!!!!!!!!!!!!!!!!!!!!!!!!!!!!!!!!!!!!!!!!!!!!!!!!!!!!!!!!!!!!!!!!!

!!!!!!!!!!!!!!!!!!!
!!!!!!!!!!!!!!!!!!!
!!                 !!
!! next time step !!
!!                 !!
!!!!!!!!!!!!!!!!!!!
!!!!!!!!!!!!!!!!!!!

do 3020 i=1,m
   do 3010 j=1,n


      h(i,j)=(hc(i,j)+hp(i,j))/2.0
      if(h(i,j).lt.0.02) h(i,j)=0.02
      u(i,j)=(uc(i,j)+up(i,j))/2.0
      u(1,j)=0.0
  !   v(1,j)=0.0
      v(i,j)=(vc(i,j)+vp(i,j))/2.0
      v(i,1)=0.0
      v(i,n)=0.0
   !  u(i,n)=0.0
   !  sfx(i,j)=(mann**2)*u(i,j)*sqrt(u(i,j)**2+v(i,j)**2)&
   !  /((h(i,j)**(1.33)))
```

```
   !    sfy(i,j)=(mann**2)*v(i,j)*sqrt(u(i,j)**2+v(i,j)**2)&
   !    /((h(i,j)**(1.33)))

   3010 continue
3020 continue

if(MOD(k,60000).eq.0) then
print*,k
print 10700,((h(i,j),i=1,m),j=1,n)
write(100,*)k
write(100,10700)((h(i,j),i=1,m),j=1,n)
write(100,*)
print*
endif


if(KEY.eq.'n') goto 3999

!!!!!!!!!!!!!!!!!!!!!!!!!
!!!!!!!!!!!!!!!!!!!!!!!!!
!!                       !!
!! artificial viscosity !!
!!                       !!
!!!!!!!!!!!!!!!!!!!!!!!!!
!!!!!!!!!!!!!!!!!!!!!!!!!

!do 3990 zz=1,3

!if(zz.eq.1)then

do 3035 i=1,m
  do 3030 j=1,n

  var(i,j)=h(i,j)

3030 continue
3035 continue

!elseif(zz.eq.2)then

! do 3045 i=1,m
!  do 3040 j=1,n

 ! var(i,j)=v(i,j)

!3040 continue
!3045 continue

!else

!do 3055 i=1,m
!  do 3050 j=1,n

 ! var(i,j)=u(i,j)

!3050 continue
!3055 continue
```

```
!endif

do 3100 kk=1,2
if(kk.eq.1)then
i=1
else
i=m
endif
    do 3060 j=1,n-1

         parax(i,j)=abs(var(i,j+1)-var(i,j))/(abs(var(i,j+1))&
             +abs(var(i,j)))

3060     continue

         parax(i,n)=abs(var(i,n-1)-var(i,n))/(abs(var(i,n-1))&
             +abs(var(i,n)))

3100 continue


do 3200 kkk=1,2

if(kkk.eq.1)then
j=1
else
j=m
endif
    do 3150 i=1,m-1

         paray(i,j)=abs(var(i+1,j)-var(i,j))/(abs(var(i+1,j))&
             +abs(var(i,j)))

3150     continue

         paray(m,j)=abs(var(m-1,j)-var(m,j))/(abs(var(m-1,j))&
             +abs(var(m,j)))

3200 continue

do 3300 i=2,m-1
   do 3250 j=2,n-1

            parax(i,j)=abs(var(i,j+1)-2.0*var(i,j)+var(i,j-1))/&
            (abs(var(i,j+1))+abs(2.0*var(i,j))+abs(var(i,j-1)))

              paray(i,j)=abs(var(i+1,j)-2.0*var(i,j)+var(i-1,j))/&
            (abs(var(i+1,j))+abs(2.0*var(i,j))+abs(var(i-1,j)))

3250  continue
3300 continue

do 3400 i=1,m
  do 3350 j=1,n-1

   epsylx(i,j)=discof*max(parax(i,j),parax(i,j+1))
```

```
3350  continue
3400  continue

do 3550 i=1,m-1
  do 3500 j=1,n

  epsyly(i,j)=discof*max(paray(i,j),paray(i+1,j))

3500  continue
3550  continue

do 3650 i=2,m-1
  do 3600 j=2,n-1

            var(i,j)=var(i,j)+epsylx(i,j)*(var(i,j+1)-var(i,j))-&
                     epsylx(i,j-1)*(var(i,j)-var(i,j-1))&
                     +epsyly(i,j)*(var(i+1,j)-var(i,j))-&
                     epsyly(i-1,j)*(var(i,j)-var(i,j-1))

3600 continue
3650 continue

!if(zz.eq.1)then

do 3750 i=1,m
  do 3700 j=1,n

  h(i,j)=var(i,j)

3700 continue
3750 continue

!elseif(zz.eq.2)then

 !do 3850 i=1,m
  !do 3800 j=1,n

   !v(i,j)=var(i,j)

!3800 continue
!3850 continue

!else

!do 3950 i=1,m
!  do 3900 j=1,n

!  u(i,j)=var(i,j)

!3900 continue
!3950 continue

!endif

!3990 continue
```

```
if(MOD(k,60000).eq.0) then
print 10700,((h(i,j),i=1,m),j=1,n)
print*
print*
write(100,10700)((h(i,j),i=1,m),j=1,n)
write(100,*)

endif
!!!!!!!!!!!!!!!!!!!
!!!!!!!!!!!!!!!!!!!
!!                 !!
!! interpolation  !!
!!                 !!
!!!!!!!!!!!!!!!!!!!
!!!!!!!!!!!!!!!!!!!


3999 do 4100 i=1,n-1
         do 4000 j=1,m-1

       vbar(i,j)=(v(i,j)+v(i+1,j)+v(i,j+1)+v(i+1,j+1))*0.25
       ubar(i,j)=(u(i,j)+u(i+1,j)+u(i,j+1)+u(i+1,j+1))*0.25
       hbar(i,j)=(h(i,j)+h(i+1,j)+h(i,j+1)+h(i+1,j+1))*0.25

   4000 continue
4100 continue

   havg=(h(m,1)+h(m,2)+h(m,3)+h(m,4)+h(m,5)+h(m,m))/6.0

   vavg=(sqrt((v(m,1)**2)+(u(m,1)**2))+sqrt((v(m,2)**2)+(u(m,2)**2))+&
   sqrt((v(m,3)**2)+(u(m,3)**2))+sqrt((v(m,4)**2)+(u(m,4)**2))+&
   sqrt((v(m,5)**2)+(u(m,5)**2))+sqrt((v(m,m)**2)+(u(m,m)**2)))/6.0

   Qavg=(((sqrt((v(m,1)**2)+(u(m,1)**2))*h(m,1))+(sqrt((v(m,2)**2)+&
   (u(m,2)**2))*h(m,2))+(sqrt((v(m,3)**2)+(u(m,3)**2))*h(m,3))&
   +(sqrt((v(m,4)**2)+(u(m,4)**2))*h(m,4))+(sqrt((v(m,5)**2)+&
   (u(m,5)**2))*h(m,5))+(sqrt((v(m,m)**2)+(u(m,m)**2))*h(m,m)))/6.0)&
   *2000.0

    if(MOD(k,50).eq.0) then

    if(k.le.5000000)then
    write(41,10200)((hbar(i,j),j=1,n-1),i=1,m-1)
    write(51,10200)((vbar(i,j),j=1,n-1),i=1,m-1)
    write(61,10200)((ubar(i,j),j=1,n-1),i=1,m-1)
    else
    write(42,10200)((hbar(i,j),j=1,n-1),i=1,m-1)
    write(52,10200)((vbar(i,j),j=1,n-1),i=1,m-1)
    write(62,10200)((ubar(i,j),j=1,n-1),i=1,m-1)
    endif

      endif

    if(MOD(k,60000).eq.0) then
    time=k*delt
    write(4,10300)Qavg
    print 10400,time,havg,vavg,Qavg,net
```

```
      write(71,10400)time,havg,vavg,Qavg
      else
      endif

      count=count+1
      if(count.eq.4) count=0

do 4800 i=1,m
do 4750 j=1,n

        sfx(i,j)=(mann**2)*u(i,j)*sqrt(u(i,j)**2+v(i,j)**2)&
          /((h(i,j)**(1.33)))
        sfy(i,j)=(mann**2)*v(i,j)*sqrt(u(i,j)**2+v(i,j)**2)&
          /((h(i,j)**(1.33)))

4750 continue
4800 continue



!10000    format(5F13.10)
!10100    format(6F13.10)
10200    format(5F8.5)
10300    format(F10.5)
10400    format(5F12.5)
10500    format(5X,'time(s)',4X,'havg(cm)',2X,'vavg(cm/s)',2X,&
                'Qavg(cc/s)',7x,'net')
10600    format(5x,'-------',4X,'--------',2X,'----------',2X,&
                '----------',6x,'------')
10700    format(6F9.6)


5000 continue


9000     time=time/60.0
     print*,' the simulation stoped after',time,'minutes'


end
```

```
! THIS PROGRAM CALCULATES THE SUSPENDED SOLID CONCENTRATION
! BY SIAMAK ESFANDIARY
!=============================================================

implicit none
integer n, m, time, maxnode
parameter (maxnode=10)
parameter (n=5, m=5)
double precision v(maxnod,maxnod), u(maxnod,maxnod), h(maxnod,maxnod)
double precision falvel(maxnod,maxnod), mann ,  bedcon(maxnod,maxnod)
double precision shevel(maxnod,maxnod), tsp(maxnod,maxnod)
double precision exdtdx(maxnod,maxnod)
double precision eydtdy(maxnod,maxnod), susavg, qsorc(maxnod,maxnod)
double precision DmDt(maxnod,maxnod), taw(maxnod,maxnod)
double precision Ex(maxnod,maxnod),  Ey(maxnod,maxnod),vavg,havg
double precision susm(maxnod,maxnod), susmp(maxnod,maxnod)
double precision susmph(maxnod,maxnod)
double precision susmc(maxnod,maxnod), susmch(maxnod,maxnod)
parameter (max=32400, g=981.0, shecrt=0.1 )
parameter (const=0.00156, sheros= 0.0000045)
parameter (Econst=0.0000002,wdens=1.0)
parameter (shedep=0.000002, KO=0.5)
parameter (delx=400.0, dely=400.0, delt=0.05)




! OPENING THE INPUT FILES
!========================

open(unit=7 ,file='test.txt',status='unknown')
open(unit=8 ,file='susm.txt',status='unknown')
open(unit=9 ,file='qsorc.txt',status='unknown')
open(unit=11,file='Qavg.txt',status='unknown')
open(unit=41,file='outhbar.txt',status='unknown')
open(unit=51,file='outvbar.txt',status='unknown')
open(unit=61,file='outubar.txt',status='unknown')



print*,'please wait'
print 10500



! INITIAL CONDITIONS
!===================


do 120 i=1,m
do 110 j=1,n

susm(i,j)=0.0
falvel(i,j)=0.0
Ex(i,j)=0.0
```

```
Ey(i,j)=0.0
exdtdx(i,j)=0.0
eydtdy(i,j)=0.0


110 continue
120 continue



dtdx=delt/delx
dtdy=delt/dely

mann=0.15

!READING THE INPUT FILES
!=======================

do 50000 time=1,max

read(51,10200)((v(i,j),j=1,n),i=1,m)
read(61,10200)((u(i,j),j=1,n),i=1,m)
read(41,10200)((h(i,j),j=1,n),i=1,m)



! COMPUTING THE VAIABLES
!=======================

! shevel(i,j) = shear velocity
! manning coefficient= 0.035
! tsp(i,j)= transport stage parameter
! shecrt = critical bed shear velocity given by Shield's diagram
! bedcon(i,j)= reference concentration or near bed concentration
! const = 0.035*D50/(a2*a*(D*)**.3)
! taw(i,j)= bed shear stress
! DmDt(i,j) = mass eroded per unit area per unit time
! sheros = limiting bed shear for erosion
! Econst = erosion constant
! qsorc(i,j)= source/sink term
! shedep= limiting bed shear stress for deposition
! falvel(i,j)= fall velocity
!=================================================================



do 320 i=1,m
do 300 j=1,n

shevel(i,j)=(mann*sqrt(g)*sqrt(u(i,j)**2 + v(i,j)**2))/(h(i,j)**(1/6))

tsp(i,j)=((shevel(i,j)/shecrt)**2)-1
if(tsp(i,j).lt.0)  tsp(i,j)=0

bedcon(i,j)=const*(tsp(i,j)**(1.5))
```

```
taw(i,j)=wdens*(shevel(i,j)**2)


if(taw(i,j).ge.sheros) then
DmDt(i,j)=Econst*((taw(i,j)/sheros)-1)
else
DmDt(i,j)=0
endif


if(taw(i,j).lt.shedep) then
qsorc(i,j)=(-(taw(i,j)/shedep)*falvel(i,j)*susm(i,j))*delt
elseif(taw(i,j).ge.shedep .and. taw(i,j).lt.sheros) then
qsorc(i,j)=-(falvel(i,j)*susm(i,j))*delt
else
qsorc(i,j)=(DmDt(i,j)- falvel(i,j)*susm(i,j))*delt
endif

300   continue
320 continue


! FINITE DIFFERENCE COMPUTATIONS
!==============================

! prediction step
! boundary conditions
! i=1   ,   j=2,n-1
!================

do 400 j=2,n-1

susmph(1,j)=susm(1,j)*h(1,j)-
dtdx*(susm(1,j)*u(1,j)*h(1,j)+susm(2,j)*u(2,j)*h(2,j))&
-dtdy*(susm(1,j)*v(1,j)*h(1,j)-susm(1,j-1)*v(1,j-1)*h(1,j-
1))+exdtdx(1,j)*(2*susm(2,j)&
*h(2,j)-2*susm(1,j)*h(1,j))+eydtdy(1,j)*(susm(1,j+1)*h(1,j+1)-
2*susm(1,j)*h(1,j)-susm(1,j-1))&
+qsorc(1,j)

susmp(1,j)=susmph(1,j)/h(1,j)

400 continue



! j=1   ,   i=2,m-1
!================

do 450 i=2,m-1

susmph(i,1)=susm(i,1)*h(i,1)-dtdx*(susm(i,1)*u(i,1)&
*h(i,1)-susm(i-1,1)*u(i-1,1)*h(i-1,1))-&
dtdy*(susm(i,1)*v(i,1)*h(i,1)+susm(i,2)*v(i,2)&
*h(i,2))+exdtdx(i,1)*(susm(i+1,1)*h(i+1,1)-2*&
susm(i,1)*h(i,1)+susm(i-1,1)*h(i-1,1))+eydtdy(i,1)&
*(2*susm(i,2)*h(i,2)-2*susm(i,1)*h(i,1))+qsorc(i,1)
```

```
susmp(i,1)=susmph(i,1)/h(i,1)

450 continue


! j=n   ,   i=2,m-1
!================

do 480 i=2,m-1

susmph(i,n)=susm(i,n)*h(i,n)-dtdx*(susm(i,n)*u(i,n)*h(i,n)&
-susm(i-1,n)*u(i-1,n)*h(i-1,n))&
-dtdy*(susm(i,n)*v(i,n)*h(i,n)-susm(i,n-1)*v(i,n-1)&
*h(i,n-1))+exdtdx(i,n)*(susm(i+1,n)*h(i+1,n)-2*&
susm(i,n)*h(i,n)+susm(i-1,n)*h(i-1,n))+eydtdy(i,n)*&
(2*susm(i,n-1)*h(i,n-1)-2*susm(i,n)*h(i,n))+qsorc(i,n)

susmp(i,n)=susmph(i,n)/h(i,n)

480 continue


!point(1,1) & point(1,n)
!=======================

susmp(1,1)=(susmp(1,2)+susmp(2,1))*0.5
susmp(1,n)=(susmp(1,n-1)+susmp(2,n))*0.5


! i=m   ,   j=1,n
!==============

do 500 j=1,n

susmp(m,j)=susmp(m-1,j)

500 continue


! inside points
!===============

do 600 i=2,m-1
do 550 j=2,n-1

susmph(i,j)=susm(i,j)*h(i,j)-dtdx*(susm(i,j)*u(i,j)*h(i,j)&
-susm(i-1,j)*u(i-1,j)*h(i-1,j))&
-dtdy*(susm(i,j)*v(i,j)*h(i,j)-susm(i,j)*v(i,j-1)&
*h(i,j-1))+exdtdx(i,j)*(susm(i+1,j)*h(i+1,j)-2*&
susm(i,j)*h(i,j)+susm(i-1,j)&
*h(i-1,j))+eydtdy(i,j)*(susm(i,j+1)*h(i,j+1)&
-2*susm(i,j)*h(i,j)+&
susm(i,j-1)*h(i,j-1))+qsorc(i,1)

susmp(i,j)=susmph(i,j)/h(i,j)
```

```
550 continue
600 continue

!------------------------------     SEPERATING THE PREDICTION STEP ----
--------------------
!------------------------------    FROM THE CORRECTION STEP    --------
-----------------


! correction step
! boundary conditions
! i=1   ,   j=2,n-1
!====================================


do 700      j=2,n-1

susmch(1,j)=susm(1,j)*h(1,j)-dtdx*(susmp(2,j)*u(2,j)&
*h(2,j)-susmp(1,j)*u(1,j)*h(1,j))&
-dtdy*(susmp(1,j+1)*v(1,j+1)*h(1,j+1)&
-susmp(1,j)*v(1,j)*h(1,j))+exdtdx(1,j)*(2*susmp(2,j)&
*h(2,j)-2*susmp(1,j)*h(1,j))+eydtdy(1,j)*(susmp(1,j+1)*h(1,j+1)&
-2*susmp(1,j)*h(1,j)-susmp(1,j-1))&
+qsorc(1,j)

susmc(1,j)=susmch(1,j)/h(1,j)

700 continue

! j=1   ,   i=2,m-1
!================

do 750 i=2,m-1

susmch(i,1)=susm(i,1)*h(i,1)-dtdx*(susmp(i+1,1)*u(i+1,1)&
*h(i+1,1)-susmp(i,1)*u(i,1)*h(i,1))&
-dtdy*(susmp(i,2)*v(i,2)*h(i,2)&
-susmp(i,1)*v(i,1)*h(i,1))+exdtdx(i,1)*(susmp(i+1,1)&
*h(i+1,1)-2*susmp(i,1)*h(i,1)+susmp(i-1,1)&
*h(i-1,1))+eydtdy(i,1)*(2*susmp(i,2)*h(i,2)-2*susmp(i,1)*h(i,1))&
+qsorc(i,1)

susmc(i,1)=susmch(i,1)/h(i,1)

750 continue

! j=n   ,   i=2,m-1
!================

do 780 i=2,m-1

susmch(i,n)=susm(i,n)*h(i,n)-dtdx*(susmp(i+1,n)*u(i+1,n)&
*h(i+1,n)-susmp(i,n)*u(i,n)*h(i,n))&
+dtdy*(susmp(i,n+1)*v(i,n+1)*h(i,n+1)+susmp(i,n)&
*v(i,n)*h(i,n))+exdtdx(i,n)*(susmp(i+1,n)*h(i+1,n)-2*&
susmp(i,n)*h(i,n)+susmp(i-1,n)*h(i-1,n))+eydtdy(i,n)*&
(2*susmp(i,n-1)*h(i,n-1)-2*susmp(i,n)*h(i,n))+qsorc(i,n)
```

```
susmc(i,n)=susmch(i,n)/h(i,n)

780 continue

!point(1,1) & point(1,n)
!=======================

susmc(1,1)=(susmc(1,2)+susmc(2,1))*0.5
susmc(1,n)=(susmc(1,n-1)+susmc(2,n))*0.5



! i=m  ,  j=1,n
!==============

do 800 j=1,n

susmc(m,j)=susmc(m-1,j)

800 continue


! inside points
!===============

do 870 j=2,m-1
do 820 i=2,n-1

susmch(i,j)=susm(i,j)*h(i,j)-dtdx*(susmp(i+1,j)*u(i+1,j)&
*h(i+1,j)-susmp(i,j)*u(i,j)*h(i,j))&
+dtdy*(susmp(i,j+1)*v(i,j+1)*h(i,j+1)+susmp(i,j)&
*v(i,j)*h(i,j))+exdtdx(i,j)*(susmp(i+1,j)*h(i+1,j)-2*&
susmp(i,j)*h(i,j)+susmp(i-1,j)*h(i-1,j))+eydtdy(i,j)*&
(2*susmp(i,j-1)*h(i,j-1)-2*susmp(i,j)*h(i,j))+qsorc(i,j)


susmc(i,j)=susmch(i,j)/h(i,j)


820 continue
870 continue

! next time step
!===============

do 920 i=1,m
do 900 j=1,n

susm(i,j)=(susmp(i,j)+susmc(i,j))*0.5
if(susm(i,j).lt.0.0000001) susm(i,j)=0

falvel(i,j)=KO*(susm(i,j)**(4.0/3.0))

Ex(i,j)=0.5*shevel(i,j)*h(i,j)
Ey(i,j)=Ex(i,j)

exdtdx(i,j)=delt/(delx**2)*Ex(i,j)
```

```
eydtdy(i,j)=delt/(dely**2)*Ey(i,j)


900 continue
920 continue


susavg=(susm(m,1)+susm(m,2)+susm(m,3)+susm(m,4)&
+susm(m,5)+susm(m,6))/6.0


! WRITING THE OUTPUT FILES INTO test.txt FILE
!============================================

write(8,10300)((susm(i,j),j=1,n),i=1,m)
write(9,10300)((qsorc(i,j),j=1,n),i=1,m)

if(MOD(time,10).eq.0) then

write(7,*)'time step=',time
write(7,*)
write(7,*)'velocity in the y direction'
write(7,10300)((v(i,j),j=1,n),i=1,m)
write(7,*)
write(7,*)'velocity in the x direction'
write(7,10300)((u(i,j),j=1,n),i=1,m)
write(7,*)
write(7,*)'flow depth'
write(7,10300)((h(i,j),j=1,n),i=1,m)
write(7,*)
write(7,*)'shear velocity'
write(7,10300)((shevel(i,j),j=1,n),i=1,m)
write(7,*)
write(7,*)'transport stage parameter'
write(7,10300)((tsp(i,j),j=1,n),i=1,m)
write(7,*)
write(7,*)'near bed concentration'
write(7,10300)((bedcon(i,j),j=1,n),i=1,m)
write(7,*)
write(7,*)'bed shear stress'
write(7,10300)((taw(i,j),j=1,n),i=1,m)
write(7,*)
write(7,*)'mass eroded per unit area per unit time'
write(7,10300)((DmDt(i,j),j=1,n),i=1,m)
write(7,*)
write(7,*)'fall velocity'
write(7,10300)((falvel(i,j),j=1,n),i=1,m)
write(7,*)
write(7,*)'Ex and Ey'
write(7,10300)((Ex(i,j),j=1,n),i=1,m)
write(7,*)
write(7,*)'source/sink term'
write(7,10300)((qsorc(i,j),j=1,n),i=1,m)
write(7,*)
write(7,*)'suspended solid concentration'
write(7,10300)((susm(i,j),j=1,n),i=1,m)
write(7,*)
```

```
write(7,*)'========== end of time step',time,'==========='
write(7,*)
!write(11,*)susavg

endif

susavg=(susm(5,1)+susm(5,2)+susm(5,3)+susm(5,4)+susm(5,5))/5.0

vavg=(sqrt((v(5,1)**2)+(u(5,1)**2))+sqrt((v(5,2)**2)+(u(5,2)**2))+&
sqrt((v(5,3)**2)+(u(5,3)**2))+sqrt((v(5,4)**2)+(u(5,4)**2))+&
sqrt((v(5,5)**2)+(u(5,5)**2)))/5.0

havg=(h(5,1)+h(5,2)+h(5,3)+h(5,4)+h(5,5))/5.0

Qavg=vavg*havg*susavg*2000

if(MOD(time,1200).eq.0) then



write(11,10300)Qavg
print 10400,time,susavg,vavg,havg,qavg



endif

10200 format(5F8.5)
10300 format(5F15.7)
10400 format(I7,3X,4F15.4)
10500 format(4X,'time',11X,'g/cc',11X,'cm/s',13X,'cm',12X,'g/s',/&
             4X,'----',11X,'----',11X,'----',13X,'--',12X,'---')

50000 continue

print*,'normal termination'



end
```

```
! THIS PROGRAM COMPUTES THE RADIOACTIVE TRANSPORT
! IN RUNOFF AS WELL AS  THE CHANGE OF THE CONCENTRATION
! ON THE INTERFACE (SOIL)
! BY SIAMAK ESFANDIARY
!================================================================



implicit none
integer m,n, maxnod
double precision v(maxnod,maxnod), u(maxnod,maxnod), h(maxnod,maxnod)
double precision qsorc(maxnod,maxnod),susm(maxnod,maxnod)
double precision Fdw(maxnod,maxnod)Fpw(maxnod,maxnod)
double precision Fds(maxnod,maxnod),Fps(maxnod,maxnod)
double precision erosn(maxnod,maxnod), advec(maxnod,maxnod)
double precision decay(maxnod,maxnod),difmas(maxnod,maxnod)
double precision wcon(maxnod,maxnod),wconph(maxnod,maxnod)
double precision wconch(maxnod,maxnod), wconp(maxnod,maxnod)
double precision wconc(maxnod,maxnod),q1(maxnod,maxnod)
double precision q2(maxnod,maxnod),scon(maxnod,maxnod)
double precision kdw, kds, dnsty, KO, lambda
parameter (max=32400, delx=400.0, dely=400.0, delt=0.05 )
parameter (vd=0.000007447, infilt=0.0033)
parameter (n=5, m=5)
integer time


print*,'please wait'
print 10600

! OPENING THE INPUT FILES
!========================

open(unit=8 ,file='susm.txt',status='unknown')
open(unit=9 ,file='qsorc.txt',status='unknown')
open(unit=10,file='sconini.txt',status='unknown')
open(unit=11,file='outs.txt',status='unknown')
open(unit=12,file='outw.txt',status='unknown')
open(unit=13,file='outinf.txt',status='unknown')
open(unit=14,file='fraction.txt',status='unknown')
open(unit=41,file='outhbar.txt',status='unknown')
open(unit=51,file='outvbar.txt',status='unknown')
open(unit=61,file='outubar.txt',status='unknown')
open(unit=71,file='polhyd.txt',status='unknown')



! INITIAL CONDITIONS
!====================

do 110 i=1,m
do 100 j=1,n

wcon(i,j)=0.0
```

```
100 continue
110 continue

read(10,*)((scon(i,j),j=1,n),i=1,m)
!print 10200,((scon(i,j),j=1,n),i=1,m)


! CONSTANSTS
!=====================

poro=0.4
Ex=.0002
Ey=.0002
dnsty=2.5
kdw=0.5
kds=0.5
KO=0.8
lambda=0.0

dtdx=delt/delx
dtdy=delt/dely
exdtdx=Ex*delt/(delx**2)
eydtdy=Ey*delt/(dely**2)


do 10000 time=1,max


!READING THE INPUT FILES
!========================

read(8,10300)((susm(i,j),j=1,n),i=1,m)
read(9,10300)((qsorc(i,j),j=1,n),i=1,m)
read(51,10200)((v(i,j),j=1,n),i=1,m)
read(61,10200)((u(i,j),j=1,n),i=1,m)
read(41,10200)((h(i,j),j=1,n),i=1,m)




! COMPUTING THE VARIABLES
!========================
!Fdw(i,j)=dissolved fraction in water
!Fpw(i,j)=particulate fraction in water
!Fds(i,j)=dissolved fraction in soil
!Fps(i,j)=particulate fraction in soil
!scon(i,j)=concentration in soil
!wcon(i,j)=concentration in water
!poro=porosity
!dnsty= soil density
!wcon(i,j)=concentration in water
!scon(i,j)=concentration on soil interface
```

```
do 210 i=1,m
do 200 j=1,n

Fdw(i,j)=1.0/(1.0+kdw*susm(i,j))
Fpw(i,j)=1.0-Fdw(i,j)
Fds(i,j)=1.0/(poro+(kds*dnsty*(1.0-poro)))
Fps(i,j)=1.0-Fds(i,j)
erosn(i,j)=qsorc(i,j)*kds*(Fps(i,j)*scon(i,j))*delt
q1(i,j)=erosn(i,j)
decay(i,j)=lambda*h(i,j)*wcon(i,j)
difmas(i,j)=vd*(Fds(i,j)*scon(i,j)-Fdw(i,j)*wcon(i,j))
advec(i,j)=infilt*Fdw(i,j)*wcon(i,j)
q2(i,j)=(difmas(i,j)-decay(i,j)-advec(i,j))*delt



200 continue
210 continue

!if (mod(time,1000).eq.0)then
!print*,'qsorce'
!print 10200,((qsorc(i,j),j=1,n),i=1,m)
!print*,'Fds'
!print 10200,((Fds(i,j),j=1,n),i=1,m)
!print*,'scon'
!print 10200,((scon(i,j),j=1,n),i=1,m)
!print*,'q1'
!print 10200,((q1(i,j),j=1,n),i=1,m)
!print*
!endif

! FINITE DIFFERENCE COMPUTATIONS (concentration in water)
!=======================================================

! prediction step
! boundary conditions
! i=1   ,   j=2,n-1
!================

do 400 j=2,n-1

wconph(1,j)=wcon(1,j)*h(1,j)-dtdx*(wcon(1,j)*u(1,j)*h(1,j)+wcon(2,j)&
*u(2,j)*h(2,j))-dtdy*(wcon(1,j)*v(1,j)*h(1,j)-wcon(1,j-1)*v(1,j-1)*&
h(1,j-1))+exdtdx*(2*wcon(2,j)*h(2,j)-2*wcon(1,j)*h(1,j))+eydtdy*&
(wcon(1,j+1)*h(1,j+1)-2*wcon(1,j)*h(1,j)-wcon(1,j-1))+q1(1,j)+q2(1,j)

wconp(1,j)=wconph(1,j)/h(1,j)

400 continue
```

```
! j=1   ,   i=2,m-1
!================

do 450 i=2,m-1

wconph(i,1)=wcon(i,1)*h(i,1)-dtdx*(wcon(i,1)*u(i,1)*h(i,1)&
-wcon(i-1,1)*u(i-1,1)*h(i-1,1))&
-dtdy*(wcon(i,1)*v(i,1)*h(i,1)+wcon(i,2)*v(i,2)*h(i,2))&
+exdtdx*(wcon(i+1,1)*h(i+1,1)-2*wcon(i,1)*h(i,1)+wcon(i-1,1)*h(i-1,1))&
+eydtdy*(2*wcon(i,2)*h(i,2)-2*wcon(i,1)*h(i,1))+q1(i,1)+q2(i,1)

wconp(i,1)=wconph(i,1)/h(i,1)

450 continue



! j=n   ,   i=2,m-1
!================

do 480 i=2,m-1

wconph(i,n)=wcon(i,n)*h(i,n)-dtdx*(wcon(i,n)*u(i,n)&
*h(i,n)-wcon(i-1,n)*&
u(i-1,n)*h(i-1,n))-dtdy*(wcon(i,n)*v(i,n)*h(i,n)-wcon(i,n-1)*v(i,n-1)*&
h(i,n-1))+exdtdx*(wcon(i+1,n)*h(i+1,n)-2*wcon(i,n)*h(i,n)+wcon(i-1,n)*&
h(i-1,n))+eydtdy*(2*wcon(i,n-1)*h(i,n-1)&
-2*wcon(i,n)*h(i,n))+q1(i,n)+q2(i,n)

wconp(i,n)=wconph(i,n)/h(i,n)

480 continue


!point(1,1) & point(1,n)
!======================

wconp(1,1)=(wconp(1,2)+wconp(2,1))*0.5
wconp(1,n)=(wconp(1,n-1)+wconp(2,n))*0.5



! i=m   ,   j=1,n
!==============

do 500 j=1,n

wconp(m,j)=wconp(m-1,j)

500 continue
```

```
! inside points
!===============

do 600 i=2,m-1
do 550 j=2,n-1

wconph(i,j)=wcon(i,j)*h(i,j)-dtdx*(wcon(i,j)*u(i,j)*h(i,j)-wcon(i-1,j)&
*u(i-1,j)*h(i-1,j))-dtdy*(wcon(i,j)*v(i,j)*h(i,j)-wcon(i,j)*v(i,j-1)*&
h(i,j-1))+exdtdx*(wcon(i+1,j)*h(i+1,j)-2*wcon(i,j)*h(i,j)+wcon(i-1,j)*&
h(i-1,j))+eydtdy*(wcon(i,j+1)*h(i,j+1)-2*wcon(i,j)*h(i,j)+wcon(i,j-1)*&
h(i,j-1))+q1(i,1)+q2(i,1)

wconp(i,j)=wconph(i,j)/h(i,j)

550 continue
600 continue

!---------------------  SEPERATING THE PREDICTION STEP ----------------
!--------------------     FROM THE CORRECTION STEP     ----------------


! correction step
! boundary conditions
! i=1  ,  j=2,n-1
!====================================


do 700      j=2,n-1

wconch(1,j)=wcon(1,j)*h(1,j)-dtdx*(wconp(2,j)*u(2,j)&
*h(2,j)-wconp(1,j)*&
u(1,j)*h(1,j))-dtdy*(wconp(1,j+1)*v(1,j+1)*h(1,j+1)-wconp(1,j)*v(1,j)*&
h(1,j))+exdtdx*(2*wconp(2,j)*h(2,j)-2*wconp(1,j)*h(1,j))+eydtdy*&
(wconp(1,j+1)*h(1,j+1)-2*wconp(1,j)*h(1,j)&
-wconp(1,j-1))+q1(1,j)+q2(1,j)

wconc(1,j)=wconch(1,j)/h(1,j)

700 continue



 ! j=1  ,  i=2,m-1
!================

do 750 i=2,m-1

wconch(i,1)=wcon(i,1)*h(i,1)-dtdx*(wconp(i+1,1)*u(i+1,1)*h(i+1,1)-&
wconp(i,1)*u(i,1)*h(i,1))-dtdy*(wconp(i,2)*v(i,2)*h(i,2)-wconp(i,1)&
*v(i,1)*h(i,1))+exdtdx*(wconp(i+1,1)*h(i+1,1)-2*wconp(i,1)*h(i,1)+&
wconp(i-1,1)*h(i-1,1))+eydtdy*(2*wconp(i,2)*h(i,2)-2*wconp(i,1)*&
h(i,1))+q1(i,1)+q2(i,1)

wconc(i,1)=wconch(i,1)/h(i,1)

750 continue
```

```
! j=n   ,   i=2,m-1
!================

do 780 i=2,m-1

wconch(i,n)=wcon(i,n)*h(i,n)-dtdx*(wconp(i+1,n)*u(i+1,n)*h(i+1,n)&
-wconp(i,n)*u(i,n)*h(i,n))+dtdy*(wconp(i,n+1)*v(i,n+1)*h(i,n+1)+&
wconp(i,n)*v(i,n)*h(i,n))+exdtdx*(wconp(i+1,n)*h(i+1,n)-2*wconp(i,n)&
*h(i,n)+wconp(i-1,n)*h(i-1,n))+eydtdy*(2*wconp(i,n-1)*h(i,n-1)-2*&
wconp(i,n)*h(i,n))+q1(i,n)+q2(i,n)

wconc(i,n)=wconch(i,n)/h(i,n)

780 continue

!point(1,1) & point(1,n)
!=======================

wconc(1,1)=(wconc(1,2)+wconc(2,1))*0.5
wconc(1,n)=(wconc(1,n-1)+wconc(2,n))*0.5



! i=m   ,   j=1,n
!==============

do 800 j=1,n

wconc(m,j)=wconc(m-1,j)

800 continue



! inside points
!===============

do 900 j=2,m-1
do 850 i=2,n-1

wconch(i,j)=wcon(i,j)*h(i,j)-dtdx*(wconp(i+1,j)*u(i+1,j)*h(i+1,j)&
-wconp(i,j)*u(i,j)*h(i,j))+dtdy*(wconp(i,j+1)*v(i,j+1)*h(i,j+1)+&
wconp(i,j)*v(i,j)*h(i,j))+exdtdx*(wconp(i+1,j)*h(i+1,j)-2*wconp(i,j)&
*h(i,j)+wconp(i-1,j)*h(i-1,j))+eydtdy*(2*wconp(i,j-1)*h(i,j-1)-2*&
wconp(i,j)*h(i,j))+q1(i,j)+q2(i,j)

wconc(i,j)=wconch(i,j)/h(i,j)


850 continue
900 continue
```

```
! next time step
!===============

do 1000 i=1,m
do  950 j=1,n

wcon(i,j)=(wconp(i,j)+wconc(i,j))*0.5
if(wcon(i,j).lt.0.0000000001) wcon(i,j)=0.0
scon(i,j)=scon(i,j)-((q1(i,j)+q2(i,j))*delt)



950  continue
1000 continue



! WRITING THE OUTPUT FILES INTO test.txt FILE
!============================================


write(11,10200)((scon(i,j),j=1,n),i=1,m)
write(12,10200)((wcon(i,j),j=1,n),i=1,m)
write(14,*)'Fdw'
write(14,10200)((Fdw(i,j),j=1,n),i=1,m)
write(14,*)'=========================='
write(14,*)'Fpw'
write(14,10200)((Fpw(i,j),j=1,n),i=1,m)
write(14,*)'=========================='
write(14,*)'Fds'
write(14,10200)((Fds(i,j),j=1,n),i=1,m)
write(14,*)'=========================='
write(14,*)'Fps'
write(14,10200)((Fps(i,j),j=1,n),i=1,m)
write(14,*)'=========================='

if(MOD(time,500).eq.0) then

!print*,'time step',time
!print 10200,((scon(i,j),j=1,n),i=1,m)
!print*
write(13,*)'q1'
write(13,10400)((q1(i,j),j=1,n),i=1,m)
write(13,*)'=========================='
write(13,*)'difmas'
write(13,10400)((difmas(i,j),j=1,n),i=1,m)
write(13,*)'=========================='
write(13,*)'advec'
write(13,10400)((advec(i,j),j=1,n),i=1,m)
write(13,*)'=========================='
write(13,*)'q2'
write(13,10400)((q2(i,j),j=1,n),i=1,m)
write(13,*)'=========================='
write(13,*)'concentration in runoff'
write(13,10400)((wcon(i,j),j=1,n),i=1,m)
write(13,*)'=========================='
write(13,*)'concentration on soil surface'
```

```
write(13,10400)((scon(i,j),j=1,n),i=1,m)
write(13,*)'=========================='
write(13,*)'suspendied solid concentration'
write(13,10400)((susm(i,j),j=1,n),i=1,m)
write(13,*)'=========================='
write(13,*)'Fdw'
write(13,10400)((Fdw(i,j),j=1,n),i=1,m)
write(13,*)'=========================='
write(13,*)'Fds'
write(13,10400)((Fds(i,j),j=1,n),i=1,m)
write(13,*)'=========================='

endif

vavg=(sqrt((v(5,1)**2)+(u(5,1)**2))+sqrt((v(5,2)**2)+(u(5,2)**2))+&
sqrt((v(5,3)**2)+(u(5,3)**2))+sqrt((v(5,4)**2)+(u(5,4)**2))+&
sqrt((v(5,5)**2)+(u(5,5)**2)))/5.0

havg=(h(5,1)+h(5,2)+h(5,3)+h(5,4)+h(5,5))/5.0


wcavg=(wcon(5,1)+wcon(5,2)+wcon(5,3)+wcon(5,4)+wcon(5,5))/5.0

Qcavg=vavg*havg*wcavg*2000


if(MOD(time,1200).eq.0) then

write(71,10300)wcon
print 10500,time,vavg,havg,Qcavg

endif

10200 format(5F8.5)
10300 format(5F15.7)
10400 format(5F14.11)
10500 format(I7,3X,4F15.4)
10600 format(4X,'time',11X,'cm/s',13X,'cm',12X,'Bq/s',/&
             4X,'----',11X,'----',13X,'--',12X,'---')

10000 continue


print*,'normal termination'

end
```

Bibliography

Abbott, M.B. (1979). *Computational Hydraulics: Elements of the Theory of Free Surface Flows*. Pitman, London.

Alanson C.V., W. H. Neibling, G. R. Foster (1981). "Estimating sediment Transport Capacity in Watershed Modeling", Transactions of the ASCE, 1211-1220.

Amano, H., Matsunaga, T., Nagao, S., Hanzawa, Y., Watanaba, M., Ueno, T. and Onuma, Y. (1999). "The Transfer Capability of Long-Lived Chernobyl Radionuclides from Surface Soil to River Water in Dissolved Forms", Organic Chemistry, Vol. 30, 437-442.

Ariathurai, R. and R. B. Krone, (1976). "Finite Element Model for Cohesive Sediment Transport", Journal of Hydraulic Division, ASCE, 102(HY3), 323-337.

Armstrong, N. E. and E. Gloyna, (1967). "Mathematical Models for The Dispersion of Radionuclides in Aquatic Systems", Environmental and Health Engineering Laboratory, University of Texas, Austin.

Aziz N., Shyam N. P. (1984). "Sediment Transport in Shallow Flows", Journal of Hydraulic Engineering, ASCE, 111(10), 152-169.

Brunjes, F., H. Barnewitz, G. Kirchener, (1999), "Diffusion and Diffusion-convection Experiments for Studying the sorption of Radionuclides in Soils", Czechoslovak Journal of Physics, 49, 175-180.

Cao, Z. (1999). "Equilibrium Near-Bed Concentration of Suspended Sediment", Journal of Hydraulic Engineering, ASCE, 125(12), 1270-1278.

Carlsson, S. (1978). "A model for The Movement and Loss of ^{137}Cs in Small Watershed", Health Physics, Vol. 34, 33-37.

Chapra, S. C. (1997). *Surface Water Quality Modeling*, WCB/McGraw Hill, New York.

Chow, V. T., D. R. Maidment and L. Mays, (1994). *Applied Hydrology*, McGraw Hill, New York, NY.

Constantinidis C. A. (1981). "Two-dimensional Kinematic Overland Flow Modeling", 2nd International Conference on Urban Storm Drainage, Urbana, Illinois USA, June 14-19.

Chaudhry, M. H. (1993). *Open-Channel Flow* , Prentice Hall, Englewood Cliffs, NJ.

Coughtrey, P. J. (1988). " Models for Radionuclide Transport in Soils", Soil Use and Management, 4(1), 84-90.

David W. P., C. E. Beer, (1975). "Simulation of Soil Erosion – Part 1. Development of a Mathematical Erosion Model", Transaction of ASCE, 126-133.

Eagleson Peter S. (1970). *Dynamic Hydrology*, McGraw Hill, New York, NY.

Fetter, C. W. (1993). *Contaminant Hydrogeology*, Macmillan Publishing Company, New York.

Fennema, R. J. (1983). " Numerical Solution of Two-Dimensional Transient Free-Surface Flows", thesis presented to the Washington State University, in partial fulfillment of the requirements for the degree of Doctor in Philosophy.

Fennema, R. J. and M. H. Chaudry, (1990). "Numerical Solution to 2D Free-Surface Flows: Explicit Methods", Journal of Hydraulic Engineering, ASCE, 116(8), 1013-1034.

Govindaraju, R. S., Jones, S. E. and Kavvas, M. L. (1988). "On the Diffusion Wave Modeling of Overland Flow 1. Solution foe Steep Slopes", Water Resources Research, 25(5), 734-744.

Govindaraju, Kavvas, M. L. and R. S., Jones, S. E. (1990). "Approximate Alalytical Solution for Overland Flow", Water Resources Research, 26(12), 2903-2912.

Guo, Q. and Jin, Y. (2000). "Modeling Sediment Transport Using Depth-Averaged and Momentum Equations", Journal of Hydraulic Engineering, ASCE, 125(12), 1262-1269.

Halldin S. and A. Rodhe (1990). "Urban Storm Water Transport and wash-off of Cesium-137 After the Chernobyl Accident", Water, Air and Soil Pollution, 49, 139-158.

Hann, C.T., Jonson, H.P. and Brakensiek, D. L. (1982). *Hydrologic Modeling of Small Watersheds*, An ASAE Monograph Number 5 in series published, chapter 8.

Hillel D. (1980), *Applications of Soil Physics*, Academic Press, New York, NY.

Iwagaki, Y. (1955), *Fundamental Studies on Runoff Analysis by Characteristics*, Bull. 10, Disaster Prevention Research, Kyoto University, Kyoto, Japan.

Julien P. Y. (1995). *Erosion and Sedimentation*, Cambridge University Press, New York.

Khanbilvardi R. M., A. S. Rogowski and A. C. Miller (1984). *Rill-interrill Erosion and Deposition Model of Stripmine Hydrology*, USDA/EPA Report.

Khanbilvardi, R. M. and Sadegh, A. (1997). "Erosion-Controlled Transport of Radioactive and Agrochemical Pollutants within Agricultural Watersheds", Final Report submitted to National Science Foundation, Award Number 9508271.

Khanbilvardi, R. M., Shestopolov, V., Onishchenko, I., Bublyas, V. and Gudzenko, V. (2000). "Role of Erosion Processes in Transfer of radionuclides: Results of Field Experiments", Journal of The American Water Resources Association, 35(4), 887-898.

Koboyashi, N. and S. Nam Seo (1985)."Fluid and Sediment Interaction over a Plane Bed", Journal of Hydraulic Engineering, ASCE, 111(6), 903-921.

Konshin O. V. (1992), "Applicability of the Convection-diffusion Mechanism for Modeling Migration of ^{137}Cs and ^{90}Sr in the Soil", Health Physics 63(3) 291-300.

Konshin O. V. (1992), "Mathematical Model of ^{137}Cs Migration in Soils: Analysis of Observations Following the Chernobyl Accident", Health Physics 63(3) 301-306..

Korhonen R. (1990). "Modeling Transfer of ^{137}Cs Fallout in Large Finnish Watercourse", Health Physics, 59(4), 443-454.

Lee, H., Hsieh, H., Yang, J. and Yang, C. T. (1997). "Quasi-Two Dimensional Simulation of Scour and Deposition in Alluvial Channels", Journal of Hydraulic Engineering, ASCE, 123(7), 600-609.

Leo, C., Van Rossum, H. and Termes, P. (1991). "Field Verification of 2-D and 3-D Suspended-Sediment Models", Journal of Hydraulic Engineering, ASCE, 116 (10), 1270-1287.

Mays, L. W. (1996). *Water Resources Handbook*, MacGraw-Hill, New York.

Morris, E. M. (1978). "The Effect of the Small-Slope Approximation and Lower Boundary Conditions on Solutions of The Saint- Venant Equations", Journal of Hydrology, 40, 31-47.

Nair, S. K., Hoffman, F. O., Thiessen K. M. and Konoplev, A. V. (1996). "Modeling The Washoff of 90Sr and 137Cs from An Experimental Plot Established in The Vicinity of The Chernobyl Reactor", Health Physics, Vol. 71(6), 896-909.

Nicholson, J. and O'Connor, B. A., (1984). "Cohesive Sediment Transport Model", Journal of Hydraulic Engineering, ASCE, 112(7), 621-640.

Pearson C. P., (1989). "One-dimensional Flow Over a Plane: Criteria for Kinematic Wave Modeling", Journal of Hydrology, 111, 39-48.

Rogowski, A. S. and Tamura T., (1965). "Movement of ^{137}Cs by Runoff, Erosion and Infiltration on The Alluvial Captina Silt Loam", Health Physics, Vol. 111, 1333-1340.

Roig, L.C., B. P. Donnell, W.A. Thomas, W.H. McAnally and S.A. Adamec, Jr., (1996). *A user's manual for SED2D-WES, A Generalized Computer*

Program for Two-Dimensional, Vertically Averaged Sediment Transport, SED 2D-WES Version 1.2 Beta

Rose C. W., (1985). Development in Soil Erosion and Deposition Models, Springer-verlag, New York, NY.

Shamber, D. R. and B. E. Larock, (1981). " Numerical Analysis of Flow in Sedimentation Basins", Journal of Hydraulic Division, ASCE, 107(5), 575-591.

Sladkevich, M., A. N. Militeev, and H. Rubin, (2000). "Simulation of Transportation Phenomena in Shallow Aquatic Environment", Journal of Hydraulic Engineering, ASCE, 126(2), 123-136.

Spiegel, Murray R., (1968). *Mathematical Handbook of Formulas and Tables, Schaum's outline series*, McGraw-Hill, New York, NY.

Street, R. L., Watters, G. Z., Vennard J. K., (1996). *Elementary Fluid Mechanics*, 7th Edition, Wiley, New York, NY.

Tannehill, J.C., Anderson, D. A. and Pletcher R. H., (1997). *Computational Fluid Mechanics and Heat Transfer*, 2nd Edition, Taylor & Francis.

Tayfur, G., Kavvas, M. L., Govindaraju R. S. and Storm, D. E., (1993). "Applicability of St. Vennant Equations for Two-Dimensional Overland Flows over Rough Infiltrating Surface", Journal of Hydraulic Engineering, ASCE, 119(1) 51-63.

US Army Corps of Engineers, (1993). *HEC-6, Scour and Deposition in Rivers and Reservoirs, User's Manual*, Hydrologic Engineering Center.

Van Rijn, L. C., (1984). "Sediment Transport, Part II: Suspended Load Transport", Journal of Hydraulic Engineering, ASCE, 110(11) 1613–1641.

Wallach R. and R. Shabtai, (1992). "Modeling Surface Runoff Contaminatrion by Soil Chemicals under Transient Water Infiltration", Journal of Hydrology, 132, 263-281.

Woolhiser, D. A. and J. A. Liggett, (1967). " Unsteady, One-dimensional Flow over a Plane – The Rising Hydrograph", Water Resources Research, 3(3), 39-71.

Wu, W., W.Rodi and T.Wenka, (2000). "3D Numerical Modeling of Flow and Sediment Transport in Open Channels", Journal of Hydraulic Engineering, ASCE, 126(1) 4 -15.

Yang T. C., (1996). *Sediment Transport Theory and Practice*, McGraw Hill, New York, NY.

Zhang, W. and T. W. Cundy, (1987). "Laminar Einstein Bed Load Transportation Equation for Overland Sheet Flow", Journal of Hydraulic Engineering, ASCE, 113(12) 1525-1538.

Zhang, W. and T. W. Cundy, (1989). "Modeling of Two-Dimensional Overland Flow", Water Resources Research, 25 (9), 2019-2035.